STUDIES ON BROADBAND CONJUGATE MATCHED FEED HORN

A Thesis submitted

in partial fulfillment for the Degree of

Doctor of Philosophy

by

RANAJIT DEY

Avionics Department

INDIAN INSTITUTE OF SPACE SCIENCE AND TECHNOLOGY

THIRUVANANTHAPURAM

June, 2016

CERTIFICATE

This is to certify that the thesis entitled "**Studies on Broadband Conjugate Feed Horn**" submitted by **Ranajit Dey** to the Indian Institute of Space Science and Technology, Thiruvananthapuram, in partial fulfillment for the award of the degree of **Doctor of Philosophy** is a *bona fide* record of research work carried out by him under our supervision. The contents of this thesis, in full or in parts, have not been submitted to any other Institution or University for the award of any degree or diploma.

Dr. Basudeb Ghosh

Department of Avionics

Dr. Soumyabrata Chakrabarty

Head, Microwave Sensors Antenna Division,
Space Applications Centre, ISRO

Thiruvananthapuram

June, 2016

Counter signature of HOD with seal

DECLARATION

I declare that this thesis entitled "**Studies on Broadband Conjugate Matched Feed Horn**" submitted in partial fulfillment of the degree of **Doctor of Philosophy** is a record of original work carried out by me under the supervision of **Dr. Soumyabrata Chakrabarty** and **Dr. Basudeb Ghosh**, and has not formed the basis for the award of any other degree or diploma, in this or any other Institution or University. In keeping with the ethical practice in reporting scientific information, due acknowledgements have been made wherever the findings of others have been cited.

Ranajit Dey

SC10D009

Thiruvananthapuram - 695 547

June, 2016

ACKNOWLEDGMENTS

I am very much thankful to Dr. S. B. Chakrabarty, Head, Microwave Sensors Antenna Division, Antenna Systems Group, Space Applications Center for his continuing interaction, excellent comments and suggestions during the course of this research work.

I am also thankful to Dr. Basudeb Ghosh, Assistant Professor, Department of Avionics, Indian Institute of Space Science and Technology for his comments and suggestions.

I extend my sincere thanks to the Group Director, ASG, Shri Rajeev Jyoti, Director, SAC, Shri Tapan Misra, Chairman ISRO, Shri A.S. Kiran Kumar and the Director, Indian Institute of Space Science and Technology, Dr. K.S. Dasgupta for permitting me to work for my Ph.D. thesis and extending support of the facilities and infrastructure of the center for the completion of this work.

Special thanks are due to Shri Ila Agnihotri and all other colleagues at MSAD/ASG, SAC, Ahmedabad, for encouragement and necessary support.

Thanks are due to Shri Ulkesh Desai and his mechanical team for providing support for mechanical drawing generation and hardware development. Special thanks are due to Shri H.C. Sanandiya, Shri V. R. Seth and Shri H. S. Solanki of AMD/ASG, SAC, for providing necessary support for radiation pattern measurements.

Last but not the least I am personally indebted to my wife, father and mother for their moral support and encouragement to persevere throughout this work.

Ranajit Dey

ABSTRACT

The research work described in the thesis is mainly focused on the investigation of improving the bandwidth of the conjugate matched feed horn for offset parabolic reflector antennas. Although, the offset parabolic reflector configuration offers significant advantages as compared to the front-fed parabolic reflector antenna, it suffers from two serious drawbacks. Due to the structural asymmetry, when illuminated by a linearly polarized primary feed, it generates high cross-polarization. The presence of high cross-polarization in the antenna radiation patterns implies the loss of energy in the undesired polarization, which ultimately results into reduction of the antenna efficiency. High degree of cross-polarization degrades the performance of the communication channel and can cause measurement errors in case of remote-sensing applications. In mono-pulse tracking radars, the high cross-polarization creates bore-sight-jitter, which severely affects the tracking accuracies. Considering these undesirable effects of high cross-polarization, it becomes necessary to develop a suitable technique to suppress the unwanted cross-polarization of the offset parabolic reflector antenna over a wide bandwidth. In the present thesis, the high cross-polarization of the offset parabolic reflector has been suppressed over a wide bandwidth by using a wide band conjugate matched feed. The concept of matched feed is thoroughly described at the beginning of the thesis. Design of matched feed using symmetric triple post discontinuity is also presented. The novel wide band conjugate matched feed horn has been designed in smooth as well as in corrugated cylindrical structure. The detailed designs of these matched feed structures have been presented in the thesis. It has been verified numerically that the proposed matched feeds effectively suppress the undesired high cross-polarization of the offset parabolic reflector antenna over a wider bandwidth.

TABLE OF CONTENTS

LIST OF FIGURES

LIST OF TABLES

ABBREVIATIONS

CCPT	Conservation of complex power technique
DGR	Dual Gridded Reflector
FEM	Finite Element Method
HFSS	High Frequency Structure Simulator
MF	Matched Feed
MM	Mode Matching
PO	Physical Optics
TE	Transverse Electric
TM	Transverse Magnetic

CHAPTER 1
INTRODUCTION

1.1 Background and Literature Survey

In satellite communications, remote sensing, radar and radio astronomy, cross-polarization over a specified bandwidth is an essential parameter [1]. The cross-polarization refers to the radiation of electromagnetic energy into the polarization other than the desired polarization. The presence of high cross-polarization degrades the overall performance of the system and restricts its use for many applications. In microwave radiometers, the cross-polarization affects the beam efficiency [2]. In communication system, the high cross-polarization produces undesired interference between the two orthogonal channels [3].

The parabolic reflector antenna is the most preferred antenna system for many applications due to its higher gain over a wide bandwidth [4]. The cross-polar properties of various parabolic reflectors have been studied by many researchers and are presented in the literature [5]-[22]. It is observed from these studies that the cross-polarization in a reflector type of antenna system depends on many parameters, e. g., the geometry of the reflector, the focal-length to diameter ratio (F/D) of the antenna system, the reflector surface imperfections, support struts, etc.

An axially symmetric parabolic reflector antenna does not generate cross-polar radiation in the principle planes due to its structural symmetry [4]. Also, further improvement in the cross-polar performance of an axially symmetric front-fed parabolic reflector can be achieved by selecting a larger F/D reflector configuration [5]. However, in practical applications, where it is difficult to accommodate a reflector with large F/D ratio due to mechanical constraints, a dual reflector antenna system can be used to suppress the cross-polarization [3]-[6]. Watson and Ghobrial [6] have reported that the cross-polar isolation of a

symmetrical cassegrain reflector is better than that of the equivalent prime-focal parabolic reflector antenna.

The axially symmetric parabolic reflectors as well as the symmetric dual reflectors suffer from a serious drawback of aperture blocking. Due to this aperture blocking, gain, side-lobe levels and cross-polarization of the antenna are affected. This aperture blocking effects can be overcome by the use of offset parabolic reflector antenna [19].

In offset reflector antenna system, the feed does not obscure the aperture of the main reflector. The absence of feed blockage in an offset parabolic reflector antenna ensures high illumination efficiency as compared to the prime focal parabolic reflector antenna. Also there is a high isolation between the primary feed and the main reflector for offset reflector configuration.

However, the offset parabolic reflector antennas suffer from a high linear cross-polarization field level in the plane of asymmetry when illuminated by a conventional linearly polarized feed, operating at its dominant mode. The cross-polarization pattern has been found to become significantly worse for offset reflectors with low F/D and higher offset angle. In the applications where the available space is a limitation, the reflectors with smaller F/D are preferable.

The cross-polar properties of offset parabolic reflector antennas have been studied and reported by many researchers [7]-[11], [23]-[27]. However, very few researchers have attended the problem of suppressing the cross-polarization of an offset parabolic reflector antenna. Chu and Turrin [7] were the first to publish the numerical data on the variation of maximum cross-polarization as a function of F/D ratio and offset angle. Gans and Semplak [8] demonstrated that a single offset reflector with small offset angle can provide low cross-polarization and low side-lobes. They also presented a detailed theoretical analysis to compute the cross-polarization in the reflector aperture and extended the same to study the cross-polar performance of the offset reflector in the far-field. Rudge [9] has presented

physical optics (PO) based mathematical expressions to predict the co-polar and cross-polar radiation patterns of an offset reflector antenna with offset feeds.

Chu [23] presented a concept of using polarization-selective grids between the reflector and the feed to obtain larger cross-polarization discrimination. In this method, the cross-polarization suppression depends on the size and location of the grid. He has used a straight strip grid while Dragone [24] proposed a curved strip grid for cross-polarization cancellation. However, the polarization selective grids may add to the complexity of the antenna system and also increase the cost of the overall system. Radiation properties of offset prime focal reflector antennas with emphasis on reducing side-lobes and cross-polarization have been studied by Strutzman and Terada [25].

Dual gridded reflector (DGR) antenna also can be used to get better cross-polarization isolation [19], [52], [53]. In DGR, a dual polarized system is formed by interleaving two orthogonal polarization sensitive reflector surfaces with separate foci. Although DGR antenna is having great cross-polar isolation, the fabrication complexity and fabrication cost of the structure is very high.

The cross-polar performance of the offset parabolic reflector antennas can be improved by means of techniques based upon focal region field matching [28] using a conjugate matched feed. A matched feed concept for primary feeds used in conjunction with offset parabolic reflector antennas which makes use of a higher order asymmetric waveguide mode has been described in Rudge and Adatia [26], [27]. It has been shown that cross-polarization can be minimized by exciting proper amount of higher order mode, TE_{21} mode along with dominant TE_{11} mode. Design of multimode matched feed horn which combines TE_{11}, TM_{11} and TE_{21} modes in proper amplitude and phase to suppress the unwanted high cross-polarization in an offset parabolic reflector antenna have also been reported by K. Bahadori and Y. Rahmat-Samii [29]. The conjugate matched feed designs in rectangular as well as circular corrugated structure are presented by S.B. Sharma et. al. in [30]-[33].

The cross-polar bandwidth reported in all the above references [26]-[33] is relatively low and is of the order of 2-3%. On the basis of these exhaustive literature survey, it is clear that within the limited available literature, no efforts have been made to design a conjugate matched feed horns which can be used to suppress the high cross-polarization for a broader bandwidth typically of the order of 10% or beyond.

Thus, it is worthwhile to carry out investigations and evolve a configuration of conjugate matched feed which can mitigate the high cross-polarization component generated in the offset reflector antenna system for a broader bandwidth.

1.2 Proposition of the Problem:

Based on the above discussion and the literature survey, detailed investigations using full-wave electromagnetic simulation of the following problems have been carried out:

An investigation has been carried out on suitable waveguide discontinuities [34]-[37] in circular waveguide which can generate only TE_{21} mode cancelling all the higher-order modes. To develop conjugate matched feed, the only higher order mode required is TE_{21} mode along with TE_{11} mode. Single [34], dual [35] and triple [36] post discontinuity which can generate TM_{01}, TE_{21}, TE_{21}*, TM_{11} modes etc. in circular waveguide, have been investigated in detail for developing a mechanism by which the higher order mode TE_{21} can be generated along with TE_{11} mode. It has been found out that the symmetrically placed triple post discontinuity in the transverse plane of the circular waveguide as shown in Fig.1.1(a) can generate TE_{21} mode cancelling the higher order TM_{01} mode. Thus triple post discontinuity in circular waveguide is a good member for matched feed design. To get the broadband cross-polar performance with the post discontinuity, a cascading configuration of triple post discontinuity along the axial direction shown in Fig.1.1(b) also has been studied. It has been found that for very low F/D

and high offset angle, it is difficult to design broadband conjugate matched feed using cascaded triple post discontinuity in circular waveguide structure.

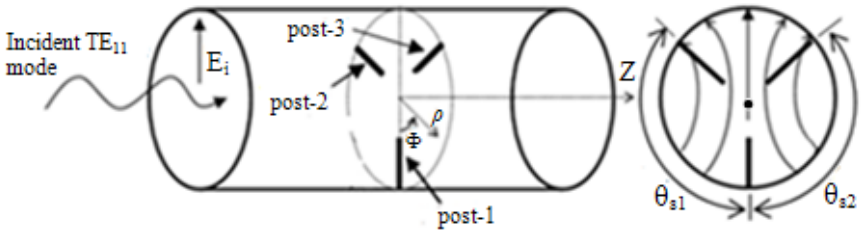

Fig. 1.1(a) A circular waveguide loaded with triple post discontinuity

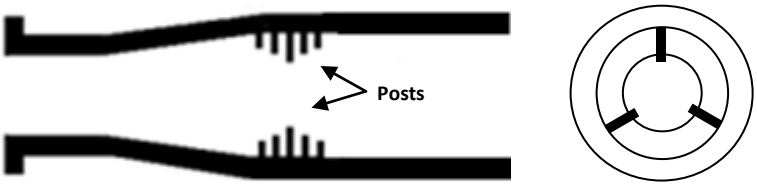

Fig.1.1(b) Schematic of conjugate matched feed horn with cascaded triple post discontinuities

Thus further studies have been carried out on the offset step discontinuities [37] in circular waveguide shown in Fig.1.2, which also can generate TM_{01}, TE_{21}, TE_{21}*, TE_{01}, TM_{11} modes etc. It has been found out that the parameters which are controlling the amplitude and phase of the higher order modes are offset distance(d) and the size of the larger waveguide supporting the higher-order modes. Thus unlike post discontinuity in circular waveguide, two parameters are there in offset step discontinuity by which modal power in higher order modes can be controlled.

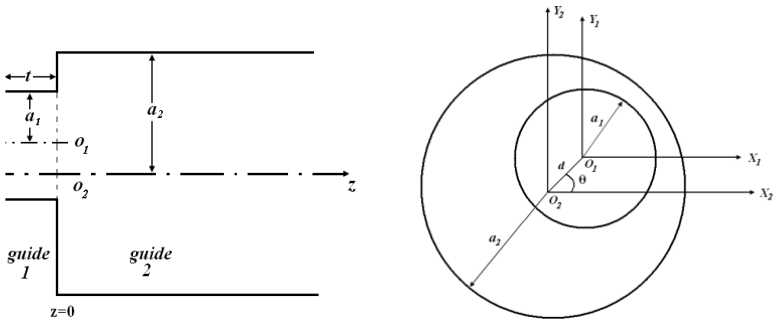

Fig. 1.2 Schematic drawing of the off-centre step junction in circular waveguide

After the detail investigation of the offset step discontinuity in circular waveguide, a novel type of symmetrical waveguide discontinuities in circular waveguide using offset step discontinuity has been configured to generate only TE_{21} mode along with TE_{11} mode. This waveguide discontinuity has been created using intersection of three off-centered junctions of circular waveguide placed symmetrically with angular spacing of 120^0 as shown in Fig.1.3. One such discontinuity which is like an iris in the waveguide has been analyzed for generating TE_{21} mode cancelling TM_{01} and TE_{21}* modes. It has been found that required amplitude and phase flatness of TE_{21} mode relative to TE_{11} mode over the designed frequency band, which is required for broadband performance of the matched feed, were not achieved. In order to enhance the cross-polar bandwidth, multiple sections with the similar iris structure shown in Fig.1.4 have been placed in the axial direction inside an oversized circular waveguide supporting TE_{11} as well as TE_{21} modes. A study has been carried out for 3, 5 and 7 irises. It has been found out that the required amplitude and phase flatness of TE_{21} mode relative to TE_{11} mode are achieved with both five and seven cascaded iris sections. The axial profile of the irises has been optimized to achieve good return loss performance. This feed is designed at Ku band for F/D=0.5 and offset angle=53^0.

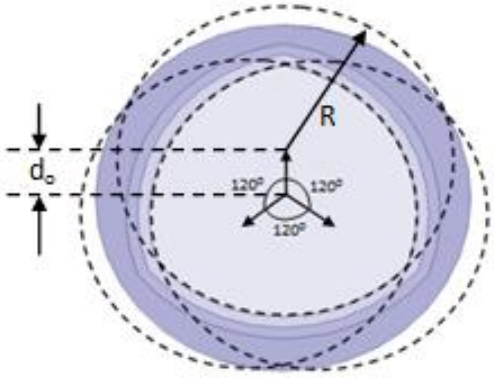

Fig.1.3 Modeling of opening of the irises (arrows indicate the offset direction of circles making 120^0 angle with each other)

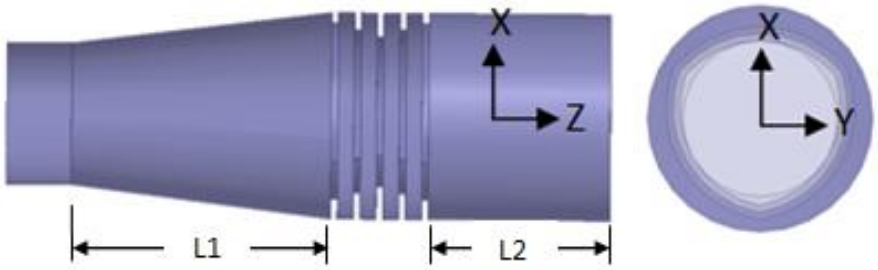

Fig.1.4 Simulation model of the proposed matched feed structure, (a) side view, (b) front view of the horn

Similar concept of the cascaded iris sections has been applied for designing broadband corrugated conjugate matched feed horn as shown in Fig.1.5 to cancel the high unwanted cross-polar components generated in offset reflector geometry having lower F/D and higher offset angle. The feed horn is specifically designed to mitigate the cross-polarization generated in 90^0 offset reflector antenna system with F/D=0.7. The secondary radiation patterns have been computed. Significant improvement in the cross polarization is achieved in 55-60GHz frequency band.

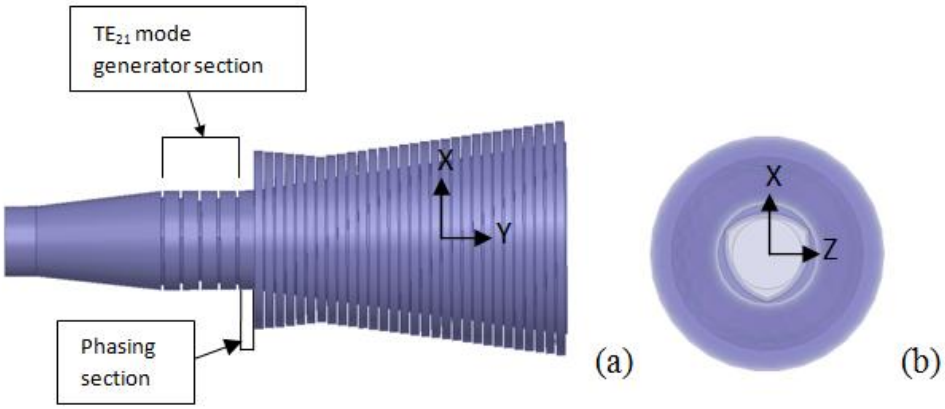

Fig.1.5 Simulation model of the proposed corrugated matched feed structure, (a) side view, (b) front view of the horn

Based on the above discussion, the thesis has been organized as per section 1.3.

1.3 Organization Of The Thesis

The research work carried out has been presented in total six chapters.

Chapter 1: The relevance of the present investigations and a brief literature survey on the low cross-polarized antenna system have been presented.

Chapter 2: In this chapter, the conjugate matched feed concept is explained. In a conjugate matched feed, the tangential electric fields in the aperture of a primary feed are to be matched with the focal region fields of an offset reflector to suppress the high cross-polarization. The higher order modes required to achieve the focal-field matching are summarized in this chapter. Also detail design and analysis of the conjugate matched feed using triple post discontinuity is presented in this chapter.

Chapter 3: This chapter deals with the scattering analysis of cascaded off-centered junctions in circular waveguide using Mode Matching Technique(MM). The study has been carried out to analyze the higher order modes characteristic for oversized circular waveguide for different offset distance for single junction. This chapter also deals with a novel structure forming with offset step junction in circular waveguide, for generating pure TE_{21} mode.

Chapter 4: A novel concept for designing a broadband conjugate matched feed horn to cancel the high unwanted cross-polar components generated because of offset reflector geometry having low F/D and high offset angle is presented in this chapter.

Chapter 5: This chapter presents the design of a broadband corrugated conjugate matched feed horn to cancel the high unwanted cross-polar components generated in offset reflector geometry having low F/D and high offset angle. The feed horn is specifically designed to mitigate the cross-pol. generated in 90^0 offset reflector antenna system with F/D=0.7.

Chapter 6: The conclusions drawn from the investigations and the scope for the future work have been discussed in this chapter.

CHAPTER 2

CONJUGATE MATCHED FEED FOR OFFSET REFLECTOR ANTENNA

This chapter discusses the basic concept of conjugate matched feed and study on the design of conjugate matched feed using triple post discontinuity. The fundamental principle of the matched feed depends on the field matching theory. According to this theory, the cross-polarization caused by the asymmetry of the offset parabolic reflector antenna can be controlled, if the tangential electric fields at the aperture of the primary feed are complex conjugate to the focal-region fields of the offset parabolic reflector antenna. In order to understand this matching process, it is necessary to first estimate the focal region fields of an offset reflector antenna. Once the focal-region fields are estimated, a multi-mode matched feed which is simpler in configuration may be designed to counter-balance the effect of the cross-polarization of the reflector antenna.

In this chapter, using the focal-region field analysis of an offset parabolic reflector antenna the cross-polarization variation as a function of F/D ratio and offset angle are presented. The higher order modes needed in circular as well as corrugated structure to provide the conjugate matching with the reflector focal-fields are also discussed. Following this, a study has been carried out on the design of conjugate matched feed horn using triple post discontinuity.

2.1 Focal Region Field Analysis

Bem [28] presented the detailed analysis to calculate the focal-region fields of an offset parabolic reflector antenna. Bem used the physical optics (PO) formulation to derive the closed form expressions of the transverse focal plane fields for a plane polarized incident plane wave. The focal field distribution of an offset parabolic reflector antenna is obtained by illuminating the reflector surface

by a linearly polarized plane wave as shown in Fig. 2.1. Figure 2.1 represents a schematic of the offset parabolic reflector antenna having projected diameter D, offset angle θ_o and focal length F. The aperture of the feed horn is placed at the focal plane of the reflector. The incident plane wave generates current on the reflector surface. Each surface element acts as an elementary dipole and produces an elementary field at a point near the focus [28]. Then the total electric field at a prescribed point can be found out by integration over the entire reflector surface.

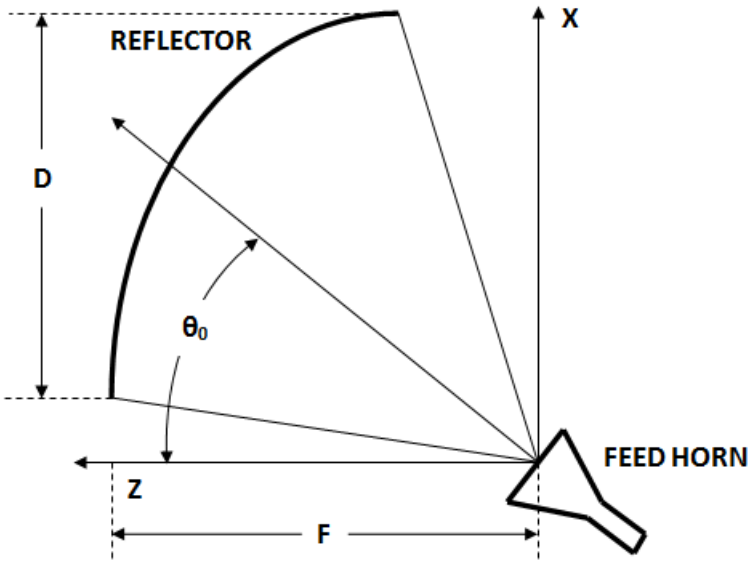

Fig. 2.1 Offset parabolic reflector antenna

Closed form expressions of the focal region fields are

$$E_x(u,\phi_o) = \frac{2J_1(u)}{u} + \frac{j\sin(\theta_o)}{2(F/D)}\frac{J_2(u)}{u}\cos(\phi_o) \qquad (2.1)$$

$$E_y(u,\phi_o) = -\frac{j\sin(\theta_o)}{2(F/D)}\frac{J_2(u)}{u}\sin(\phi_o) \qquad (2.2)$$

where, $u=(D/4F)(1+\cos(\theta_0))k.r.\sin(\theta)$, D, F and θ_o are the reflector projected diameter, focal length and offset angle respectively and r, θ are the co-ordinates of a point in the focal plane. k is the propagation constant in free space. Ey is the cross-polar component generated in the focal plane.

Investigation of equation 2.1 and 2.2 reveals that the cross-polar component E_x is an asymmetric function with a magnitude increasing with the offset angle θ_o and in phase quadrature with the principal axi-symmetric co-polar component. E_y presents the cross-polar component in the asymmetric plane. Figure 2.2 shows contour plot of the amplitude of the focal region field in the vicinity of the geometrical focus. Using the closed form expressions 2.1 and 2.2, cross-polar variation as a function of F/D and offset angle are presented in Fig. 2.3 and 2.4 respectively. It can be concluded from Fig.2.3 that the cross-polarization decreases with the increase in F/D ratio for fixed offset angle. Also Fig.2.4 describes the increase of cross-polarization with the increase in offset angle for fixed F/D.

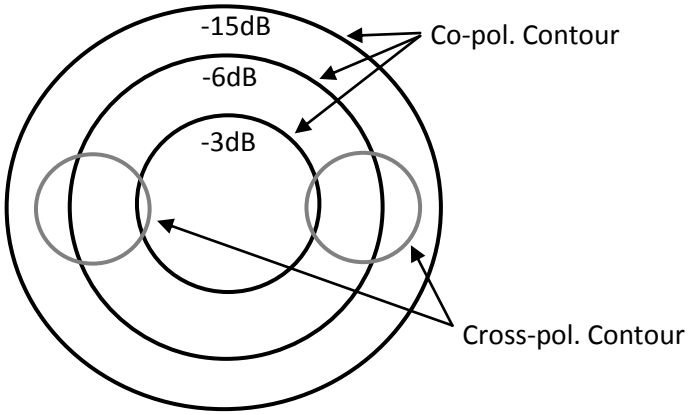

Fig.2.2 Contour plot of focal-field distribution of an offset reflector antenna

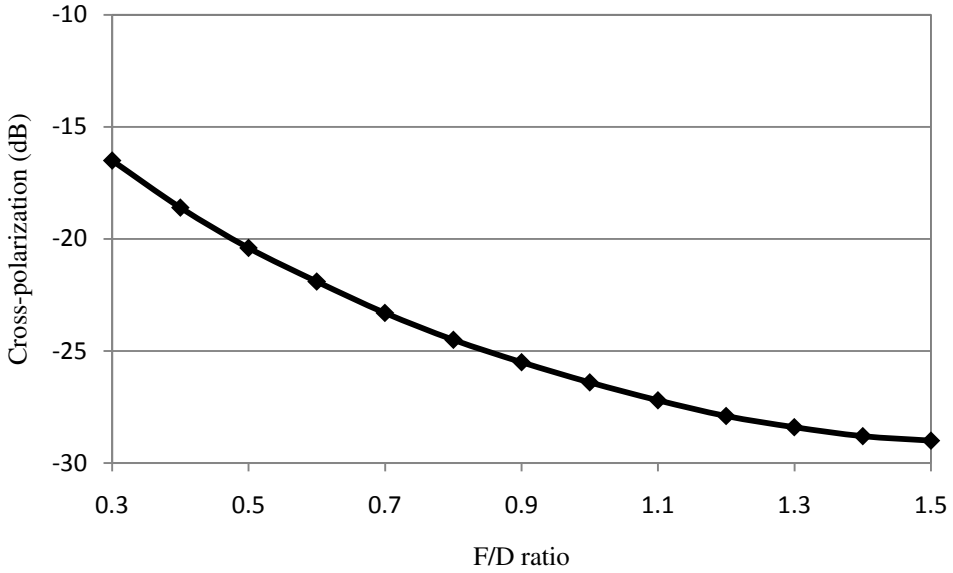

Fig. 2.3 Cross-polarization variation with the variation in F/D (θ_o=35^o)

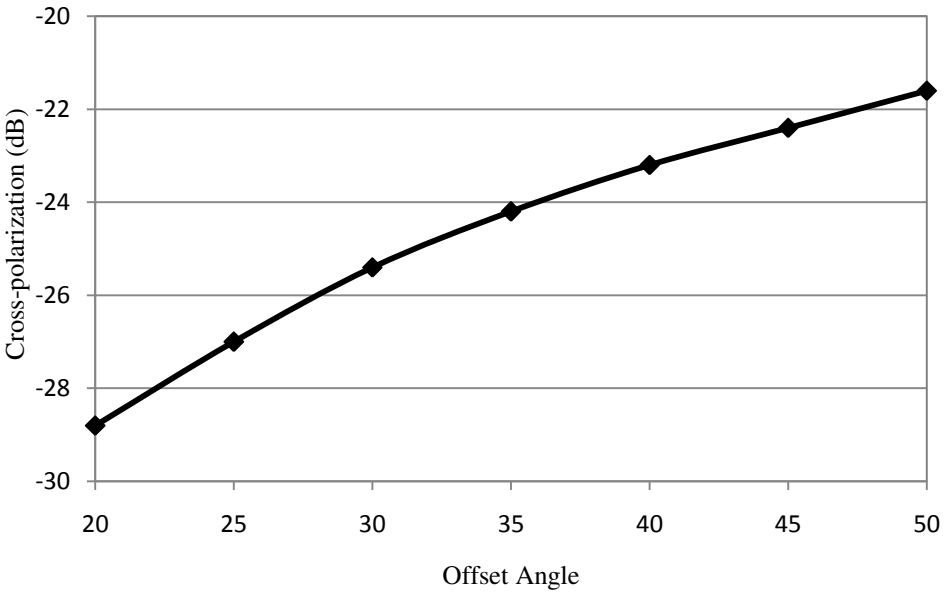

Fig. 2.4 Cross-polarization variation with the variation in offset angle(F/D=0.8)

2.2 Higher order modes for conjugate field matching

Rudge and Adatia [26] first proposed the design of matched feed for an offset parabolic reflector antenna using the concept of conjugate field. The high cross-polarization generated in the offset reflector antenna can be mitigated by matching the radiation field of the primary feed with those of the reflector. To satisfy this matching condition, the primary feed horn should support appropriate higher order mode in addition to the fundamental mode. The modal amplitudes and phases in the feed horn are to be adjusted such that, the aperture fields of the feed exhibit similar polarization characteristics as that of the focal plane fields of the offset reflector antenna. However, the cross-polar components of the feed should be in opposite phase with respect to the cross-polar components of the offset reflector. In other words, the primary feed should provide a conjugate match to the incoming fields. As a result of this anti-phase relationship between the cross-polar fields of primary feed and the offset reflector, the undesired cross-polarization, generated by the asymmetry of the reflector structure, are cancelled out.

For cylindrical circular waveguide the fundamental mode is TE_{11} mode. The higher order mode required in circular waveguide in addition to this TE_{11} mode is TE_{21} in proper amplitude and phase at the aperture of the guide to cancel the cross-polarization component generated in offset reflector antenna. The x and y-components of the electric fields of TE_{21} mode can be derived as follows.

In terms of normalized distance parameter u' and a polar angle ϕ_o, the circular waveguide's aperture fields for TE_{21} mode[19] can be written as (polarization in x-direction)

$$E_x^{TE_{21}}(u',\phi_o) = K'[J_1(u')\cos(\phi_o) + J_3(u')\cos(3\phi_o)] \quad (2.3)$$

$$E_y^{TE_{21}}(u',\phi_o) = -K'[J_1(u')\sin(\phi_o) - J_3(u')\sin(3\phi_o)] \quad (2.4)$$

Using the following recursion formula,

$$J_n(u) = \frac{2(n-1)}{u} J_{n-1}(u) - J_{n-2}(u)$$

and putting n=3, we have,

$$J_3(u) = \frac{4}{u} J_2(u) - J_1(u)$$

or $$J_3(u) + J_1(u) = \frac{4}{u} J_2(u) \quad (2.5)$$

Using the recursive relation in equation-(2.5) , E_x and E_y in the principle planes for TE_{21} mode can be written as

$$E_x^{TE_{21}}(u',\pi/2) = 0 \quad (2.6)$$

$$E_x^{TE_{21}}(u',0) = 4K' \frac{J_2(u')}{u'} \quad (2.7)$$

$$E_y^{TE_{21}}(u',0) = 0 \quad (2.8)$$

$$E_y^{TE_{21}}(u',\pi/2) = 4K' \frac{J_2(u')}{u'} \quad (2.9)$$

For TE_{11} mode, in the principle planes, E_x (co-pol.) and E_y (cross-pol.) can be written as

$$E_x^{TE_{11}}(u',0) = K \frac{J_1(u')}{u'} \quad (2.10)$$

$$E_y^{TE_{11}}(u', \pi/2) = 0 \tag{2.11}$$

The combined TE_{11} and TE_{21} modal pattern's co-polar and cross-polar components are

$$E_x^{TE_{11}+TE_{21}}(u',0) = K\frac{J_1(u')}{u'} + 4K'\frac{J_2(u')}{u'} \tag{2.12}$$

$$E_y^{TE_{11}+TE_{21}}(u', \pi/2) = 4K'\frac{J_2(u')}{u'} \tag{2.13}$$

The equations (2.12) and (2.13) are the co and cross polar components of the aperture fields of TE_{21} mode respectively. It is observed that the equation (2.13) is similar to the equation (2.2) which is cross-polar component of the focal region field. Thus mathematically it is also clear that the aperture field of TE_{21} mode can cancel the cross-polar component of the focal region field if the amplitude and phase of the TE_{21} mode is adjusted properly.

The modal power required for TE_{21} mode relative to TE_{11} mode for different F/D and offset angle can be calculated from equation (2.2).

2.3 Conjugate Matched Feed using Triple Post Discontinuity

A conjugate matched feed horn has been designed using symmetrical triple post discontinuity in circular waveguide. The HFSS simulation model of the horn is shown in Fig.2.5. A separate study has also been carried out for TE_{21} modal power and phase variation relative to TE_{11} mode at the aperture of the feed horn with posts height as a parameter. The variation of TE_{21} modal power w.r.t frequency with posts height as a parameter is shown in Fig.2.6 and Fig.2.7 shows the phase variation of TE_{21} mode relative to TE_{11} mode with different posts heights. It has been observed that TE_{21} modal power increases with the increase in posts heights and there is less variation in phase of TE_{21} mode relative to TE_{11} mode for posts height=3mm and 5mm.

The offset reflector antenna chosen for conjugate matched feed simulation are having parameters : reflector diameter=1.2m, F/D=0.8 and offset angle $\theta_0=35^0$ which is shown in Fig.2.1. The TE_{21} modal amplitude required in conjugate matched feed horn has been calculated using TICRA/GRASP software. The TE_{21} modal power required for maximum cancellation of cross-polarization in secondary pattern has been calculated to be -13.7dB and required relative phase for TE_{21} mode w.r.t TE_{11} mode is 90^0 at 10GHz. The conjugate matched feed horn has been optimized according to the above requirements. The input and aperture diameter of the horn are 22mm and 34mm respectively. The optimum height of the posts and length of the horn are 5.4mm and 57mm respectively. The simulated primary pattern of the horn is shown in Fig.2.8 at 10GHz. The simulated secondary pattern without and with posts discontinuities in the horn feed are shown in Fig.2.9 and 2.10 respectively. The cross-polar suppression bandwidth has been presented in Fig.2.11 for this designed matched feed. It is found that 15dB improvement in the cross-polarization have been observed for very narrow bandwidth i.e. for 1% bandwidth. But this improvement cannot be achieved for wide bandwidth. It is also observed that better than 10dB improvement in cross-polarization is achieved for only 2% bandwidth. 5dB improvement in cross-polarization can be achieved for 6% bandwidth.

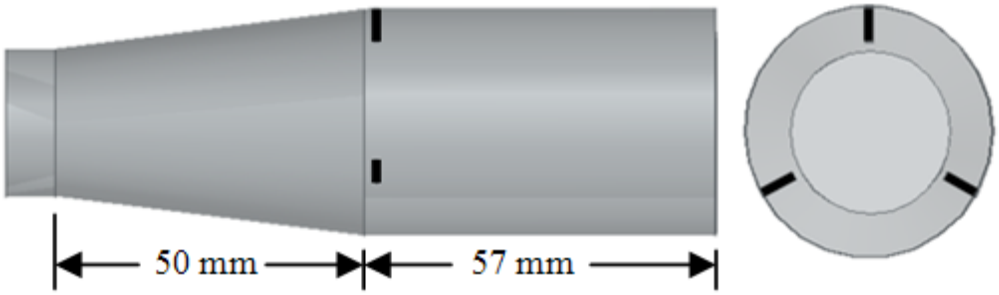

Fig.2.5 HFSS simulation model of conjugate matched feed (post height=5.4mm, post diameter=2mm)

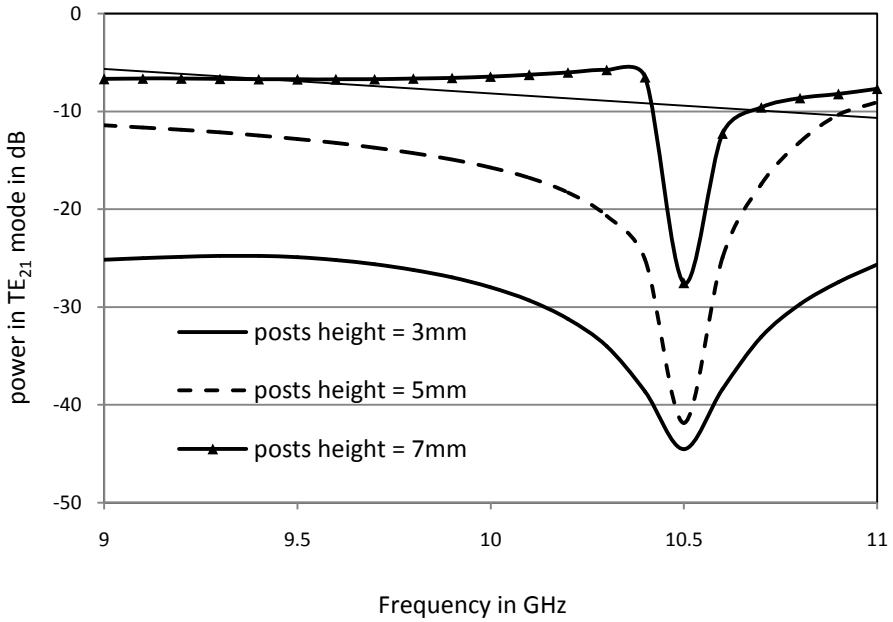

Fig.2.6 Simulated power coupling to TE_{21} mode

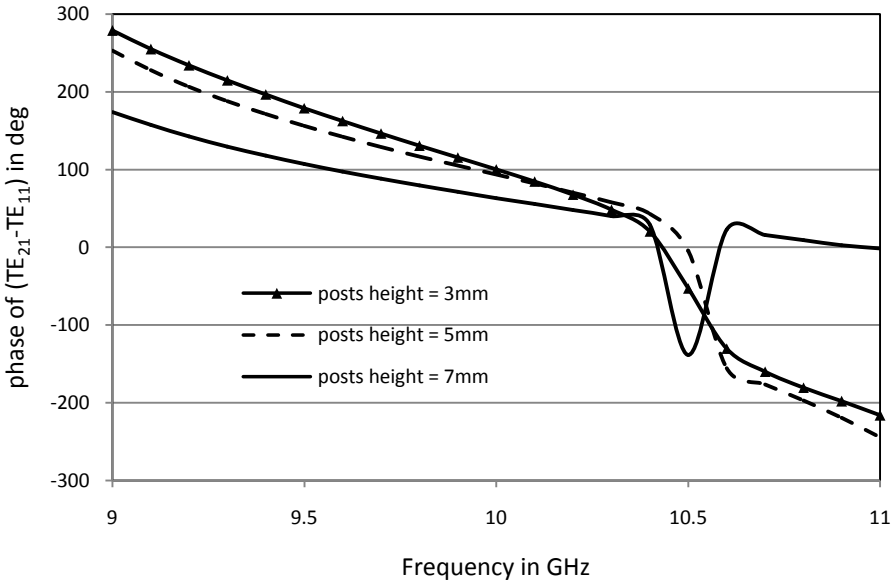

Fig.2.7 Simulated phase difference of TE_{21} and TE_{11} mode at aperture

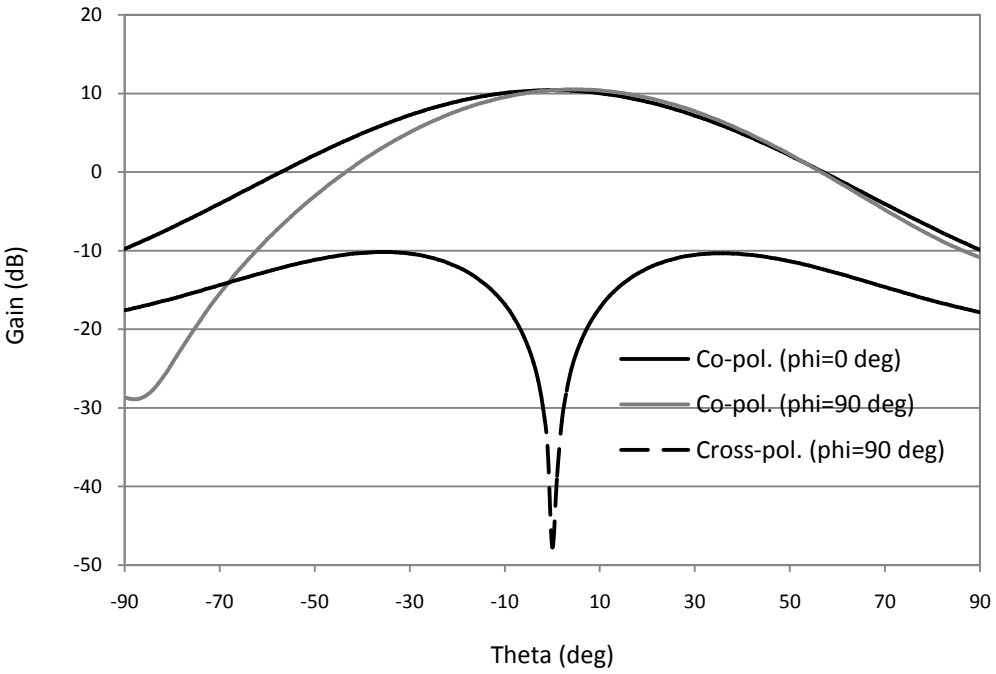

Fig.2.8 Simulated radiation pattern of the feed horn at 10GHz

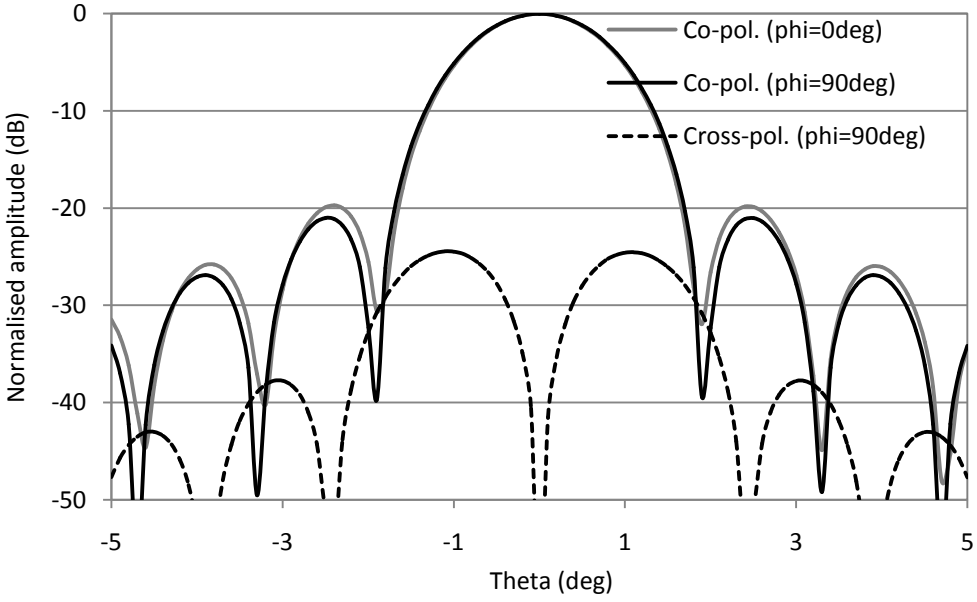

Fig.2.9 Simulated secondary pattern without posts discontinuities at 10GHz

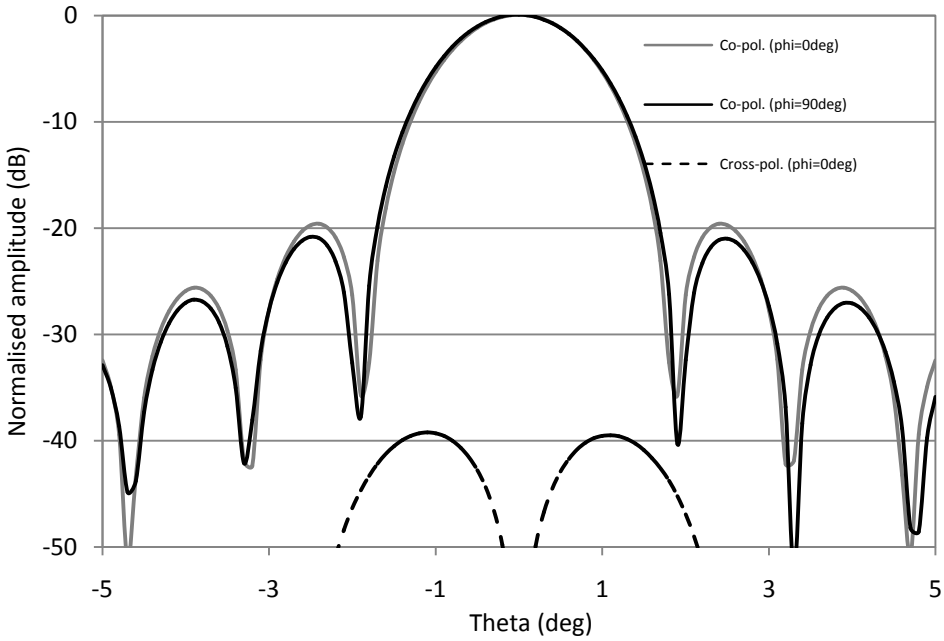

Fig.2.10 Simulated secondary pattern with posts discontinuities (MF) at 10GHz

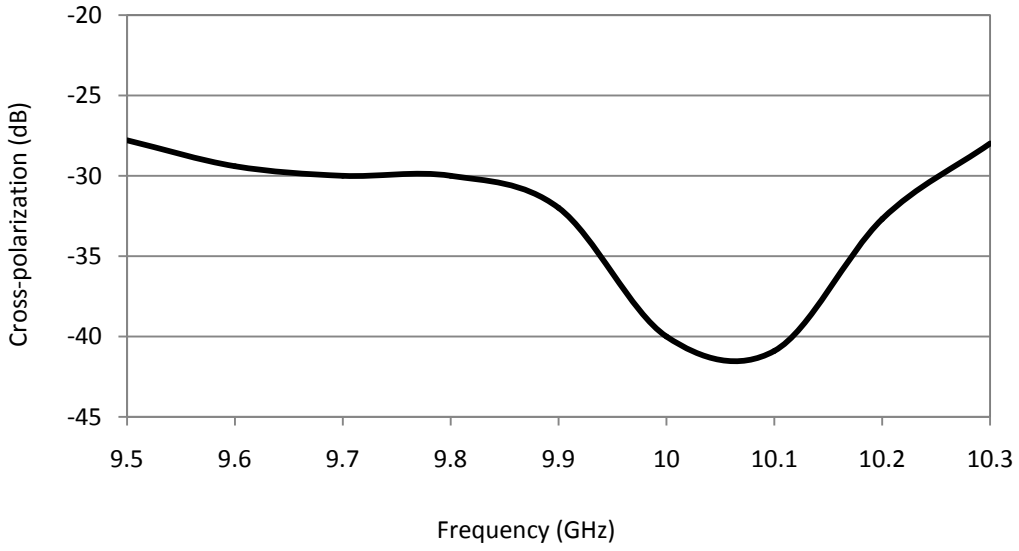

Fig.2.11 Cross-polar suppression bandwidth

The design has been extended for broader bandwidth using cascaded posts discontinuity along the axial direction of the horn as shown in Fig.2.12. The design has been carried out for offset parabolic reflector having D=1.2m, F/D=0.8 and offset angle $\theta_0=35^0$. The input and aperture diameter of the horn are 21mm and 32mm respectively. The diameter of the posts are 2mm. The height of the posts are 2.5mm, 3.2mm, 3.8mm, 3.2mm and 2.5mm. The gap between the posts is 5mm. The secondary cross-polarization has been calculated and the cross-polar suppression bandwidth is shown in Fig.2.13. It has been found that better than -30dB cross-polarization i.e. cross-polarization improvement of 5dB can be achieved for 13% bandwidth. But the cross-polarization improvement better than 10dB is achieved for only 3% bandwidth. Thus it is difficult with cascaded post discontinuity to realize a wide band conjugate matched feed for better than 10dB improvement in cross-polarization.

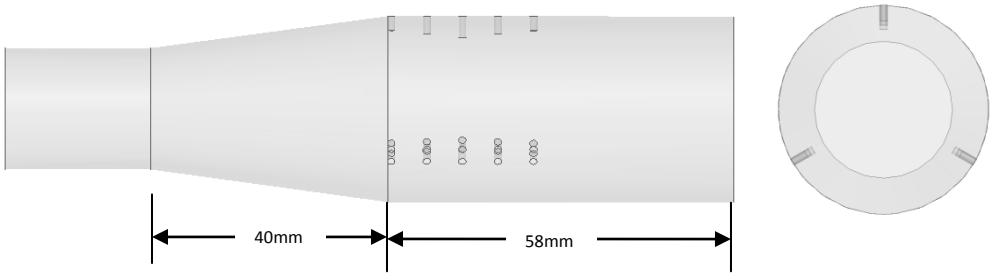

Fig. 2.12 HFSS model of Conjugate matched feed with multiple post along the axis

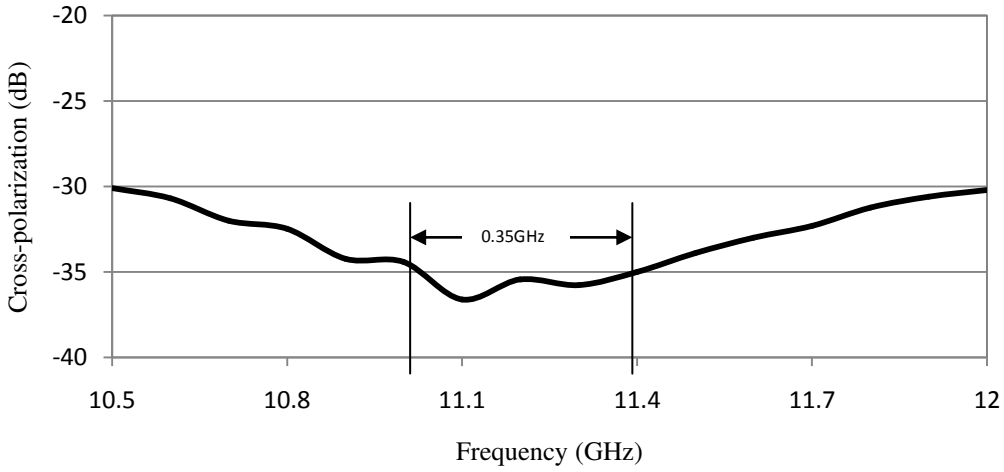

Fig. 2.13 Cross-polarization suppression bandwidth of the horn of Fig.2.12

2.4 Discussion

In the present chapter, the concept of matched feed for the offset parabolic reflector has been discussed. From the focal-region field analysis of the offset parabolic reflector antenna, it has been observed that, the offset reflector generates high cross-polarization because of the structural asymmetry. It has been also observed that the cross-polarization increases with the increase in offset angle and decrease in F/D ratio. This undesired high cross-polarization can be controlled by using a multi-mode matched feed. The higher order mode required for conjugate field matching has been discussed. The mathematical expression for TE_{21} mode at the aperture of the horn feed has also been discussed in this chapter. Also a detail analysis of conjugate matched feed using triple post discontinuity in circular waveguide has been presented in this chapter. For 10dB improvement in cross-polarization, the bandwidth of the matched feed with symmetric triple post discontinuity is 2%. It has also been found out that for cascaded triple post discontinuity in conjugate matched feed, 5dB improvement in cross-polarization is achieved for 13% bandwidth and cross-polarization improvement better than 10dB is achieved for only 3% bandwidth. Thus it is difficult with cascaded post discontinuity to realize a wide band conjugate matched feed for better than 10dB improvement in cross-polarization. In the following chapters, the investigation has been carried out for widening the cross-polar suppression bandwidth of the conjugate matched feed horn.

CHAPTER 3

ASYMMETRICAL STEP DISCONTINUITY IN CIRCULAR WAVEGUIDE AND GENERATION OF PURE TE_{21} MODE

In the present chapter, off-centered junction of two circular waveguide has been analyzed using Mode Matching technique. Detail derivations of the scattering matrix of the present problem have been presented. A convergence analysis of the problem has been carried out. The reflection coefficient for TE_{11} mode and coupling coefficient for TM_{01}, TE_{21}, TE_{01} and TM_{11} modes have been calculated for a particular offset distance and direction. All the results have been compared with Ansys HFSS and very good matching between them has been observed. This chapter also presents a concept of a novel structure using this offset step discontinuity to get pure TE_{21} mode along with TE_{11} mode eliminating TM_{01} and TE_{21}* modes.

3.1 Analysis of offset junction

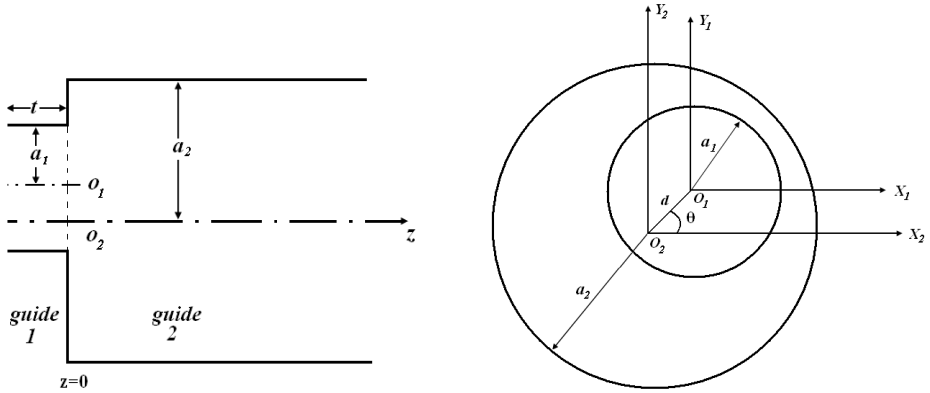

Fig.3.1 Schematic drawing of the off-centre step junction in circular waveguide

The geometry of the off-centre circular waveguide junction is shown in Fig.3.1. The conservation of complex power technique (CCPT), which has been used to obtain theoretically exact solutions with numerically convergent results to the problem of scattering at certain waveguide junctions [40], [41], and [42], and Graf's addition theorem for Bessel functions [44] are employed to obtain an analytical solution for the scattering matrix of a junction between two circular waveguides with their axes offset. In Fig.3.1 offset distance is denoted as d and θ is the direction of the offset.

The E-field mode matching matrix whose (nm, kp) th element is given by [40]

$$M_{nm,kp} = \int_{S_1} \left(\vec{e}_{2,nm} . \vec{e}_{1,kp} \right) ds \tag{3.1}$$

where, $\vec{e}_{i,nm} = \begin{cases} \hat{z} \text{ x } \nabla_t \psi^h_{i,nm} & \text{for TE modes} \\ \nabla_t \psi^e_{i,nm} & \text{for TM modes} \end{cases}$

which satisfy the boundary conditions $\frac{\partial \psi^h}{\partial n} = 0$ and $\psi^e = 0$ on 'C', where 'C' is the contour of the junction, and 'n' is the unit normal to the contour.

where, $\psi^h_{i,nm} = N^h_{nm} J_n \left(\frac{\rho_i x'_{nm}}{a_i} \right) \begin{pmatrix} \sin(n\phi_i) \\ \cos(n\phi_i) \end{pmatrix}$ (3.2)

$$\psi^e_{i,nm} = N^e_{nm} J_n \left(\frac{\rho_i x'_{nm}}{a_i} \right) \begin{pmatrix} \cos(n\phi_i) \\ \sin(n\phi_i) \end{pmatrix} \tag{3.3}$$

with, $N^h_{nm} = \sqrt{\frac{\epsilon_n}{\pi}} \frac{1}{\sqrt{(x'_{nm})^2 - n^2} J_n(x'_{nm})}$

$$N^e_{nm} = \sqrt{\frac{\epsilon_n}{\pi}} \frac{1}{x_{nm} J_{n+1}(x_{nm})}$$

as normalization constant, $\in_n = \begin{cases} 1 & \text{for } n = 0 \\ 2 & \text{for } n > 0 \end{cases}$ and x'_{nm} and x_{nm} are the m[th] zeros of $J'_n(x)$ and $J_n(x)$ respectively.

Since the integration in (1) is over the cross section of the small waveguide, we must employ a coordinate transformation between (ρ_1, ϕ_1) and (ρ_2, ϕ_2) to express $\vec{e}_{2,nm}$ in terms of (ρ_1, ϕ_1). In order to do so, Graf's addition theorem for Bessel functions [40], [44] is used

$$J_n(\lambda\rho_2)\begin{pmatrix}\cos(n\phi_i)\\ \sin(n\phi_i)\end{pmatrix} = \sum_{q=-\infty}^{\infty}(-1)^{q+n}J_q(\lambda\rho_1).J_{q-n}(\lambda d)\begin{pmatrix}\cos\left[q\phi_1-(q-n)\theta\right]\\ \sin\left[q\phi_1-(q-n)\theta\right]\end{pmatrix} \tag{3.4}$$

where, λ is an arbitrary constant.

The overall E-field mode-matching matrix *M* has the following form

$$M = \begin{bmatrix}\left[M^{hh}_{nm,kp}\right] & \left[M^{he}_{nm,kp}\right]\\ \left[M^{eh}_{nm,kp}\right] & \left[M^{ee}_{nm,kp}\right]\end{bmatrix} \tag{3.5}$$

From [41] the components for the M matrix can be written as

$$<\vec{e}^{\,h}_{nm,}\vec{e}^{\,h}_{kp}>_S = \left(\kappa^h_{kp}\right)^2\iint_S \psi^h_{2,nm}\psi^{h*}_{1,kp}ds \tag{3.6}$$

$$<\vec{e}^{\,e}_{nm,}\vec{e}^{\,e}_{kp}>_S = \left(\kappa^e_{nm}\right)^2\iint_S \psi^e_{2,nm}\psi^{e*}_{1,kp}ds \tag{3.7}$$

$$<\vec{e}^{\,h}_{nm,}\vec{e}^{\,e}_{kp}>_S = \iint_S \nabla_t\psi^e_{1,kp}\ \mathrm{x}\ \nabla_t\psi^{h*}_{2,nm}d\vec{s} = 0 \tag{3.8}$$

$$<\vec{e}^{\,e}_{nm},\vec{e}^{\,h}_{kp}>_S = \iint_S \nabla_t\psi^{e*}_{2,nm}\ \mathrm{x}\ \nabla_t\psi^h_{1,kp}d\vec{s} \tag{3.9}$$

After some rigorous derivation, the components of the coupling matrix can be written in closed form as

$$M^{hh}_{nm,kp} = <e^h_{2,nm}.e^h_{1,kp}> = (-1)^k\left(\frac{\pi}{a_1a_2}\right)N^h_{nm}N^h_{kp}\left(x_{kp}'\right)^2 x_{nm}'\frac{J_k\left(x_{kp}'\right)J_k'\left(\frac{a_1x_{nm}'}{a_2}\right)}{\left(\frac{x_{kp}'}{a_1}\right)^2-\left(\frac{x_{nm}'}{a_2}\right)^2}Q_1 \tag{3.10}$$

$$M_{nm,kp}^{eh} = (-1)^k N_{nm}^e N_{kp}^h k J_k\left(x_{kp}{}'\right) J_k{}'\left(\frac{a_1 x_{nm}{}'}{a_2}\right) Q_2 \tag{3.11}$$

$$M_{nm,kp}^{ee} =< e_{2,nm}^e . e_{1,kp}^e >= (-1)^{k+1} \pi N_{nm}^e N_{kp}^e x_{kp} \left(\frac{x_{nm}}{a_2}\right)^2 \frac{J_k{}'\left(x_{kp}\right) J_k\left(\frac{a_1 x_{nm}}{a_2}\right)}{\left(\frac{x_{kp}}{a_1}\right)^2 - \left(\frac{x_{nm}}{a_2}\right)^2} Q_3 \tag{3.12}$$

where,

$$Q_1 = J_{k+n}\left(\frac{x_{nm}{}'d}{a_2}\right) C_1(k+n) + (-1)^n J_{k-n}\left(\frac{x_{nm}{}'d}{a_2}\right) C_2(k-n)$$

$$Q_2 = -J_{k-n}\left(\frac{x_{nm}d}{a_2}\right) C_2(k+n) + (-1)^n J_{k-n}\left(\frac{x_{nm}d}{a_2}\right) C_1(k-n)$$

$$Q_3 = J_{k+n}\left(\frac{x_{nm}d}{a_2}\right) C_3(k+n) + (-1)^n J_{k-n}\left(\frac{x_{nm}d}{a_2}\right) C_4(k-n)$$

$$C_1(k+n) = \begin{bmatrix} -(\varepsilon_k - 1)\cos(k+n)\theta & \sin(k+n)\theta \\ (\varepsilon_k - 1)\sin(k+n)\theta & \cos(k+n)\theta \end{bmatrix}$$

$$C_2(k-n) = \begin{bmatrix} (\varepsilon_k - 1)\cos(k-n)\theta & -\sin(k-n)\theta \\ (\varepsilon_k - 1)\sin(k-n)\theta & \cos(k-n)\theta \end{bmatrix}$$

$$C_3(k+n) = \begin{bmatrix} \cos(k+n)\theta & (\varepsilon_k - 1)\sin(k+n)\theta \\ \sin(k+n)\theta & -(\varepsilon_k - 1)\cos(k+n)\theta \end{bmatrix}$$

$$C_4(k-n) = \begin{bmatrix} \cos(k-n)\theta & (\varepsilon_k - 1)\sin(k-n)\theta \\ -\sin(k-n)\theta & (\varepsilon_k - 1)\cos(k-n)\theta \end{bmatrix}$$

$$C_1(k-n) = \begin{bmatrix} -\cos(k-n)\theta & \sin(k-n)\theta \\ \sin(k-n)\theta & \cos(k-n)\theta \end{bmatrix}$$

$$C_2(k+n) = \begin{bmatrix} \cos(k+n)\theta & -\sin(k+n)\theta \\ \sin(k+n)\theta & \cos(k+n)\theta \end{bmatrix}$$

where, $\varepsilon_k = 1$ for k=0 and $\varepsilon_k = 2$ for k>0

Now the scattering matrix of the junction is given as

$$[S]=\begin{bmatrix} S_{22} & S_{21} \\ S_{12} & S_{11} \end{bmatrix} \tag{3.13}$$

where,

$$S_{11}=\left(Y_1+M^T Y_2 M\right)^{-1}\left(Y_1-M^T Y_2 M\right) \tag{3.14}$$

$$S_{12}=2\left(Y_1+M^T Y_2 M\right)^{-1} M^T Y_2 \tag{3.15}$$

$$S_{21}=2\left(Y_2+Y_2 M Y_1^{-1} M^T Y_2\right)^{-1} M^T Y_2 \tag{3.16}$$

$$S_{22}=-\left(Y_2+Y_2 M Y_1^{-1} M^T Y_2\right)^{-1}\left(Y_2-Y_2 M Y_1^{-1} M^T Y_2\right) \tag{3.17}$$

If there are two scattering matrices $[S^a]$ and $[S^b]$corresponding two sections of a waveguide, then the cascaded scattering matrix $[S^c]$is given by

$$[S^c{}_{11}]=[S^a{}_{12}][[I]-[S^b{}_{11}][S^a{}_{22}]]^{-1}[S^b{}_{11}][S^a{}_{21}]+[S^a{}_{11}] \tag{3.18}$$

$$[S^c{}_{21}]=[S^b{}_{21}][[I]-[S^a{}_{22}][S^b{}_{11}]]^{-1}[S^a{}_{21}] \tag{3.19}$$

$$[S^c{}_{12}]=[S^a{}_{12}][[I]-[S^b{}_{11}][S^a{}_{22}]]^{-1}[S^b{}_{12}] \tag{3.20}$$

$$[S^c{}_{22}]=[S^b{}_{21}][[I]-[S^a{}_{22}][S^b{}_{11}]]^{-1}[S^a{}_{22}][S^b{}_{12}]+[S^b{}_{22}] \tag{3.21}$$

3.2 Results and Discussion

Using the formulation as described in section-3.1, a computer program has been developed in MATLAB. This code can analyze multiple step junctions as well as corrugated structures in circular waveguide. In the present chapter, two types of structures have been analyzed. First the single step junction as shown in Fig.3.1 having 22mm smaller waveguide diameter and 36mm larger waveguide diameter has been considered. The simulation has been carried out in 9GHz-15GHz frequency range. The present analysis has been carried out for incident TE_{11} mode in guide-I having polarization in the x-coordinate direction as shown in Fig.3.1. Basically in the circular waveguide the type of modes will be TE_{mn}, TE_{mn}*, TM_{mn} and TM_{mn}* modes where index terms m and n are azimuthal and radial variations of fields respectively in circular waveguide. Let maximum allowable limit for both m and n be N. Then the total number of modes in the waveguide will be 4*N*N. For our convergence analysis, variation of N= 4 to 16 has been considered. The convergence curves of reflection coefficient of TE_{11} mode and coupling coefficient of TM_{01} mode have been presented in Fig.3.2 and Fig.3.3 respectively for offset d=2mm and $\theta=0^0$. It is clear from the convergence analysis that around 484 modes in guide-II will be sufficient for the convergence of the present method. The number of modes in guide-I has been calculated from the following relation.

Number of modes in guide-I= (a_1/a_2)*Number of modes in guide-II (3.22)

Reflection coefficient characteristics with frequency for TE_{11} mode with $\theta=0^0$ and $\theta=90^0$ are shown in Figures 3.4 and 3.5 respectively. Figure 3.6 presents the power coupling to first higher order mode TM_{01} with $\theta=0^0$. Power coupling to next modes TE_{21} and TE_{01} are shown in Fig.3.7 and 3.8 respectively. TE_{21} mode will be generated for $\theta=0^0$ only. For $\theta=0^0$, there will be no TE_{01} modes generated in guide-II. Power coupled to TM_{11} mode is shown in Fig.3.9. All the results obtained using the present analysis method have been compared with HFSS and a good agreement is observed. For the present offset junction, the simulated amplitude of all the generated higher order modes at 12GHz is presented in Table 3.1 for $\theta=0^0$. It has been observed from Table 3.1 that significant amount of power present in TM_{01} and TM_{11} modes along with TE_{21} mode.

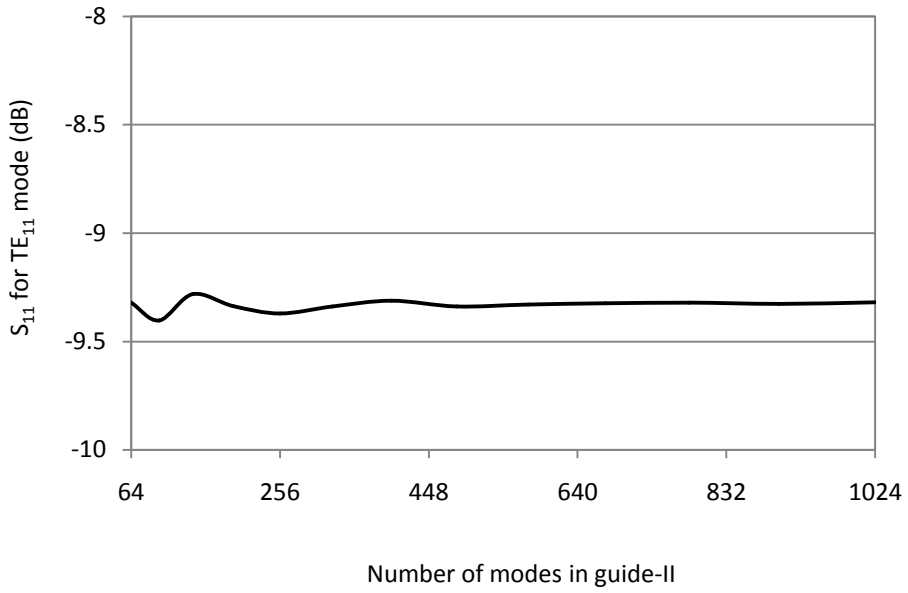

Fig.3.2 Convergence curve for reflection coefficient for TE_{11} mode

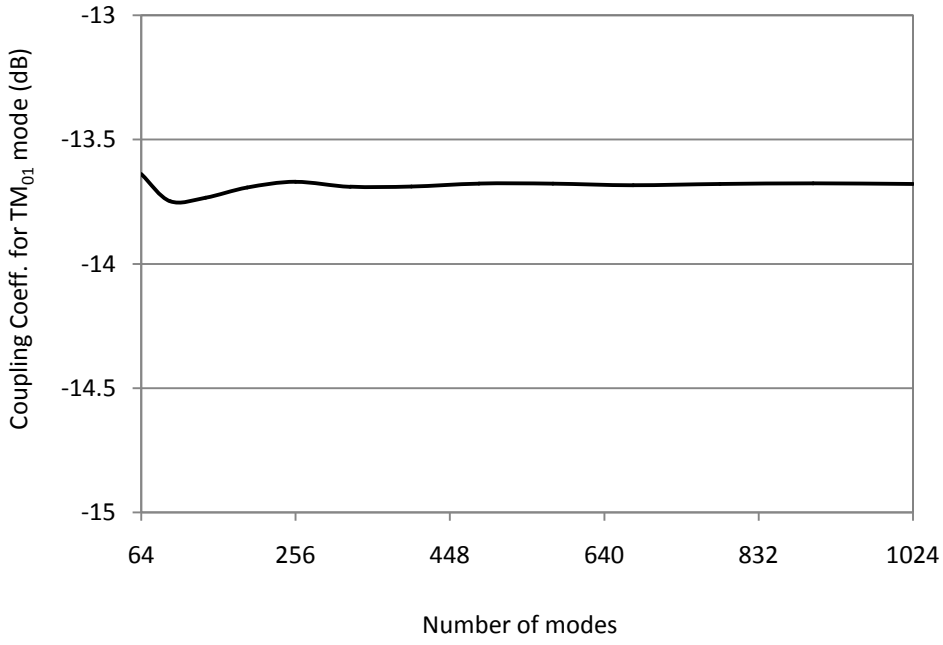

Fig.3.3 Convergence curve for coupling coefficient for TM_{01} mode

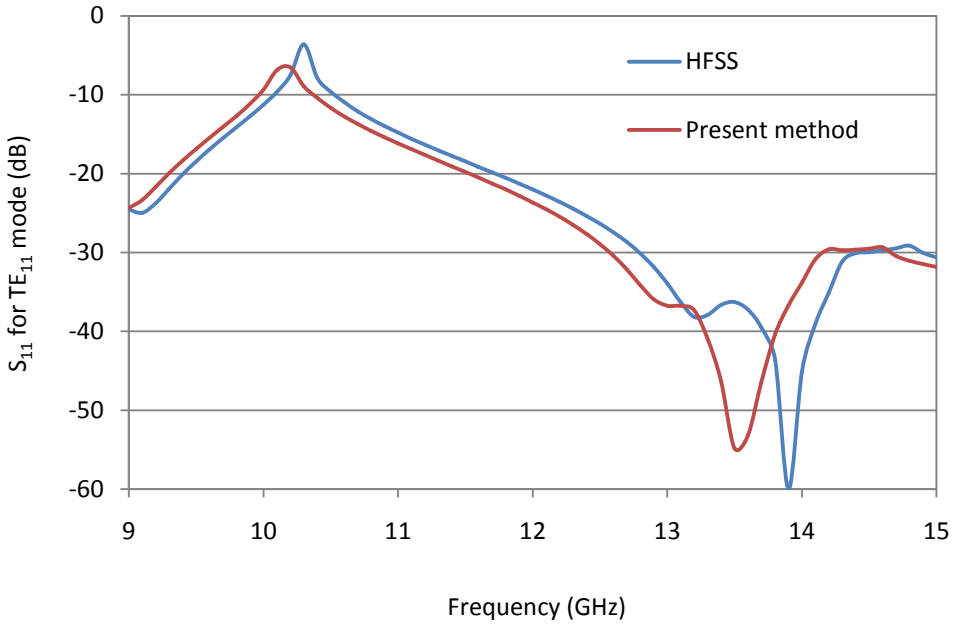

Fig.3.4 Reflection coefficient for TE_{11} mode with $\theta=0^0$ and d=2mm

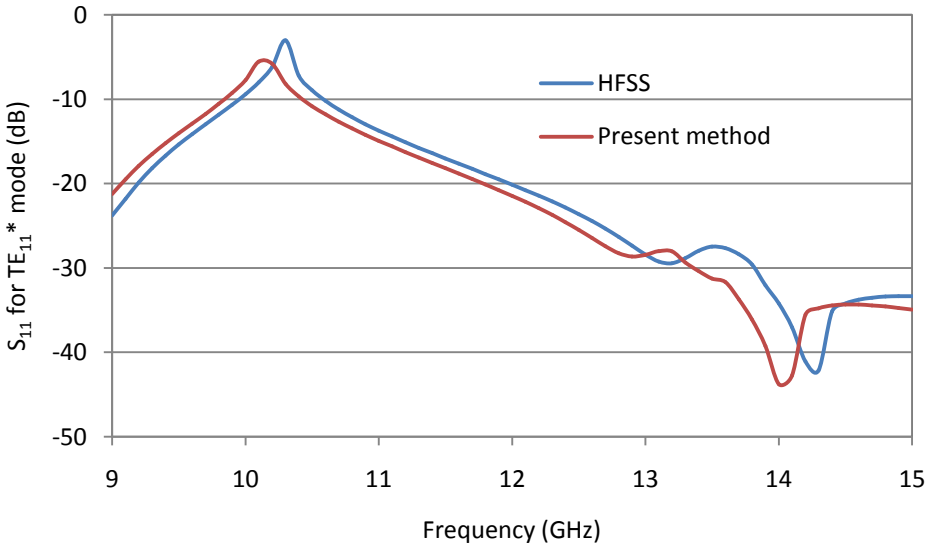

Fig.3.5 Reflection coefficient for TE_{11} mode with $\theta=90^0$ and d=2mm

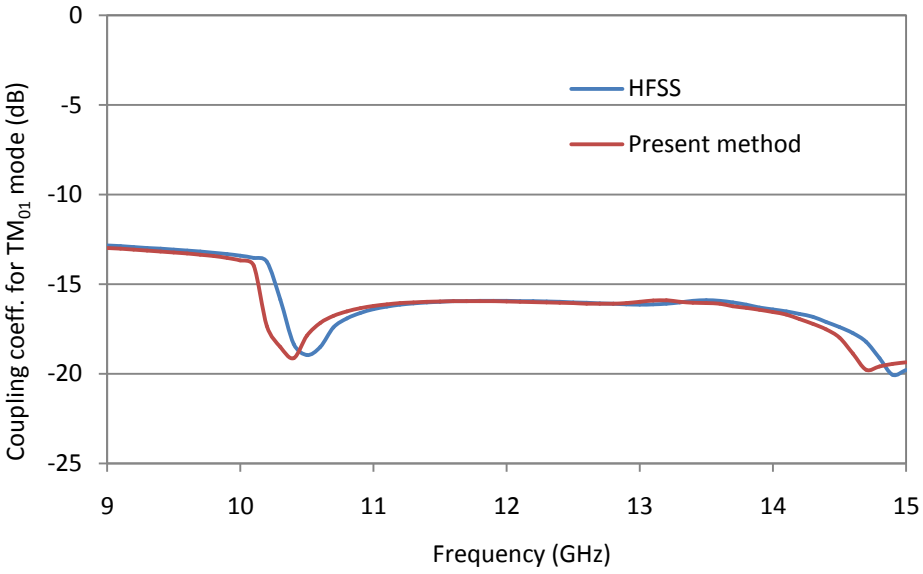

Fig.3.6 Coupling coefficient for TM_{01} mode with $\theta=0^0$ and d=2mm

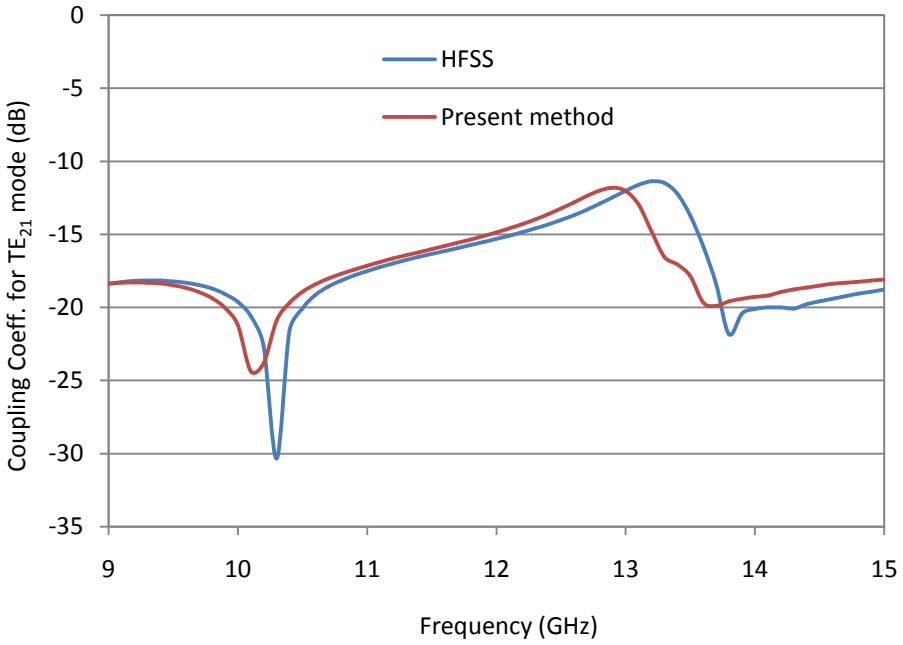

Fig.3.7 Coupling coefficient for TE_{21} mode with $\theta=0^0$ and d=2mm

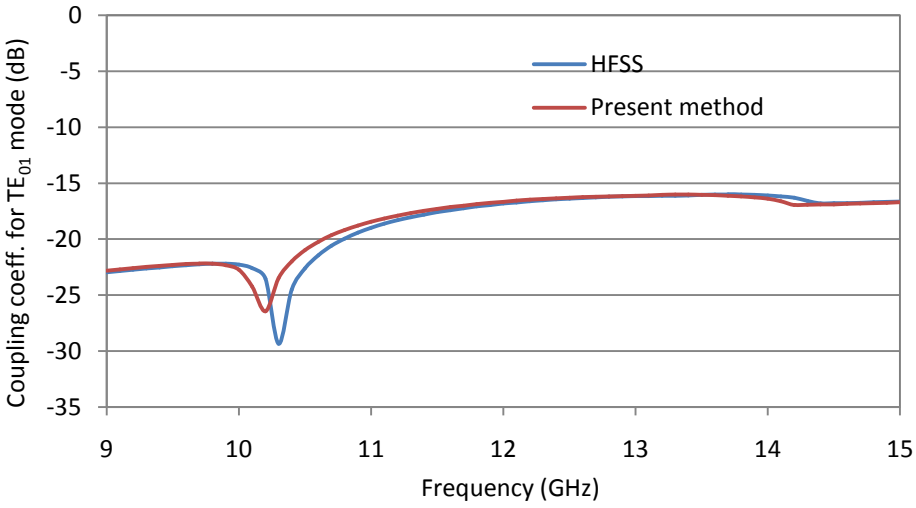

Fig.3.8 Coupling coefficient for TE_{01} mode with $\theta=90^0$ and d=2mm

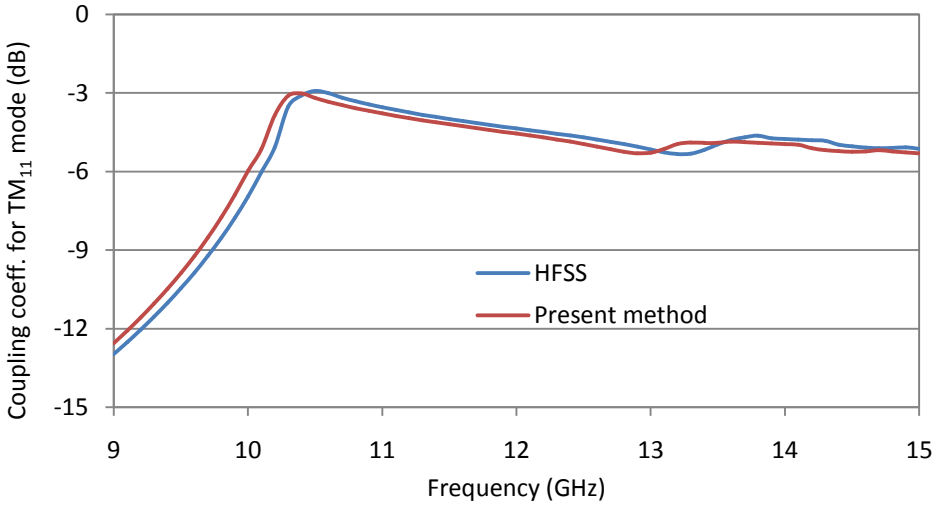

Fig.3.9 Coupling coefficient for TM_{11} mode with $\theta=0^0$ and d=2mm

Table 3.1 Modal amplitude of higher order modes at 12GHz (d=2mm)

Modes	TM_{01}	TE_{21}	TM_{11}
Amplitude	0.16	0.17	0.6

3.3 Structure for Generation of Pure TE_{21} Mode

The results shown in section 3.2 reveals that single offset step discontinuity in circular waveguide generates higher order modes like TM_{01}, TE_{21}, TM_{11} etc. for incident TE_{11} mode. So if the cutoff of the waveguide is chosen in such a way that only TM_{01} and TE_{21} modes propagate then it is possible to produce TM_{01} and TE_{21} modes at the junction of the off-centered circular waveguide as shown in Fig.3.10. Now if three such offset-centered junctions are cascaded very close to each other but the offset directions are 120^0 with each other, then TM_{01} mode will be minimized.

In the present design three such off-centered junctions placed in the same plane to make TM_{01} modal power zero as shown in Fig.3.11. In this figure it is shown that the second and third offset waveguides are cancelling the generated TM_{01} modal E fields to wipe out TM_{01} mode. Also it is observed from Fig.3.11 that TE_{21} modal fields are not cancelled by these two offset discontinuities. The amplitude of TM_{01} and TE_{21} modes are presented in Table 3.2 for smaller waveguide diameter 22mm, larger waveguide diameter 31mm and offset d=2mm.

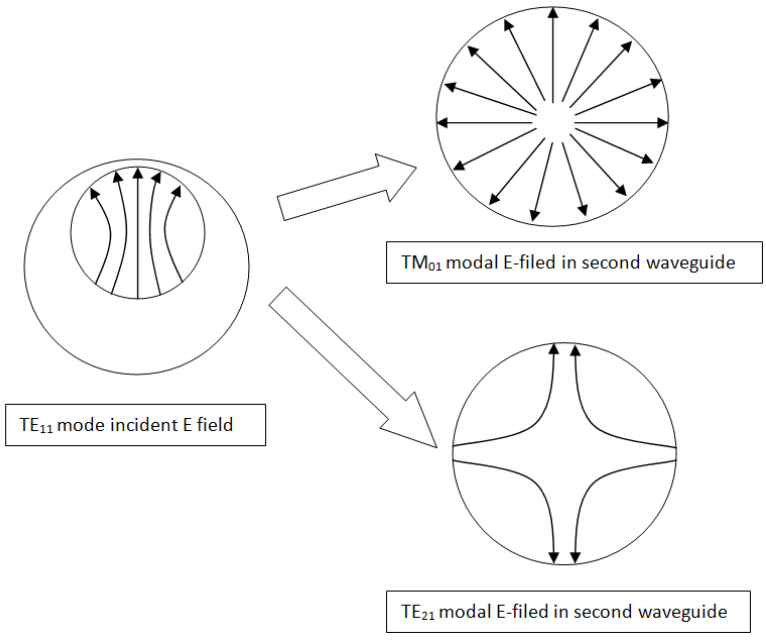

Fig.3.10 Schematic showing generation of TM_{01} and TE_{21} modes from TE_{11} mode at the offset junction (Transverse plane)

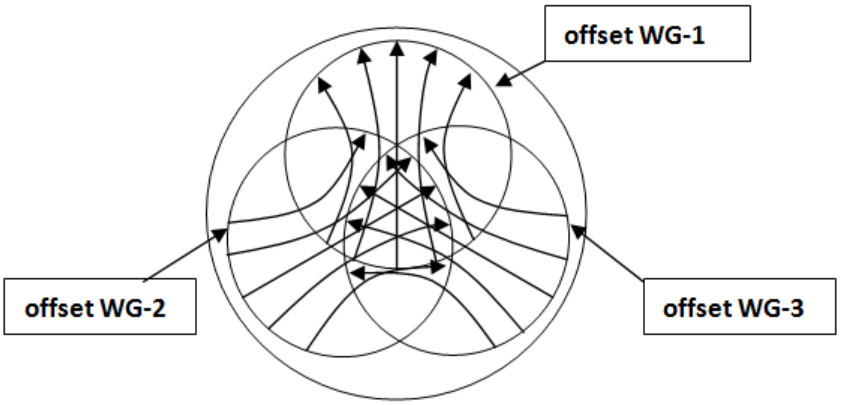

Fig.3.11 Schematic showing the fields configuration of three offset junctions co-existing at the same transverse plane 120^{o} to each other

Table 3.2 Modal amplitude of higher order modes at 12GHz for the structure of Fig.3.11

Modes	TM_{01}	TE_{21}
Amplitude	0	0.18

3.4 Conclusion

A mode matching based code has been developed to analyze off-centric junctions in circular waveguides. Convergence of the present analysis has been established in terms of number of waveguide modes. Reflection coefficient for TE_{11} mode and coupling coefficients for higher-order modes have been calculated for a single off-centric junction using mode matching technique and the calculated results have been compared with the FEM based full-wave solver HFSS. A concept of a novel structure for generating pure TE_{21} mode along with TE_{11} mode also has been discussed. This novel waveguide discontinuity which is forming an iris like structure in circular waveguide has been used to design conjugate matched feed in circular waveguide. The broad banding performance of the conjugate matched feed is obtained by cascading these irises. These have been presented in chapter 4.

CHAPTER 4

BROADBAND CONJUGATE MATCHED FEED HORN

In the present chapter, a novel type of symmetrical cascaded waveguide discontinuities has been conceptualized to achieve wide cross-polar bandwidth. One section of the waveguide discontinuity has been created using intersection of three off-centered junctions of circular waveguide placed symmetrically with angular spacing of 120^0. One such discontinuity which is like an iris in the waveguide has been analyzed for generating TE_{21} mode. It has been found that required amplitude and phase flatness of TE_{21} mode relative to TE_{11} mode over the designed frequency band, which is required for broadband performance of the matched feed, were not achieved. In order to enhance the cross-polar bandwidth, multiple sections with the similar iris structure have been placed in the axial direction inside an oversized circular waveguide supporting TE_{11} as well as TE_{21} modes. The required amplitude and phase flatness of TE_{21} mode relative to TE_{11} mode are achieved with these cascaded iris sections. The axial profile of the irises has been optimized to achieve good return loss performance. To study the broadband performance of the conjugate matched feed horn using cascaded discontinuity, three, five and seven irises have been considered and a comparative studies have been carried out.

The amplitude and phase required for TE_{21} mode to cancel cross-polar component has been calculated from the focal region field analysis [28] of the offset reflector antenna. The horn has been optimized to achieve required amplitude and phase of TE_{21} mode relative to TE_{11} mode.

4.1 Design of Broadband Conjugate Matched Feed

It is known that the field behaviour of TE_{21} mode in circular horn is close to equation-(2.2) as given in [19]. Now to cancel the cross-polar component in focal plane, feed horn has to generate TE_{21} mode along with TE_{11} mode in proper amplitude and phase. The required amplitude of TE_{21} mode is calculated with known parameters D, F ,θ and the relative phase between TE_{11} and TE_{21} modes has to be 90^0 as it is seen from equation-(2.2).

The simulation model of the proposed structure of the conjugate matched feed horn using Ansys HFSS-15 is shown in Fig.4.1-4.3. The matched feed with three, five and seven irises are shown in Fig. 4.1, 4.2 and 4.3 respectively. In the proposed structures, multiple irises have been inserted in equal interval along the Z-direction. The cross-section of the iris is shown in Fig.4.1(b). The cross-section has been realized using three offset circular waveguide junctions as shown in Fig.4.4. Circles are shown using dashed lines and they are showing how the smallest cross-section among the multiple irises is realized. The concept behind choosing the particular opening of the iris is that asymmetrical offset junction discontinuity between two circular waveguide produces TM_{01},TE_{21} and TE_{21}* modes. For conjugate matched feed design only TE_{21} mode is required along with dominant TE_{11} mode. So to cancel generated TM_{01} and TE_{21}* modes, three such type of discontinuities have been placed symmetrically in same plane and intersection of the three has been chosen as the iris opening as shown in Fig.4.1. The relative phase variations between TE_{21} and TE_{11} modes have been controlled and optimized by the proposed cascaded geometry. The 90^0 phase difference requirement has been achieved through straight section L2 of the horn after discontinuities shown in Fig.4.1. Main parameters which are controlling the amplitude and relative phase of TE_{21} mode w.r.t. TE_{11} mode at the aperture of the horn are the radius (R), offset distance(d_o) of the dashed circle shown in Fig.4.4 and the gap between the irises (g) which is shown in Fig.4.1(a). For three dashed circles in same transverse plane as shown in Fig.4.4, R and d_o are equal. The flatness of relative amplitude and phase of TE_{21} mode w.r.t. TE_{11} mode can be

controlled by the parameter g, which is essential for broadband operation of this feed horn.

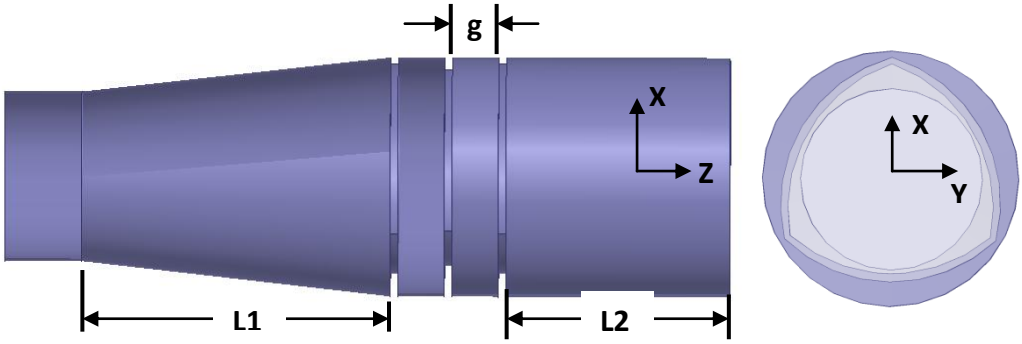

(a) (b)

Fig.4.1 Simulation model of the proposed structure having three irises, (a) side view, (b) front view of the horn

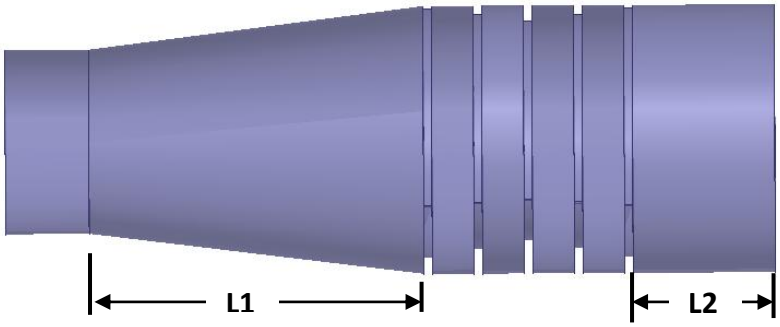

Fig.4.2 Simulation model of the proposed structure having five irises

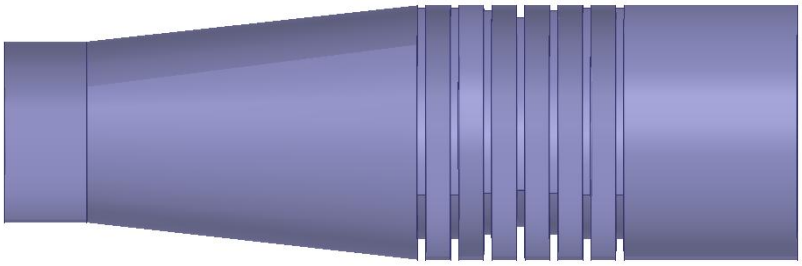

Fig.4.3 Simulation model of the proposed structure having seven irises

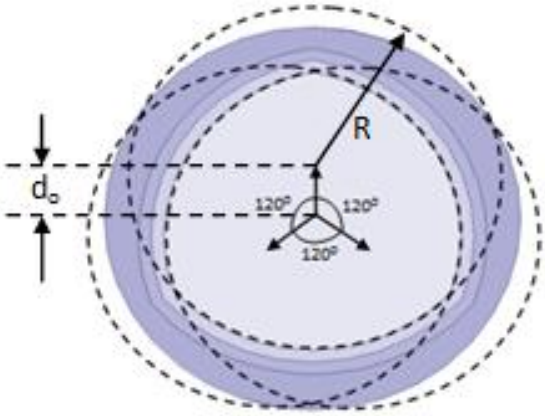

Fig.4.4 Modeling of opening of the irises (arrows indicate the offset direction of circles making 120^0 angle with each other)

The designs have been carried out for three, five and seven irises in the conjugate matched feed horn. The details of the same has been discussed in section 4.1.1.

4.1.1 Studies of Conjugate Matched Feed using three, five and seven irises

All the designs have been carried out for offset reflector having F/D=0.5, offset angle $\theta_o=53^o$ as shown in Fig.2.1. The amplitude required in TE_{21} mode relative to TE_{11} has been calculated using the equation-(4.2). For the above said reflector geometry, to cancel cross-polarization component, the amplitude required in TE_{21} mode relative to TE_{11} mode is -8dB. For conjugate matching, the phase of the TE_{21} mode relative to TE_{11} mode should be 90^o.

For the single iris discontinuity, the relative amplitude and phase of TE_{21} mode w.r.t. TE_{11} mode are presented in Fig.4.5 and Fig.4.6 respectively. It has been found that the variations of amplitude and phase of TE_{21} mode relative to TE_{11} mode are large. Thus it is impossible to design a broadband matched feed using single iris configuration. Only very narrowband (1%) conjugate matched feed can be designed using single iris discontinuity.

For cascaded three iris configuration, as shown in Fig. 4.1. The optimize R=18.5mm and d_o for three irises are 6mm, 7mm and 6mm respectively for having required TE_{21} mode amplitude relative to TE_{11} mode amplitude. The input and output diameter of the horn are 22mm and 31mm respectively. The flaring length L1=40mm and length L2=28mm. The amplitude and phase of TE_{21} w.r.t TE_{11} have been presented in Fig.4.7 and Fig.4.8 respectively for different gap between the irises. It has been found out that maximum flatness of amplitude and phase of TE_{21} w.r.t TE_{11} mode for 11-12GHz band has been obtained for g=7mm. Thus it is clear that multiple iris configuration can provide amplitude and phase flatness of TE_{21} mode relative to TE_{11} mode. The cross-polarization in the secondary pattern of the offset reflector antenna (F/D=0.5 and offset angle=53^o) for the TE_{11} mode feed is -18dB which is shown in Fig.4.9. The secondary cross-polarization has been calculated using this feed and the cross-polarization suppression bandwidth has been plotted in Fig.4.10.. It is clear from Fig.4.10 that better than 11dB improvement in cross-polarization can be obtained for 9.5% bandwidth and 15dB improvement can be obtained for 2.5% bandwidth.

Similar study has been carried out for five and seven irises. The amplitude and phase of TE_{21} w.r.t. TE_{11} have been presented in Fig.4.11 and Fig.4.12 respectively for different gap between the five irises having R=18.5mm and d_o for five irises, 5.5mm, 6mm, 7mm, 6mm and 5.5mm respectively. It has been found out that the maximum amplitude as well as phase flatness w.r.t frequency of TE_{21} mode relative to TE_{11} mode for five irises are obtained for g=5mm. Similarly, the amplitude and phase variation of TE_{21} mode relative to TE_{11} mode of seven iris configuration are presented in Fig.4.13 and Fig.4.14 respectively. The maximum amplitude and phase flatness can be obtained for g=4mm. Finally, it has been found out that the amplitude and phase flatness with respect to frequency for five and seven irises are comparable and the amplitude and phase flatness are better than three iris discontinuity. Finally, these two designs have been considered and details of the design and results are discussed in the following sections.

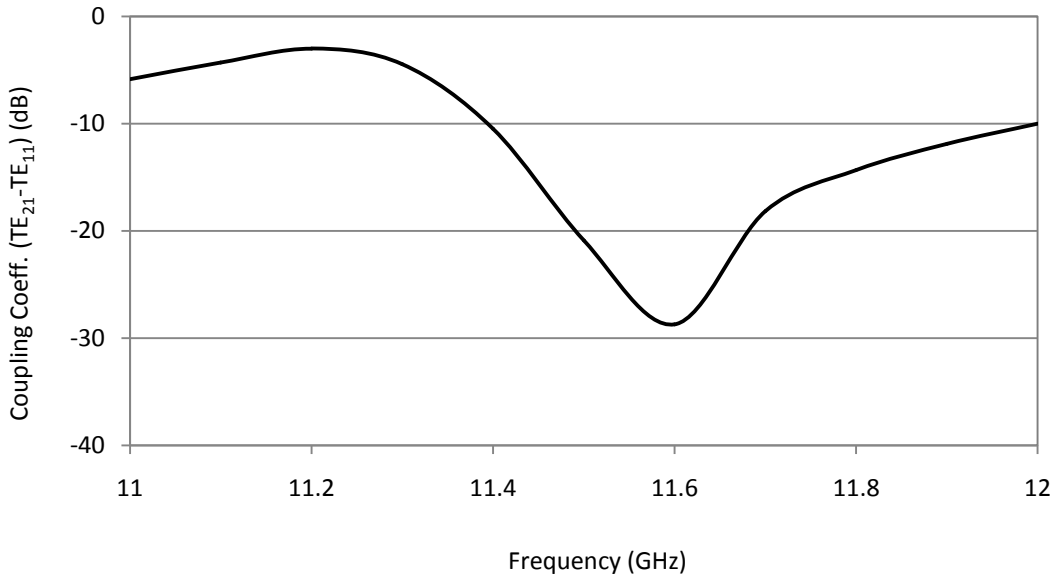

Fig. 4.5 Coupled power to TE_{21} mode relative to TE_{11} mode for single iris (R=18.5, d_o=8mm)

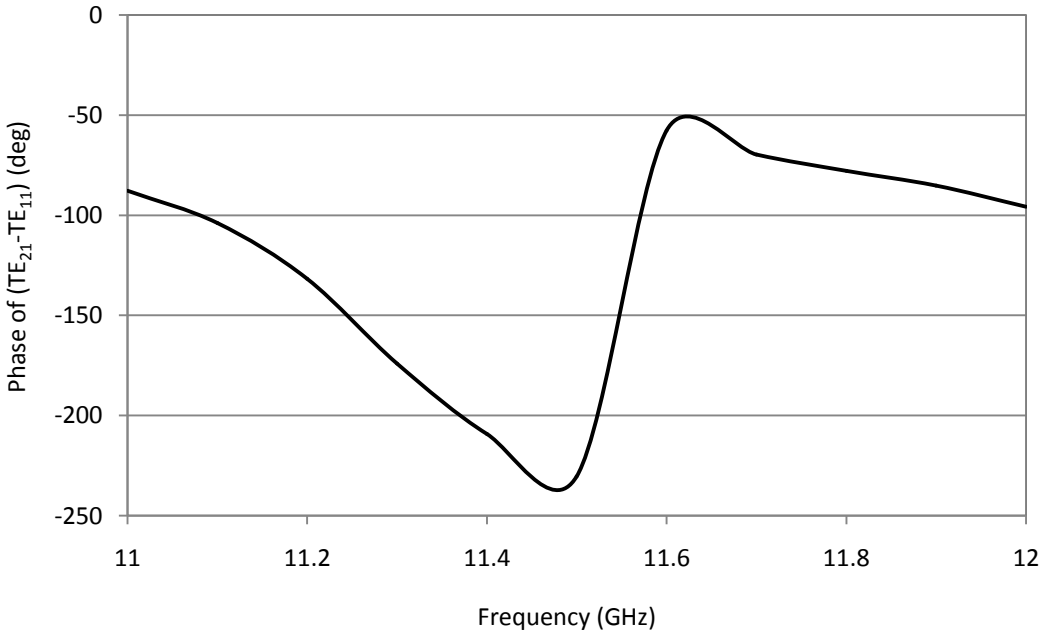

Fig. 4.6 Relative phase of TE_{21} mode w.r.t. TE_{11} mode for single iris (R=18.5, d_o=8mm)

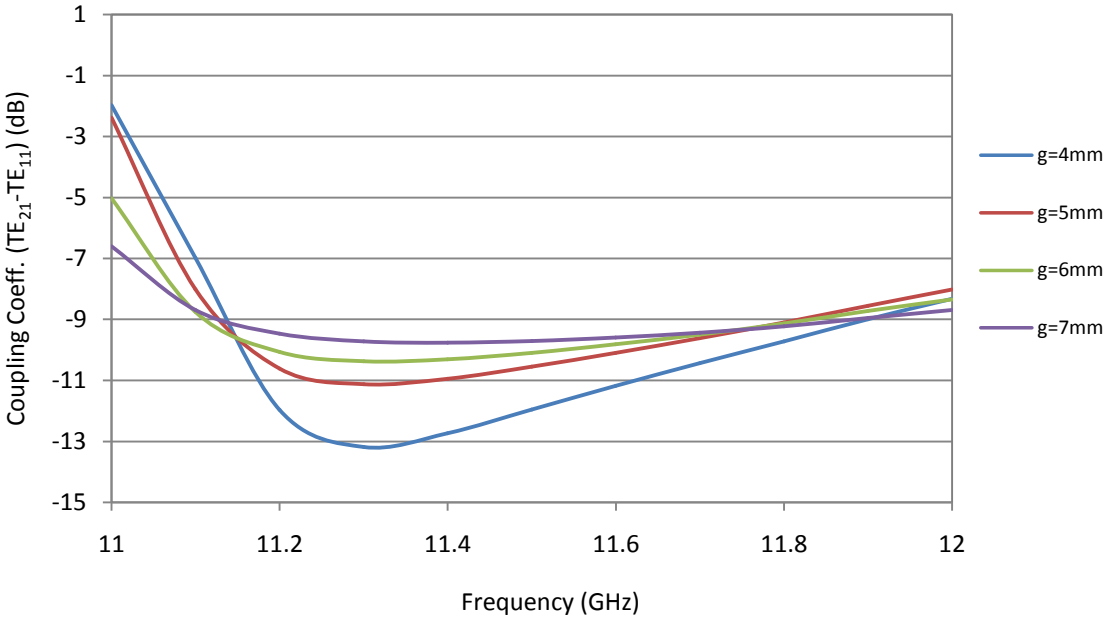

Fig.4.7 Coupled power of TE_{21} mode relative to TE_{11} mode for different gaps g between irises(R=18.5, d_o for 3 irises are 6mm, 7mm and 6mm)

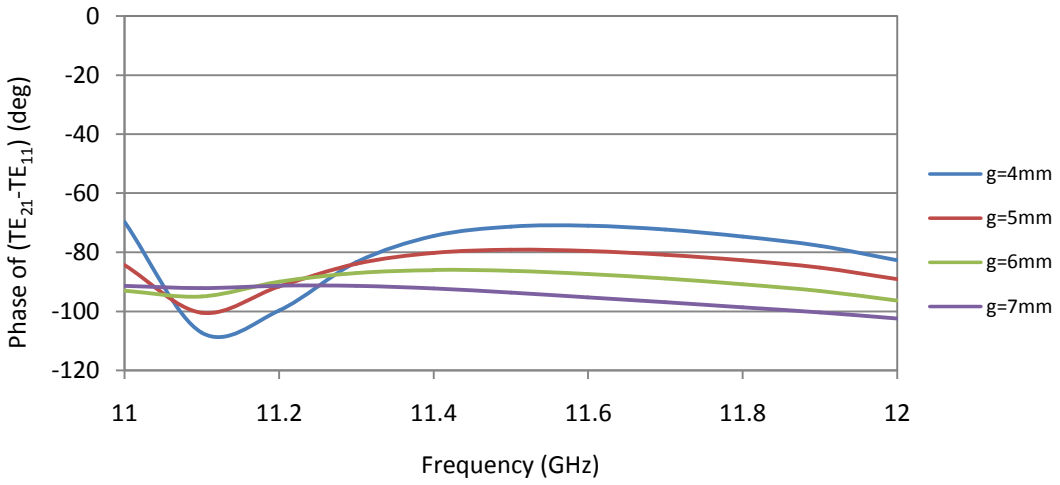

Fig.4.8 Relative phase of TE_{21} mode relative to TE_{11} mode for different gaps g between irises(R=18.5, d_o for 3 irises are 6mm, 7mm and 6mm)

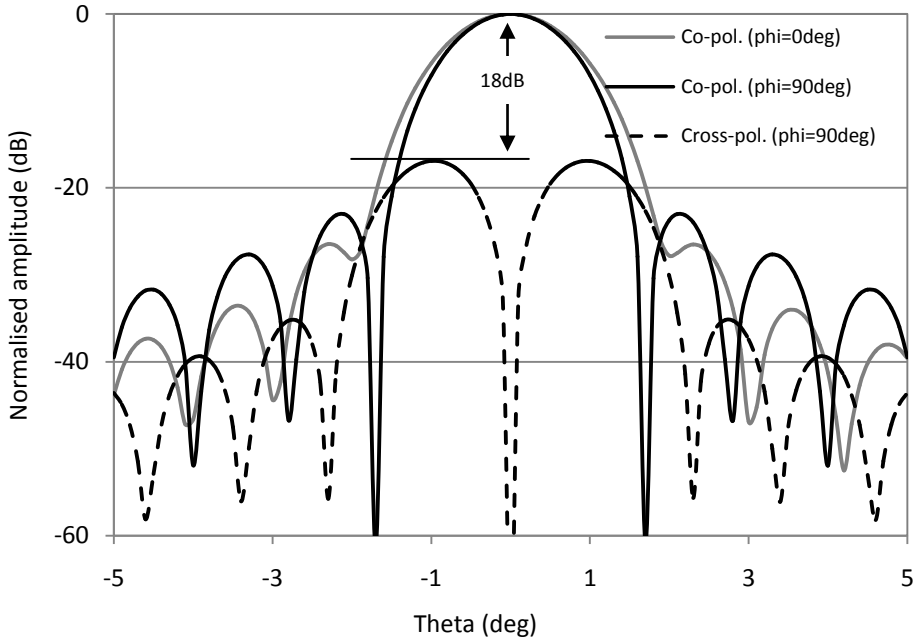

Fig.4.9 Simulated secondary pattern with TE_{11} mode feed horn at 11.5 GHz

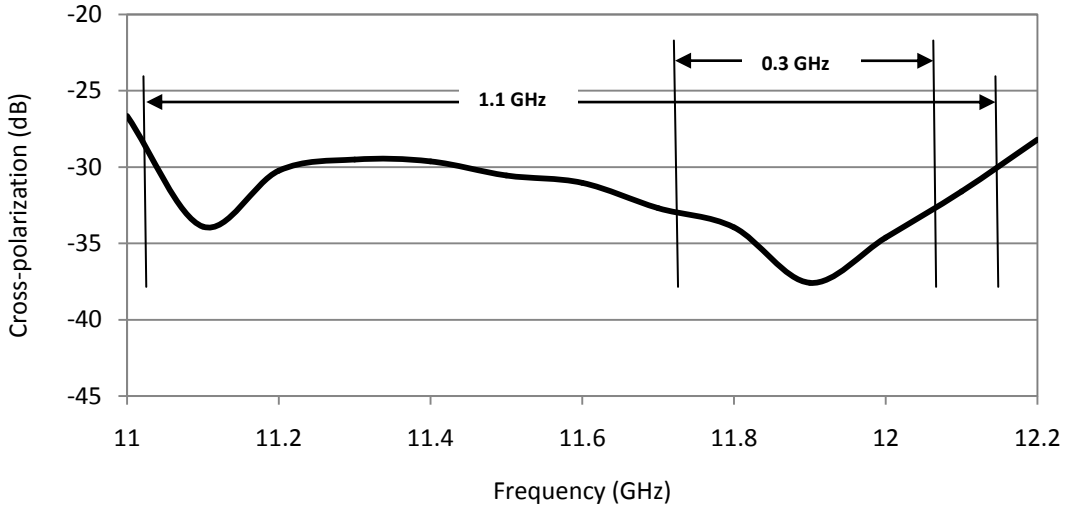

Fig.4.10 Cross-polarization suppression bandwidth for the MF with 3 irises (F/D=0.5)

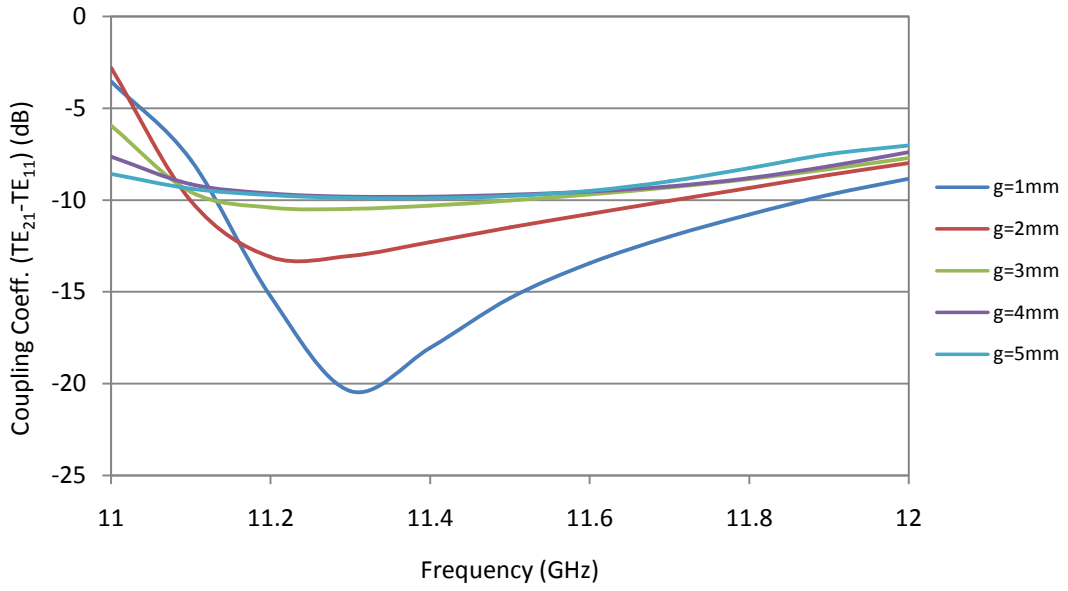

Fig.4.11 Coupled power of TE_{21} mode relative to TE_{11} mode for different gaps g between irises (R=18.5, d_o for 5 irises are 5.5mm, 6mm,7mm, 6mm and 5.5mm)

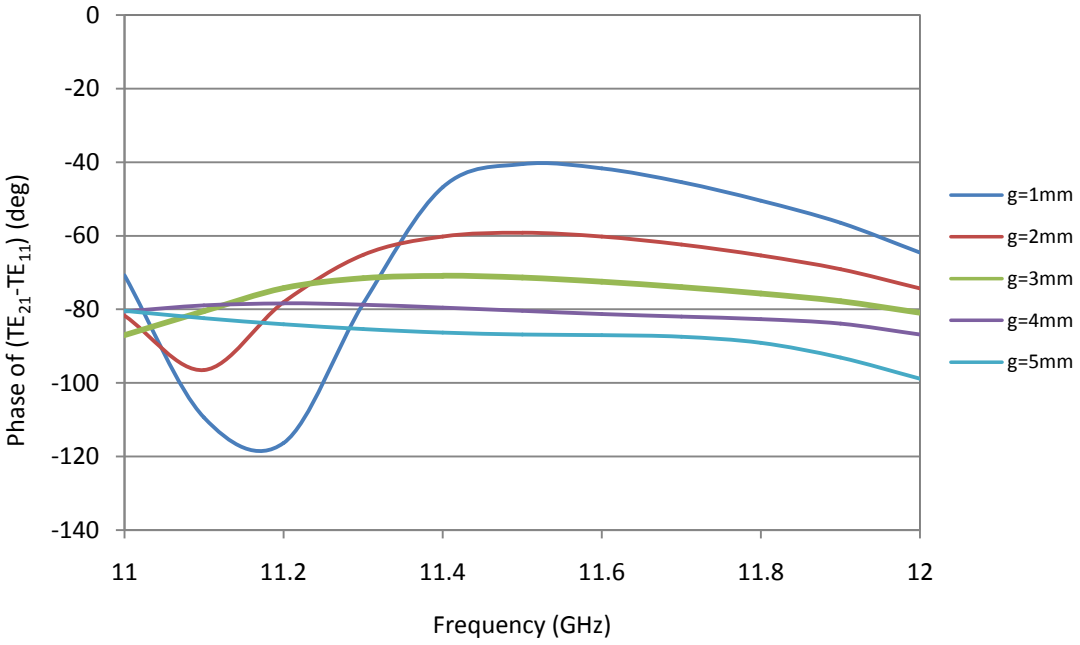

Fig.4.12 Relative phase of TE_{21} mode w.r.t TE_{11} mode for different gap=g between irises (R=18.5, d_o for 5 irises are 5.5mm, 6mm,7mm, 6mm and 5.5mm)

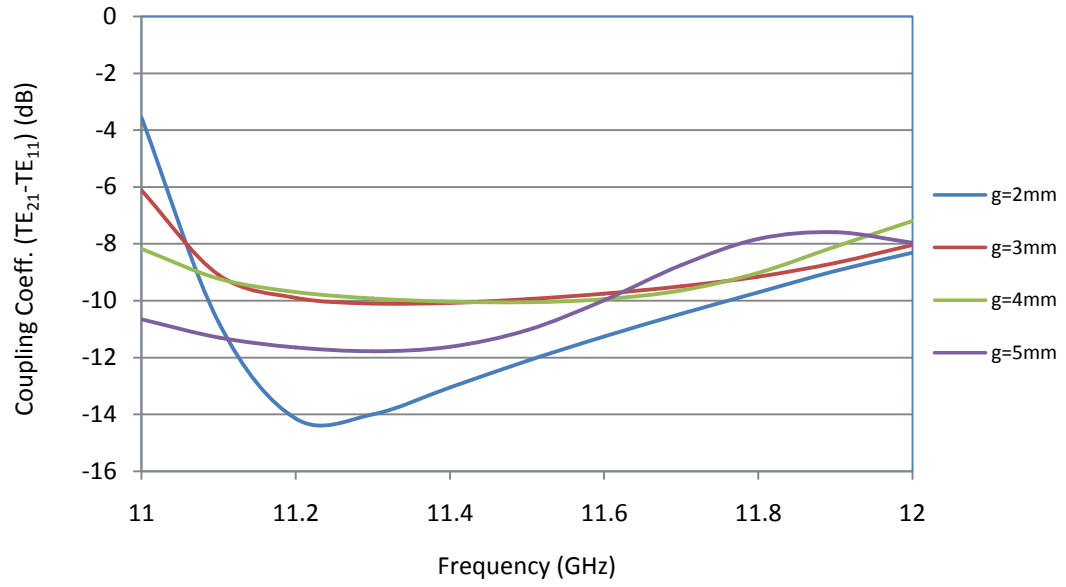

Fig.4.13 Coupled power of TE_{21} mode relative to TE_{11} mode for different gap g between irises (R=18.5, d_o for 7 irises are 5.5mm, 5.5mm, 6mm, 7mm, 6mm, 5.5mm and 5.5mm)

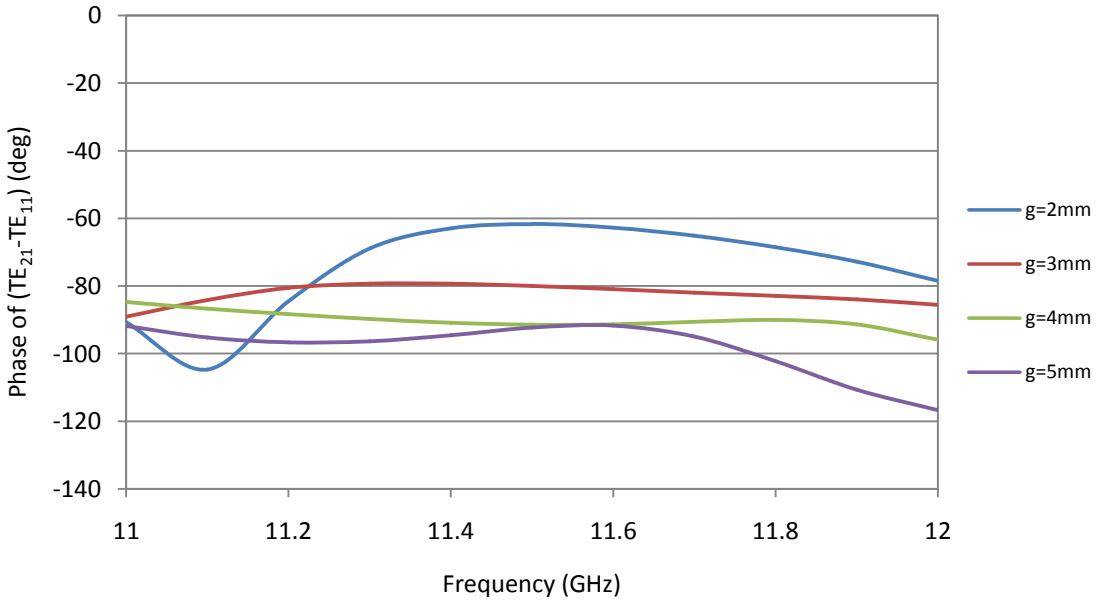

Fig.4.14 Relative phase of TE_{21} mode w.r.t TE_{11} mode for different gap g between irises (R=18.5, d_o for 7 irises are 5.5mm, 5.5mm, 6mm, 7mm, 6mm, 5.5mm and 5.5mm)

4.1.2. Design of Conjugate Matched Feed using five irises

Two designs of broadband conjugate matched feed horns using the five iris discontinuity have been carried out for the offset reflector having F/D=0.8, offset angle $\theta_o=35^0$ and F/D=0.5, $\theta_o=53^0$ respectively.

For the first design i.e. for F/D=0.8 and $\theta_o=35^0$, the optimized design parameters R=16mm, g=2.5mm and L2=28mm and d_o are different for five irises and they are 3mm, 4mm, 5mm, 4mm and 3mm. Input diameter of the horn is 22mm whereas the output diameter is 32mm. Thickness of each iris is 1mm and L1=40mm. For the second design i.e. for F/D=0.5 and $\theta_o=35^0$, the optimized design parameters R=18.5mm, g=5mm and L2=22mm and d_o are 5.5mm, 6mm, 7mm, 6mm and 5.5mm. Output diameter is 31mm. Input diameter, thickness of each iris and L1 are same as the previous design.

The first design of the horn has been carried out for offset reflector as having diameter D=1.2m, F/D=0.8 and offset angle $\theta_0=35^0$. The horn has been simulated and designed in Ansys HFSS-15. The operating region of the horn is 11-12GHz. In this region the return loss is better than 24dB. The coupling power in TE_{21} mode relative to TE_{11} mode is shown in Fig.4.15. The coupled power is varied within 1dB over the frequency band of operation. Also the relative phase of TE_{21} w.r.t TE_{11} mode at the aperture of the horn is shown in Fig.4.16. It is shown in Fig.4.16 that the variation of the relative phases are $\pm7^0$ over 90^0. Both amplitude and phase of TE_{21} mode relative to TE_{11} mode are important for designing broadband matched feed horn. Figure 4.17 shows the simulated radiation pattern of the horn at 12GHz. The asymmetry in the 0^0 plane of the radiation pattern of the horn is due to the presence of TE_{21} mode at the aperture of the horn along with TE_{11} mode [19].

The secondary pattern has been simulated using the feed horn without irises i.e. simple TE_{11} mode horn and the pattern is shown in Fig.4.18. The worst secondary cross-pol. using the above said feed horn is -25dB. The secondary radiation patterns of the reflector with the designed feed horn are shown in

Fig.4.19-4.21. There is no asymmetry in the secondary radiation pattern at 0^0 plane as bessel function of order 2 is added in conjugation with the bessel function of order 1 as shown in equation-(1). Cross-polarization of the secondary pattern over a frequency range of 10.9GHz to 12.5GHz is shown in Fig.4.22. It is clear from Fig.4.22 that we can achieve better than -35dB cross-polarization over 10% bandwidth. So there is a cross-pol. improvement of 10dB over a frequency range of 11GHz to 12.2GHz. Similarly Fig.4.22 also shows that better than -30dB cross-polarization level can be achieved for 11.5% bandwidth.

The proposed feed horn has been fabricated and is shown in Fig.4.23. A circular to rectangular transition also has been fabricated to measure the performance of the feed horn. The simulated and measured return loss performances of the horn are shown in Fig.4.24 and the measured radiation pattern is shown in Fig.4.25. It is clearly seen that the measured performance of the horn are very closely matching with the simulated performance.

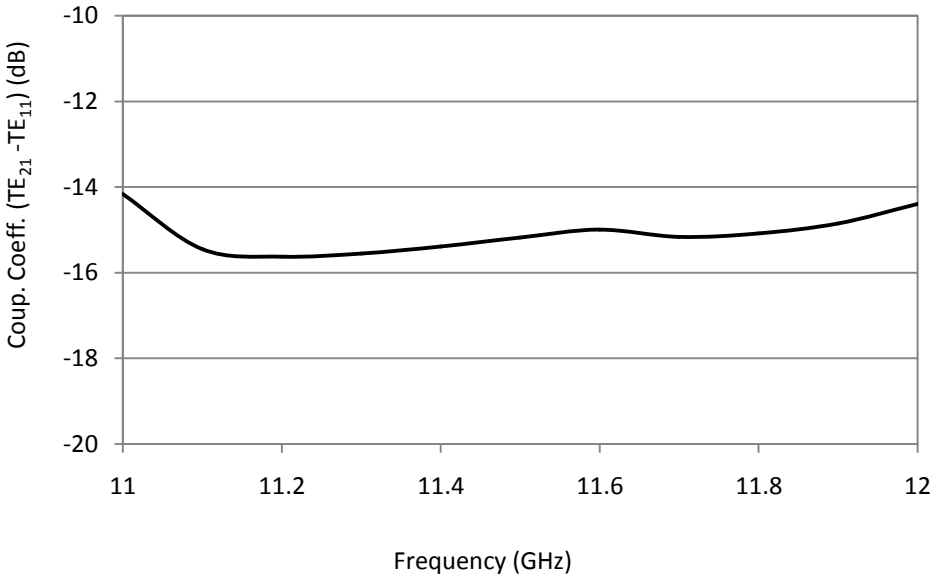

Fig.4.15 Simulated power coupling to TE_{21} mode relative to TE_{11} mode

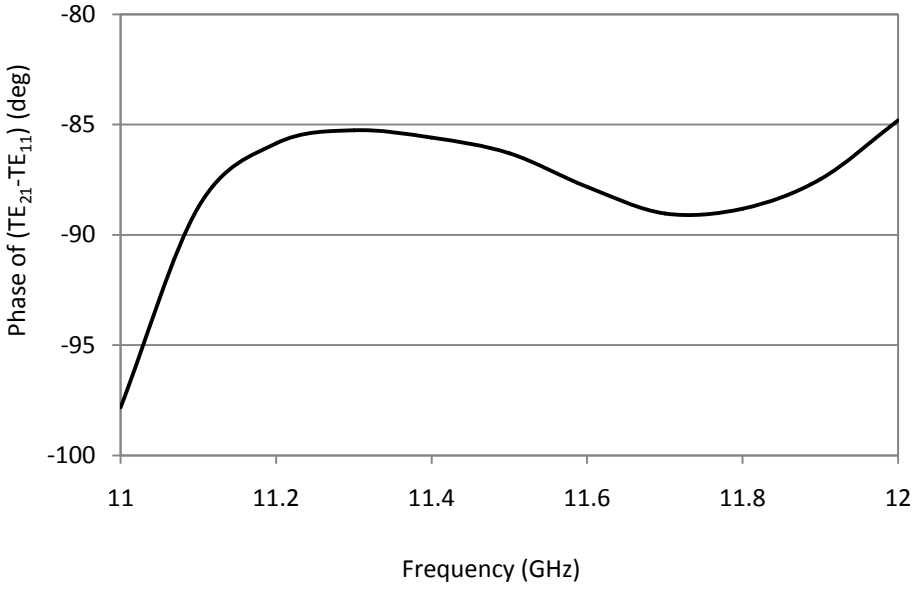

Fig.4.16 Simulated relative phase of TE_{21} mode w.r.t TE_{11} mode

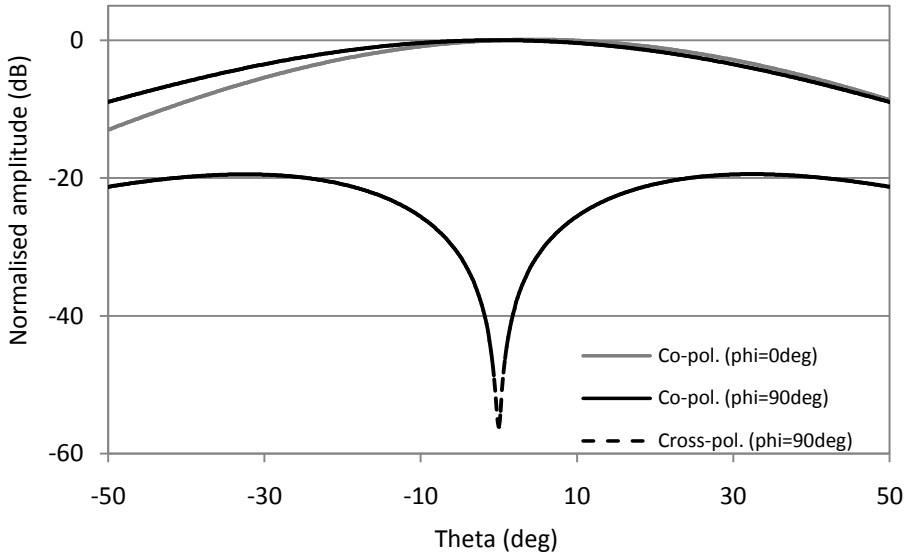

Fig.4.17 Simulated radiation pattern of the broadband conjugate matched feed horn at 12GHz

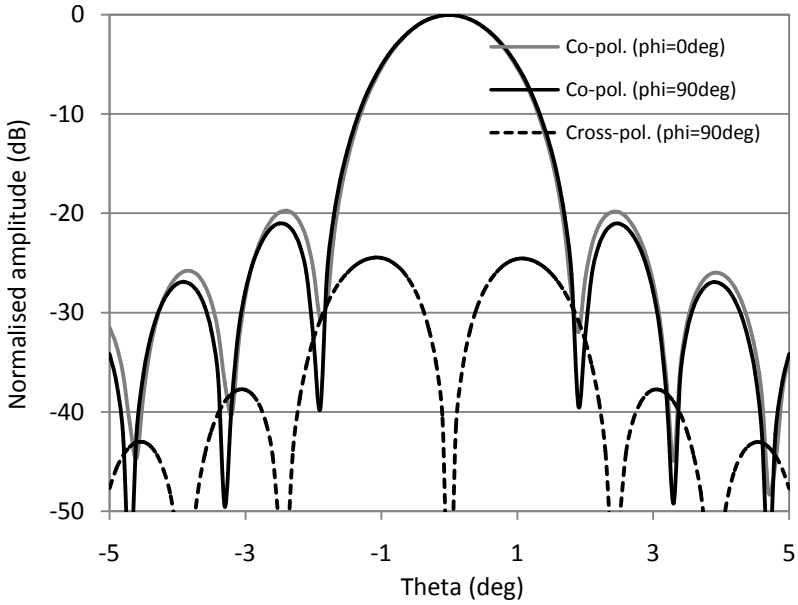

Fig.4.18 Simulated secondary pattern with TE_{11} mode feed horn at 12GHz

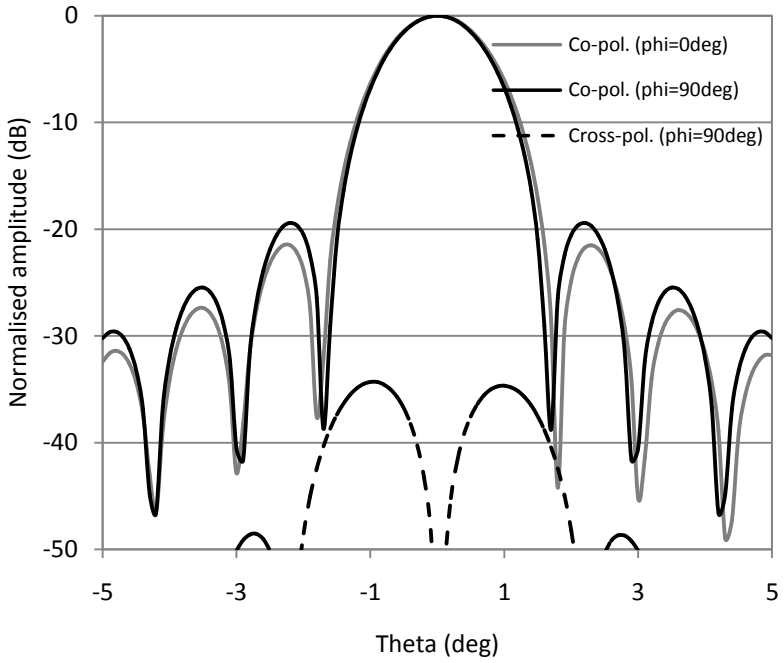

Fig.4.19 Simulated secondary pattern with conjugate matched feed horn at 11GHz

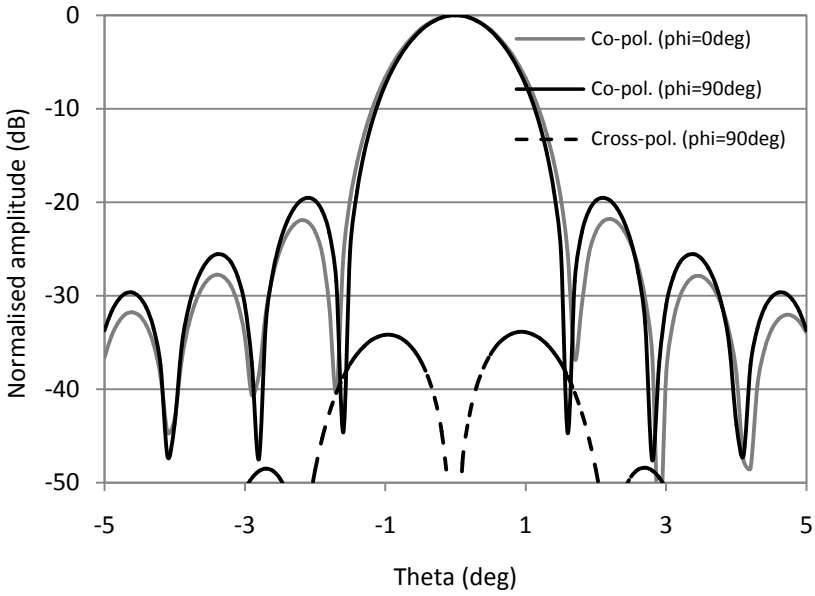

Fig.4.20 Simulated secondary pattern with conjugate matched feed horn at 11.5GHz

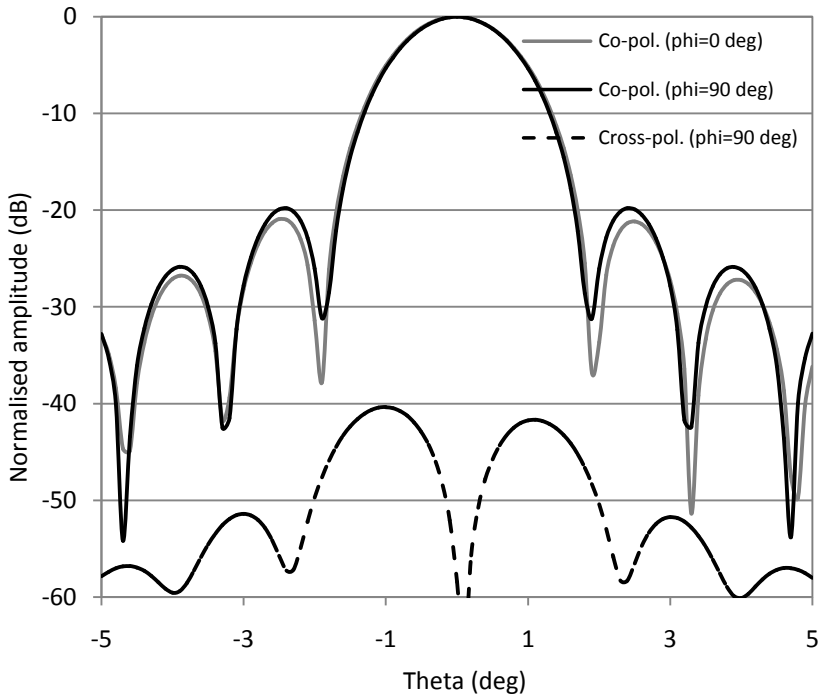

Fig.4.21 Simulated secondary pattern with conjugate matched feed horn at 12GHz

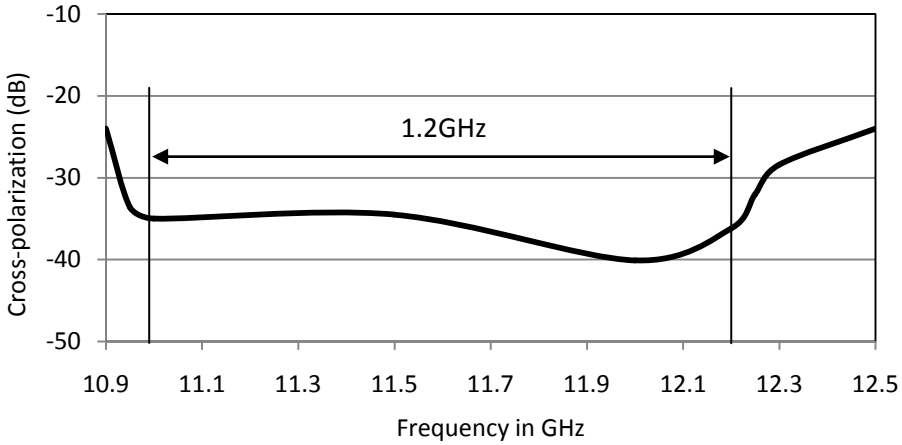

Fig.4.22 Cross-polarization suppression bandwidth for MF with 5 irises (F/D=0.8)

Fig.4.23 Fabricated broadband conjugate matched feed horn

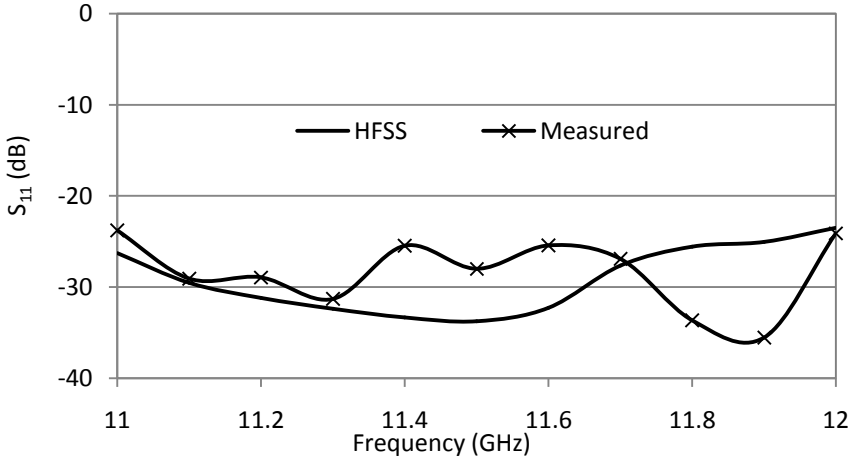

Fig.4.24 Simulated and Measured return loss characteristics of the horn

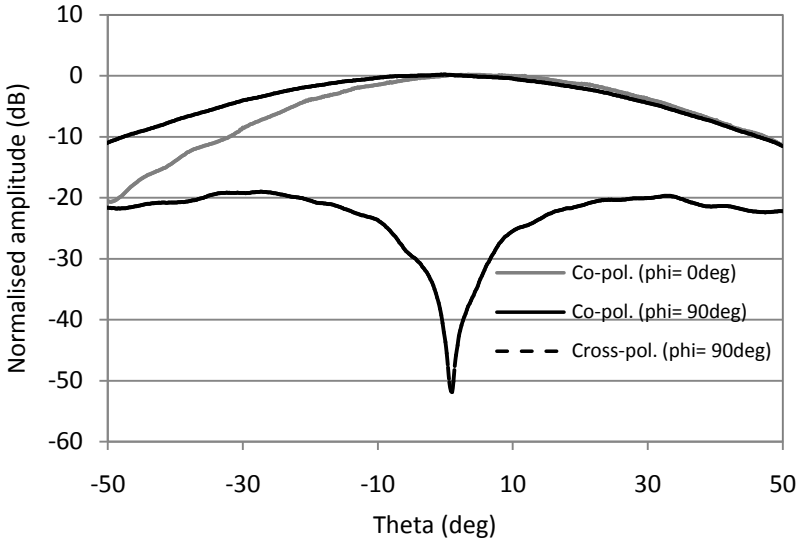

Fig.4.25 Measured radiation pattern of the horn at 12GHz

For the second design with five irises, F/D chosen is 0.5 and the corresponding offset angle $\theta_0=53^0$. The diameter of the reflector is the same as the previous design i.e. D=1.2m. The simulated return loss of the horn is better than 20dB over the band. The TE_{21} modal amplitude and phase variations relative to TE_{11} mode at the aperture of the horn with respect to frequency are shown in Fig.4.26 and 4.27 respectively. The radiation pattern of the horn at 11.8 GHz where maximum cross-polarization has been achieved in the secondary pattern is shown in Fig.4.28. The secondary pattern of the offset reflector without the iris discontinuities is shown in Fig.4.29 and with this designed matched feed at 11.8GHz has been presented in Fig.4.30. The cross-polar suppression bandwidth is shown in Fig.4.31. The maximum improvement of cross-polar component is by 23dB from -18dB to -41dB at 11.8GHz. It is also clear from Fig.4.31 that better than 10dB improvement in cross-polarization is achieved for 10% bandwidth.

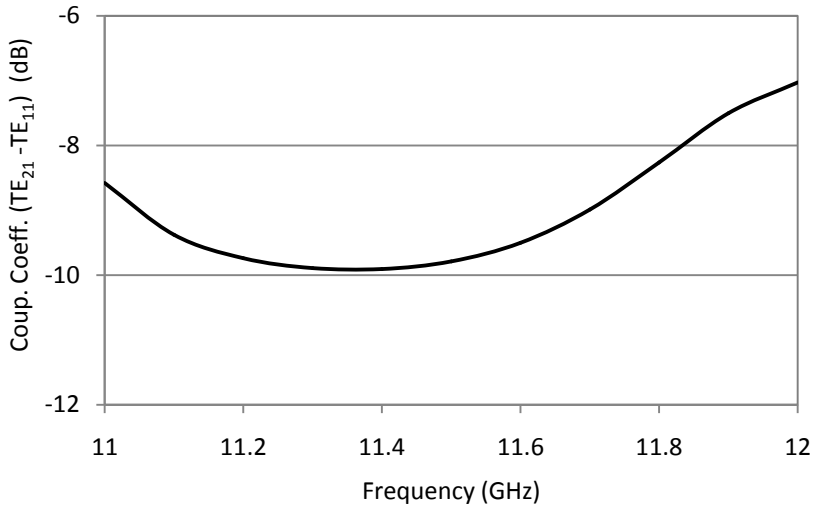

Fig.4.26 Simulated power coupling to TE_{21} mode relative to TE_{11} mode

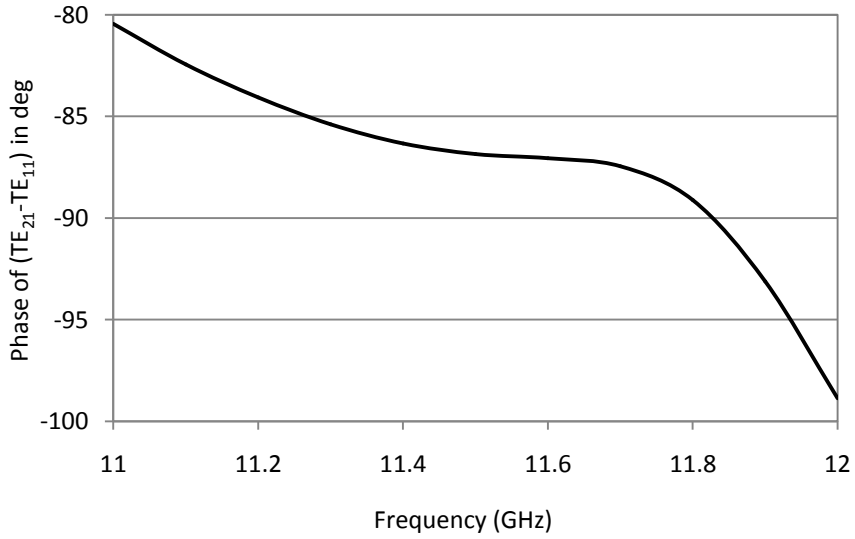

Fig.4.27 Simulated relative phase of TE_{21} mode w.r.t TE_{11} mode

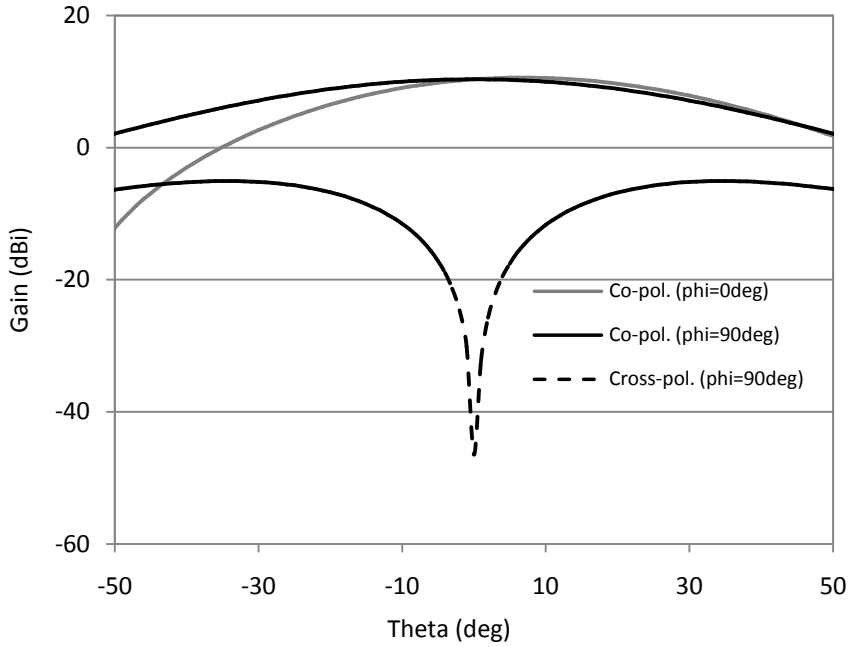

Fig.4.28 Simulated radiation pattern of the broadband conjugate matched feed horn at 11.8GHz

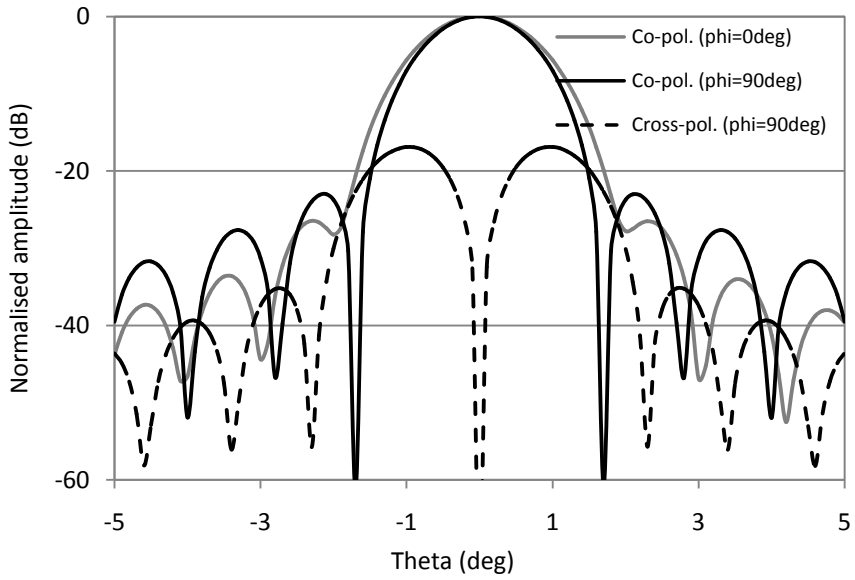

Fig.4.29 Simulated secondary pattern with TE_{11} mode feed horn at 11.8 GHz

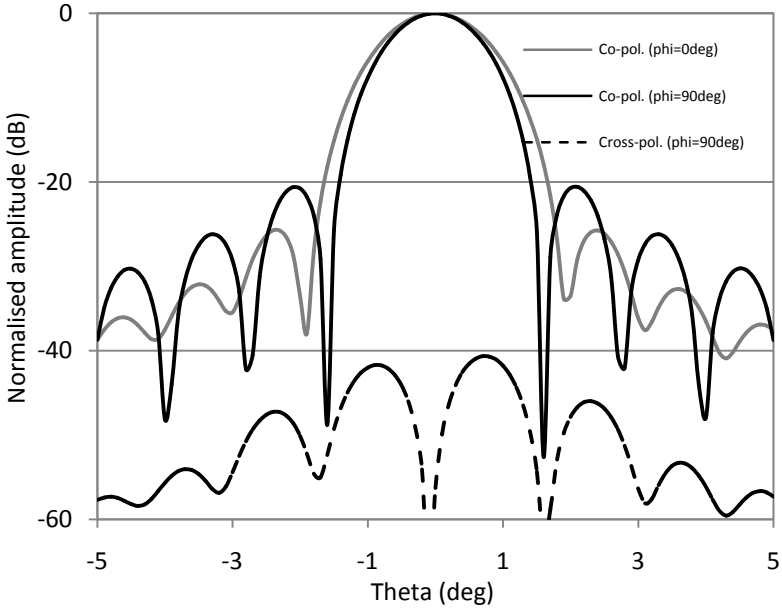

Fig.4.30 Simulated secondary pattern with conjugate matched feed horn at 11.8GHz

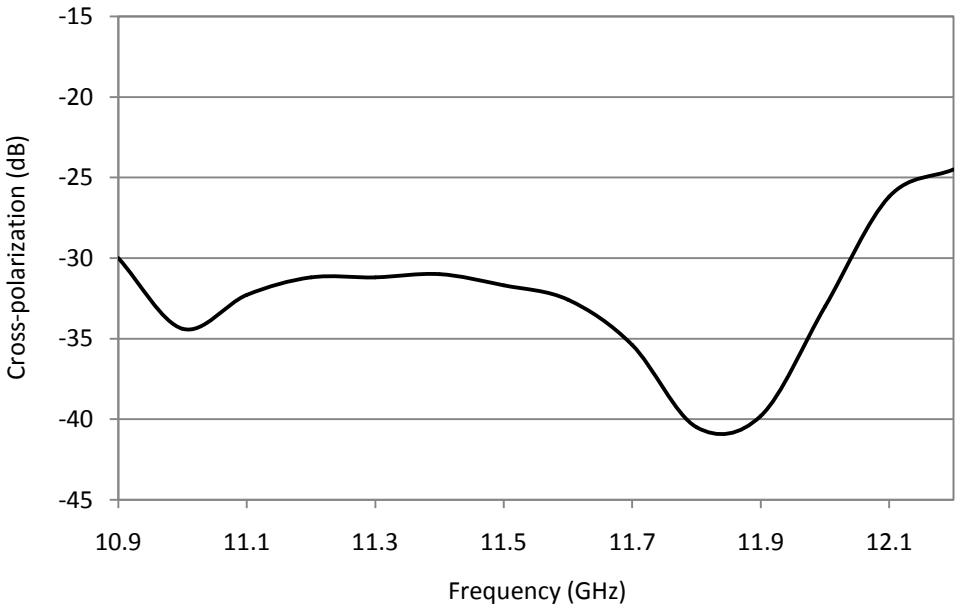

Fig.4.31 Cross-polarization suppression bandwidth for MF with 5 irises (F/D=0.5)

4.1.3. Design of Conjugate Matched Feed using seven irises

The design of broadband conjugate matched feed horns using the seven iris discontinuity have been carried out for the offset reflector having F/D=0.5, $\theta_o=53^0$. For this design, the optimized design parameters R=18.5mm, g=4mm and L2=21mm and d_o are different for seven irises and they are 5.5mm, 5.5mm, 6mm, 7mm, 6mm, 5.5mm and 5.5mm. Input diameter of the horn is 22mm whereas the output diameter is 31mm. Thickness of each iris is 1mm and L1=40mm.

The F/D chosen is 0.5 and the corresponding offset angle $\theta_0=53^0$. The diameter of the reflector is the same as the previous design i.e. D=1.2m. The simulated return loss of the horn is better than 20dB over the band. The TE_{21} modal amplitude and phase variations relative to TE_{11} mode at the aperture of the horn with respect to frequency are shown in Fig.4.32 and 4.33 respectively. The radiation pattern of the horn at 11.9 GHz where maximum cross-polarization has been achieved in the secondary pattern is shown in Fig.4.34. The secondary pattern of the offset reflector with this designed matched feed has been presented in Fig.4.35 to Fig.4.37. The cross-polar suppression bandwidth is shown in Fig.4.38. The maximum improvement of cross-polar component is by 25dB at 11.9GHz. Here also 10% bandwidth is achieved for 10dB improvement in cross-polarization.

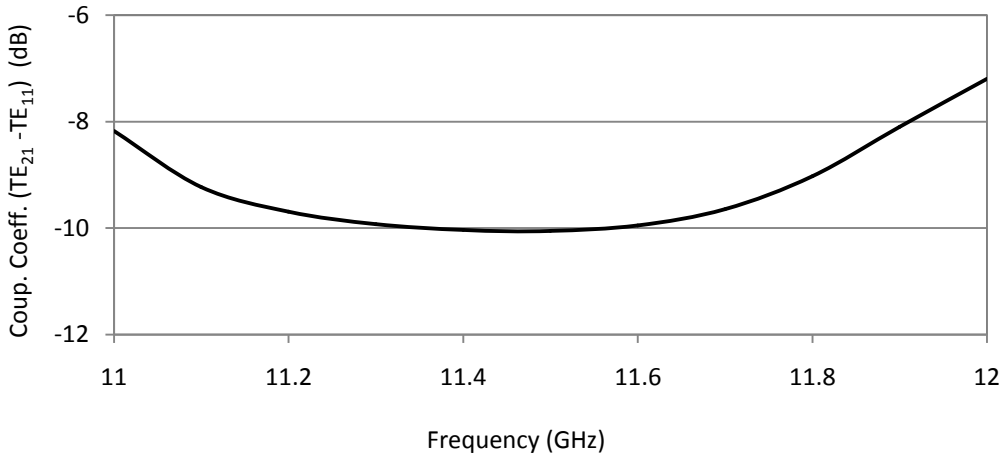

Fig.4.32 Simulated power coupling to TE_{21} mode relative to TE_{11} mode

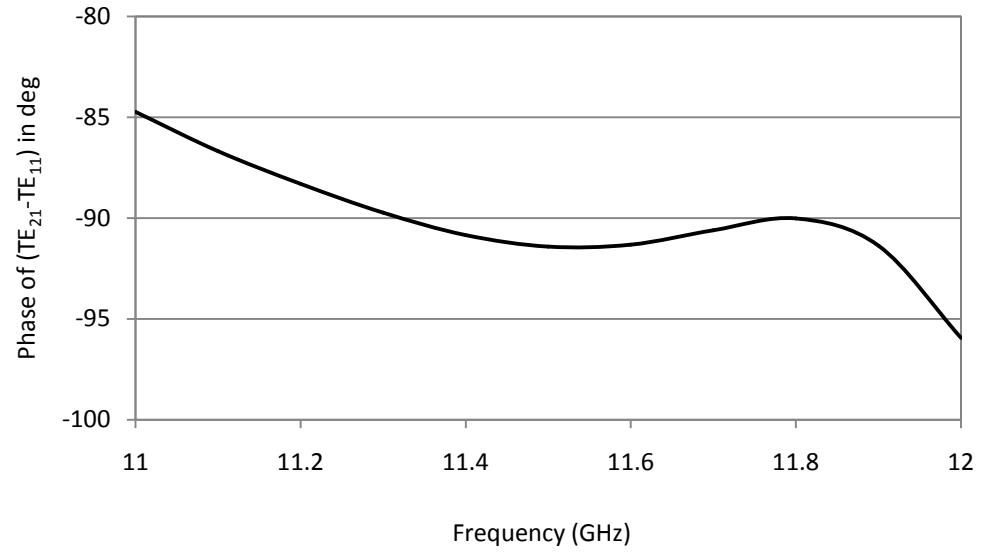

Fig.4.33 Simulated relative phase of TE_{21} mode w.r.t TE_{11} mode

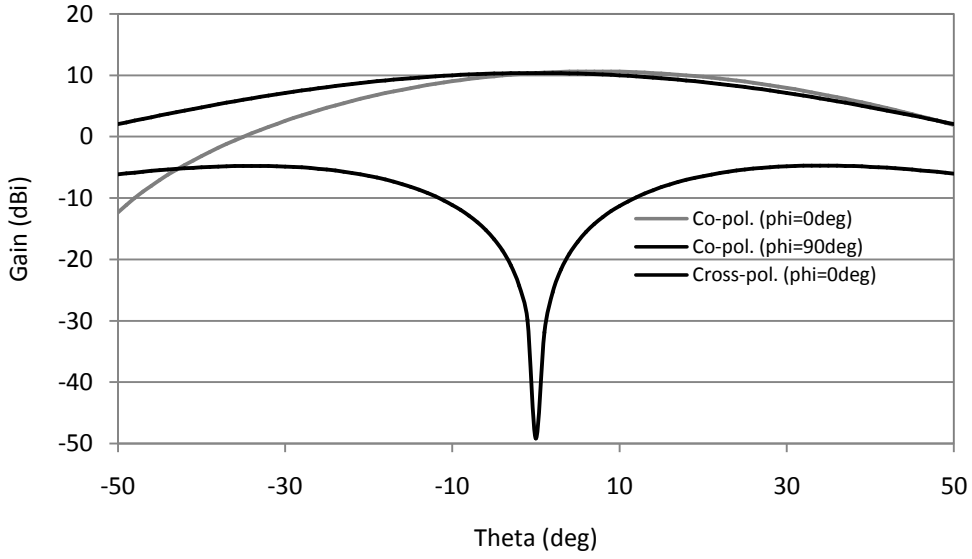

Fig.4.34 Simulated radiation pattern of the broadband conjugate matched feed horn at 11.9GHz

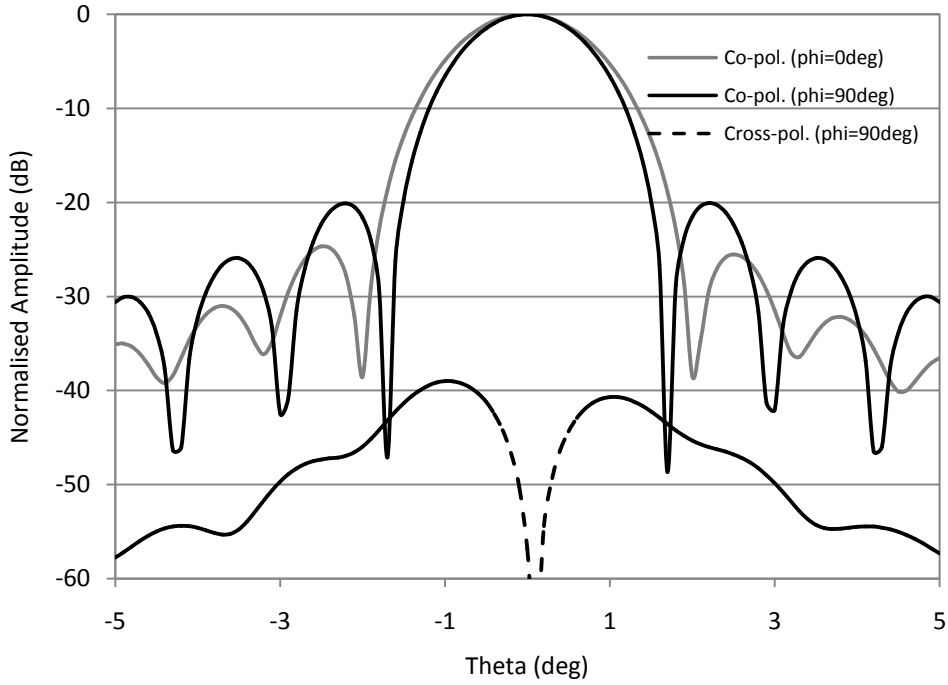

Fig.4.35 Simulated secondary pattern with conjugate matched feed horn at 11GHz

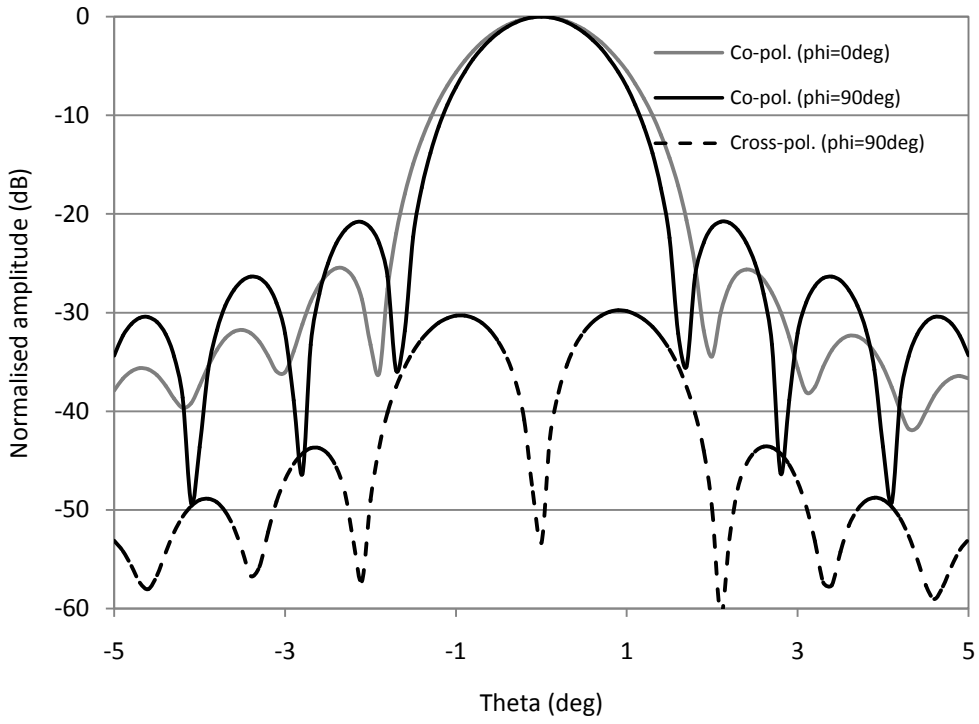

Fig.4.36 Simulated secondary pattern with conjugate matched feed horn at 11.5GHz

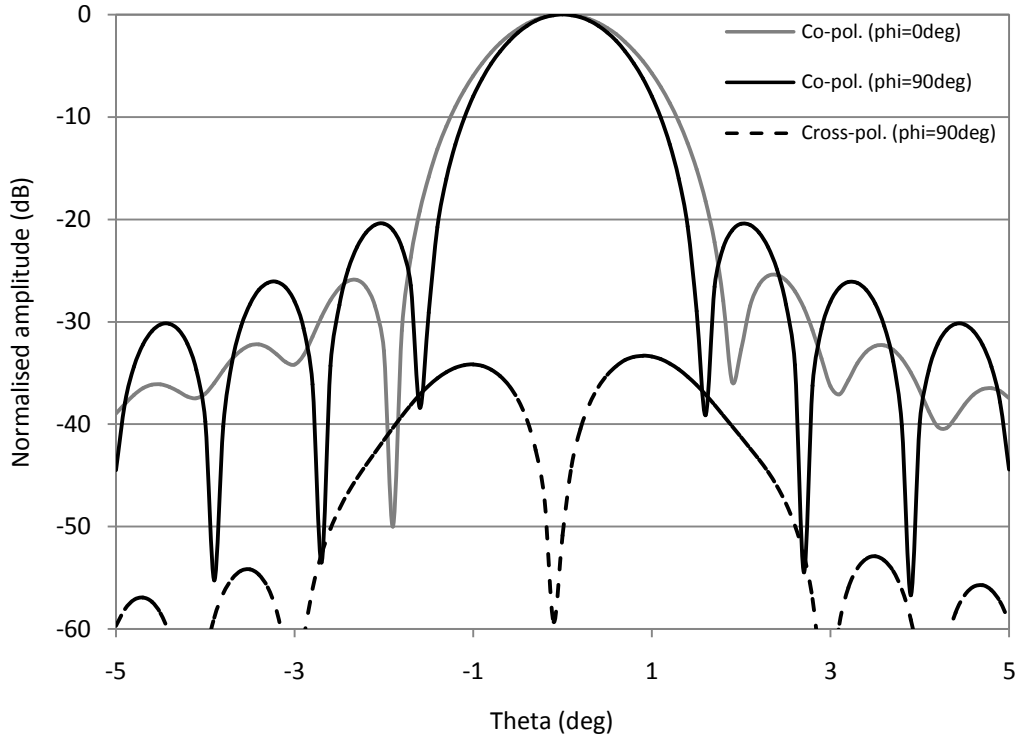

Fig.4.37 Simulated secondary pattern with conjugate matched feed horn at 12GHz

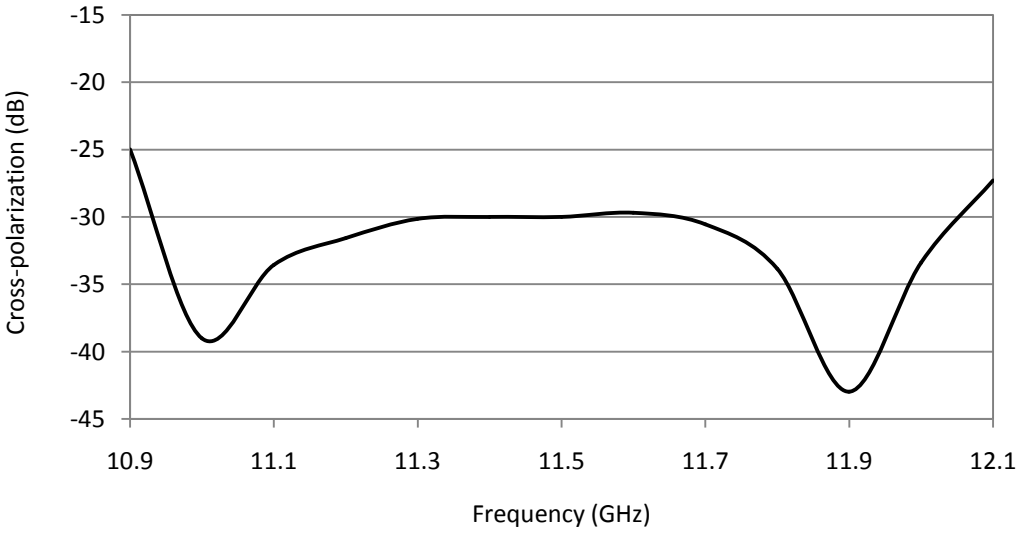

Fig.4.38 Cross-polarization suppression bandwidth for MF with 7 irises (F/D=0.5)

4.2 Conclusion

A wideband conjugate matched feed horn has been designed and developed using a novel discontinuity configuration. A detail study has been performed with this novel discontinuity to achieve wideband performance in the conjugate matched feed horn. The cross-polar performance of an offset reflector antenna with the feed horn has been simulated. It is shown that the proposed matched feed suppresses cross-polarization components by 10dB over a 10% frequency bandwidth when used as a primary feed with an offset parabolic reflector antenna having low F/D.

CHAPTER 5

BROADBAND CORRUGATED CONJUGATE MATCHED FEED HORN

The corrugated horns are in use as primary feeds for reflector antennas. In comparison to smooth walled conical horns, the corrugated horns possess two important properties, i.e., axial beam symmetry and low cross-polarization over a wide bandwidth [49],[50]. These properties ensure high antenna gain, low spillover and minimum contribution from the side-lobes. In order to produce symmetric E-plane and H-plane patterns with a very low cross-polarization, it is necessary that the horn should produce linear aperture electric fields [49]. However, it is known that a pure TE or TM mode cannot produce linear electric fields and hence the radiation patterns of smooth-walled conical horns (supporting TE and/or TM modes) are not symmetric. As reported in the published literature, the hybrid mode can only produce the required linear electric fields. The hybrid mode is basically a mixture of TE and TM modes, e.g., fundamental HE_{11} mode is a mixture of TE_{11} and TM_{11} modes. Such hybrid mode(s) can be generated by a horn, whose inner surface is corrugated. In fact, the corrugations on the walls of the horn modify the electric and the magnetic fields such that the horn produces symmetric co-polar patterns with less cross-polar radiation.

Although the fundamental HE_{11} mode guided corrugated horn is the best feed option for a symmetrical reflector, however, it is not suitable as a feed for the offset parabolic reflector antenna. This is because the conventional corrugated feed cannot suppress the cross-polarization introduced by the offset geometry of the reflector. Thus, a pure HE_{11} mode guided cylindrical corrugated feed is not suitable for an offset parabolic reflector antenna. As suggested in [19], if a corrugated matched feed can be designed, whose aperture fields are a conjugate match to the focal region fields of the reflector, it is possible to suppress the unwanted cross-polarization of the offset reflector. In a corrugated

structure, such a matched feed can be configured by adding an additional hybrid mode (HE_{21} mode) to the fundamental HE_{11} mode [33]. However, as the HE_{11} and HE_{21} modes have different phase velocity, the broadband cross-polar performance could not be achieved even with corrugated structure. For the useful performance of the onboard communication/microwave remote sensing system such low cross-polar bandwidth is not suitable. It is worthwhile to carry out investigations and develop a wideband corrugated conjugate matched feed. To the best of authors' knowledge, the design and realization of such feeds offering wideband cross-polar radiation performance are not reported in open literature.

In the present chapter, a similar type of symmetrical cascaded waveguide discontinuities which already has been presented in chapter 4, has been used to achieve wide cross-polar bandwidth in corrugated horn. One section of the waveguide discontinuity has been conceptualized using intersection of three off-centered junctions of circular waveguide placed symmetrically with angular spacing of 120^0. One such discontinuity which is like an iris in the waveguide has been analyzed for generating TE_{21} mode. When TE_{21} mode passes through corrugated structure of the horn, it is converted to HE_{21} mode at the aperture of the corrugated horn [33]. Similarly incident TE_{11} mode is converted to HE_{11} mode at the aperture of the corrugated horn. It has been found that the required amplitude and phase flatness of HE_{21} mode relative to HE_{11} mode at the aperture of the corrugated horn over the designed frequency band, which is required for broadband performance of the corrugated matched feed were not achieved. In order to enhance the cross-polar bandwidth, five sections with the similar iris structure have been placed in the axial direction inside circular waveguide at the throat section of the corrugated horn. The axial profile of the irises has been optimized to achieve good return loss performance.

The proposed configuration has been used to design a corrugated broadband conjugate matched feed horn working in 55-60GHz band i.e. for 8% bandwidth.

From the focal region field analysis [28] of the offset reflector antenna, the amplitude and phase required in HE_{21} mode to cancel cross-polar component has been calculated. The horn has been optimized to achieve required amplitude and phase of HE_{21} mode relative to HE_{11} mode.

In the present chapter, two designs of the broadband corrugated conjugate matched horn have been presented. One design is for the offset reflector having F/D=0.7 and 90^0 offset angle and another design for the offset reflector having F/D=0.4 and offset angle=90^o.

5.1 Field Expressions for the Corrugated Conjugate Matched Feed

In case of a corrugated cylindrical wave-guide structure, the matched feed is a dual-mode feed with two modes, i.e., HE_{11} and HE_{21}. The fundamental HE_{11} mode ensures that the feed itself will not radiate high cross-polarization, while a small component of HE_{21} mode compensates the asymmetric cross-polarization added by the offset geometry. For the satisfactory operation of the matched feed, it is necessary that the HE_{21} mode should maintain -90° phase relationship with the HE_{11} mode. The field expressions of the dual-mode corrugated matched feed can be written as,

$$E_\theta = E_\theta^{HE_{11}} + \gamma . E_\theta^{HE_{21}} \tag{5.1}$$

$$E_\phi = E_\phi^{HE_{11}} + \gamma . E_\phi^{HE_{21}} \tag{5.2}$$

where, γ is the arbitrary constant defining the relative power in HE_{21} mode with respect to the fundamental HE_{11} mode. Using the general expressions for E_θ and E_ϕ from [51], the expressions for $E_\theta^{HE_{11}}$, $E_\theta^{HE_{21}}$, $E_\phi^{HE_{11}}$ and $E_\phi^{HE_{21}}$ can be obtained as,

$$E_\theta^{HE_{11}} = -(j)^2 \cos(\phi)\left\{L_1(\theta)\overline{\Lambda}_1(ka + \overline{\beta}_1 ka\cos(\theta)) + Q_1(\theta)(ka\cos(\theta) + ka\overline{\beta}_1)\right\}e^{-jkR} \tag{5.3}$$

$$E_{\theta}^{HE_{21}} = -(j)^3 \cos(3\phi)\left\{L_2(\theta)\overline{\Lambda}_2(ka + \overline{\beta}_2 ka\cos(\theta)) + Q_2(\theta)(ka\cos(\theta) + ka\overline{\beta}_2)\right\}e^{-jkR} \quad (5.4)$$

$$E_{\phi}^{HE_{11}} = -(j)^2 \sin(\phi)\left\{L_1(\theta)\overline{\Lambda}_1(ka + \overline{\beta}_1 ka\cos(\theta)) + Q_1(\theta)(ka\cos(\theta) + ka\overline{\beta}_1)\right\}e^{-jkR} \quad (5.5)$$

$$E_{\phi}^{HE_{21}} = -(j)^3 \sin(3\phi)\left\{L_2(\theta)\overline{\Lambda}_2(ka + \overline{\beta}_2 ka\cos(\theta)) + Q_2(\theta)(ka\cos(\theta) + ka\overline{\beta}_2)\right\}e^{-jkR} \quad (5.6)$$

where,

a = aperture radius of the horn,

R=distance from the aperture centre to the observation point (in meter),

λ= wavelength of operation ,

k= free-space propagation constant,

$\overline{\beta}_1$ = normalized phase-change coefficients of HE_{11} mode,

$\overline{\beta}_2$ = normalized phase-change coefficients of HE_{21} mode,

$\overline{\Lambda}_1$ = normalized hybrid factor (referred as and for the HE_{11} and HE_{21} modes, respectively),

$$L_m = \frac{J_m(x_1')J_m(x_m)}{x_1' x_m \sin(\theta)}$$

$$Q_m = \frac{x_m J_m(x_m)J_m'(x_1') - x_1' J_m(x_1')J_m'(x_m)}{x_m^2 - x_1'^2 \sin(\theta)}$$

$$x_1' = ka$$

x_1 = the first root of the Bessel function for HE_{11} mode (=2.405),

x_2 = the first root of the Bessel function for HE_{21} mode (=3.8317),

$J_m(x)$ = Bessel function of the first kind and order m,

The actual values of x_1 and x_2 have been obtained by solving the characteristic equation under a balanced hybrid condition [51].

5.2 Broadband Corrugated Matched Feed Design

It is known that the field behaviour of HE_{21} mode in circular corrugated horn is close to equation-(2.2) as given in [19]. Now to cancel the cross-polar component in focal plane, corrugated feed horn has to generate HE_{21} mode along with HE_{11} mode in proper amplitude and phase. The required amplitude of HE_{21} mode is calculated with known parameters *D, F,* θ and the relative phase between HE_{11} and HE_{21} modes has to be 90^0 as it is seen from eq.(2.2).

The simulation model of the proposed broadband corrugated conjugate matched feed horn using FEM based High Frequency Structure Simulator (HFSS) is shown in Fig.5.1. In the proposed structure, the TE_{21} mode converter is modeled with five irises inserted in equal interval along the Z-direction in the throat section of the horn as shown in Fig.5.1(a). The cross-section of the horn is shown in Fig.5.1(b). The cross-section of the TE_{21} mode generator section has been realized using three offset circular waveguide junctions as shown in Fig.5.2. Circles are shown using dashed lines and they are showing how the smallest cross-section among the 5 irises is realized. The concept behind choosing the particular opening of the iris is that asymmetrical offset junction discontinuity between two circular waveguide produces TM_{01}, TE_{21} and TE_{21}* modes. For conjugate matched feed horn design only TE_{21}/HE_{21} (smooth-wall horn/Corrugated horn) mode is required along with dominant TE_{11}/HE_{11} mode. So to cancel generated TM_{01} and TE_{21}* modes, three such type of discontinuities have been placed symmetrically in same plane and intersection of the three has been chosen as the iris opening as shown in Fig.5.2.

The relative phase variations between HE_{21} and HE_{11} modes at the aperture of the horn have been controlled and optimized by the proposed cascaded geometry along with phasing sections and corrugated horn. For conjugate matching operation, the relative phase between HE_{11} and HE_{21} modes should be 90^0.

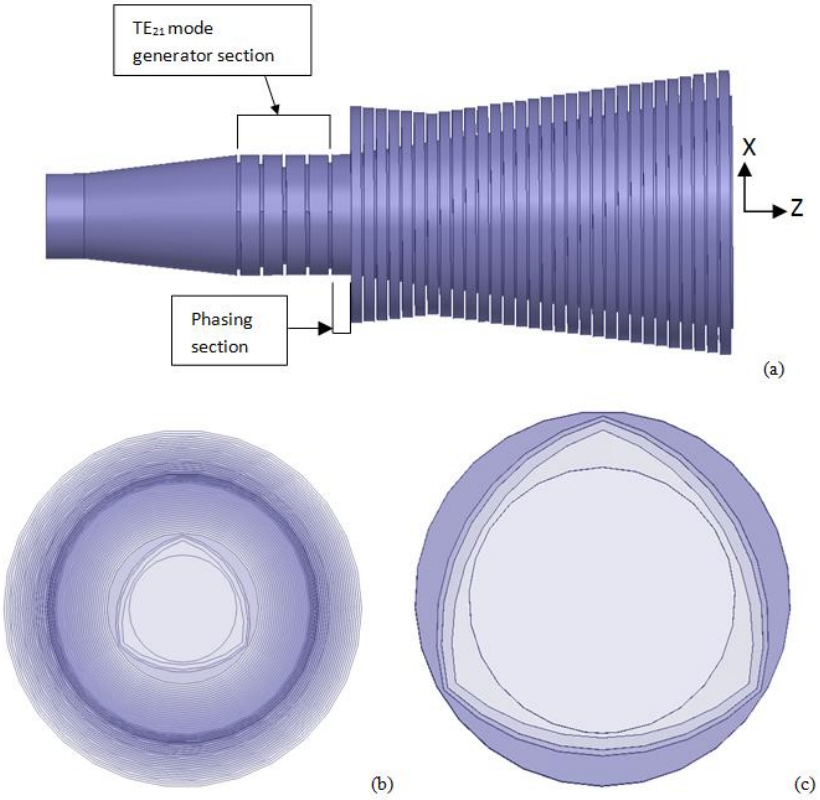

Fig.5.1 Simulation model of the proposed structure, (a) side view, (b) front view of the horn (c) enlarged view of the iris structure

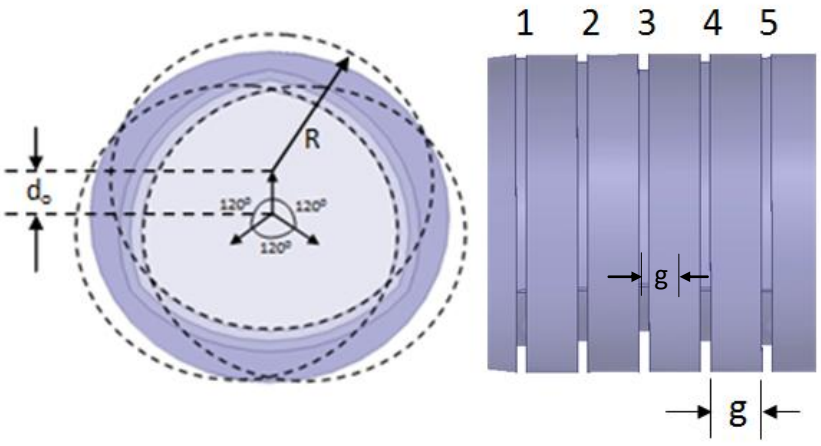

Fig.5.2 Modeling of opening of the irises (arrows indicate the offset direction of circles making 120^0 angle with each other)

Main parameters which are controlling the relative amplitude and phase of HE_{21} mode w.r.t. HE_{11} mode at the aperture of the horn are the radius R, offset distance (d_o) of the dashed circle shown in Fig.5.2 and gap between the irises (g).

For three dashed circles in the same transverse plane as shown in Fig.5.2, R and d_o are equal. The flatness of relative amplitude and phase of HE_{21} mode w.r.t. to HE_{11} mode can be controlled by parameter g, which is essential for broadband operation of this feed horn.

The present designs of the corrugated broadband conjugate matched feed have been carried out for F/D=0.7 and offset angle $\theta_o=90^0$ and also for F/D=0.4 and offset angle $\theta_o=90^0$. The optimized design parameters for the first design are R=3.7mm, g=1mm and d_o are different for five irises and they are 1.1mm, 1.2mm, 1.4mm, 1.2mm and 1.1mm. The lengths of the TE_{21} mode converter section and phasing section as shown in Fig.5.1 are 5mm and 1mm respectively. Input diameter of the horn is 4.4mm whereas diameter of the phasing section is 6.2mm. Length and aperture diameter of the corrugated horn are 20mm and 12mm respectively. The thickness of the irises is 0.2mm. For the second design, the optimized parameters R=4.3mm, g=1.2mm and d_o =1.6mm which is same for all the five irises. The lengths of the TE_{21} mode converter section and phasing section are 5.8mm and 0.2mm respectively. All other parameters are same as first design.

5.3 Results and Discussion

5.3.1 Corrugated Matched Feed For F/D=0.7

The simulated coupling power in HE_{21} mode relative to HE_{11} mode for different value of g is presented in Fig.5.3 and the relative phase of HE_{21} w.r.t HE_{11} mode for different value of g is shown in Fig.5.4. It has been found out from Fig.5.3 and Fig.5.4 that optimum amplitude and phase flatness are obtained for g=1mm. For g=1mm, the coupled power is varied within 3dB over the frequency band of operation. Also for g=1mm, the variations of the relative phases are $\pm 25^0$ over 90^0. Both amplitude and phase of HE_{21} mode relative to HE_{11} mode at the aperture of the horn are important for designing broadband matched feed horn. The simulated return loss performance of the horn is shown in Fig.5.5. Figure 5.6 shows the simulated radiation pattern of the horn at 57.5GHz.

The secondary patterns of the offset reflector having diameter D=138mm, F/D=0.7 and offset angle $\theta_0=90^0$ as shown in Fig.5.7 have been simulated using GRASP/TICRA. The secondary pattern has been simulated using the corrugated feed horn without irises i.e. simple HE_{11} mode horn and the pattern is shown in Fig.5.8. Figure 5.9 shows the secondary simulated pattern with the designed broadband corrugated matched feed horn. The worst secondary cross-polarization using HE_{11} mode feed horn is -18dB. The simulated secondary cross-polarization at 57.5GHz is -35dB when the designed broadband corrugated matched feed is used to illuminate the reflector. Secondary performance of the cross-polarization of corrugated matched feed using single iris as well as five irises as a function of frequency is shown in Fig.5.10. It is clear from Fig.5.10 that better than 7dB improvement in cross-polarization is achieved for only 2% bandwidth for corrugated matched feed having single iris discontinuity and better than 10dB cross-polarization improvement for 1% bandwidth. Figure 5.10 also shows that the corrugated matched feed having five cascaded iris discontinuity are improving the cross-polarization bandwidth. Better than 10dB improvement in cross-polarization is achieved for 8% bandwidth and 7dB improvement in cross-polarization for 9.5% bandwidth.

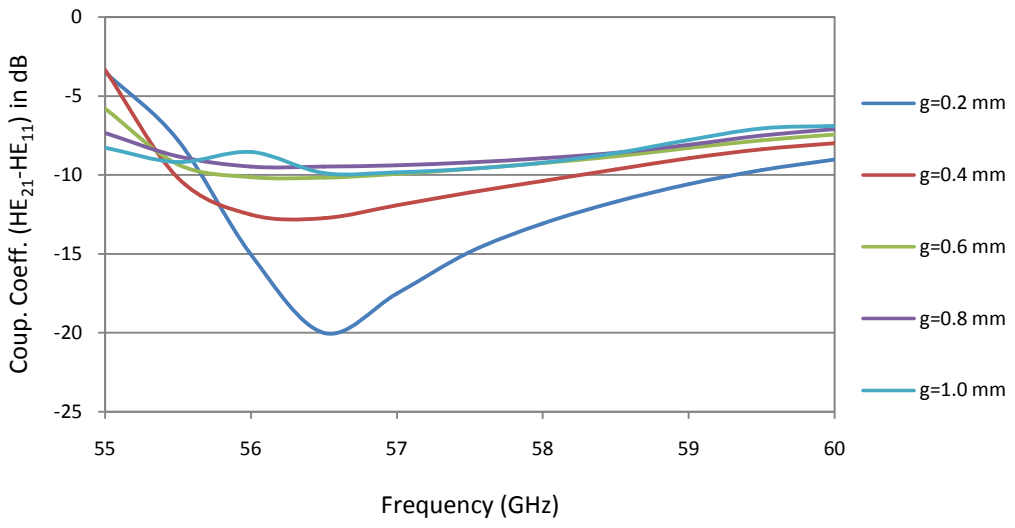

Fig. 5.3 Simulated power coupling to HE_{21} mode relative to HE_{11} mode at the aperture of the horn for different g

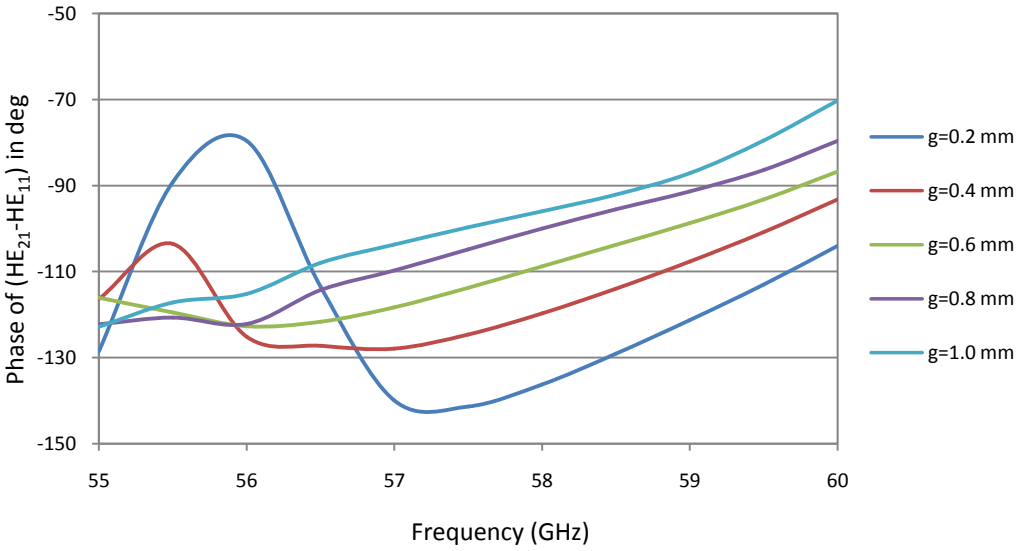

Fig. 5.4 Simulated relative phase of HE_{21} mode relative to HE_{11} mode at the aperture of the horn for different g

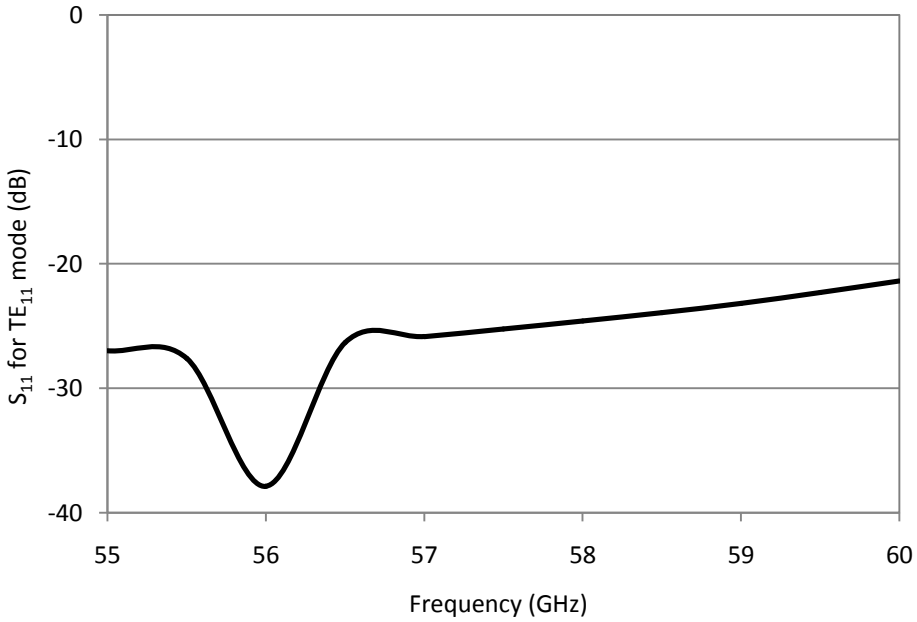

Fig.5.5 Simulated return loss characteristics of the horn

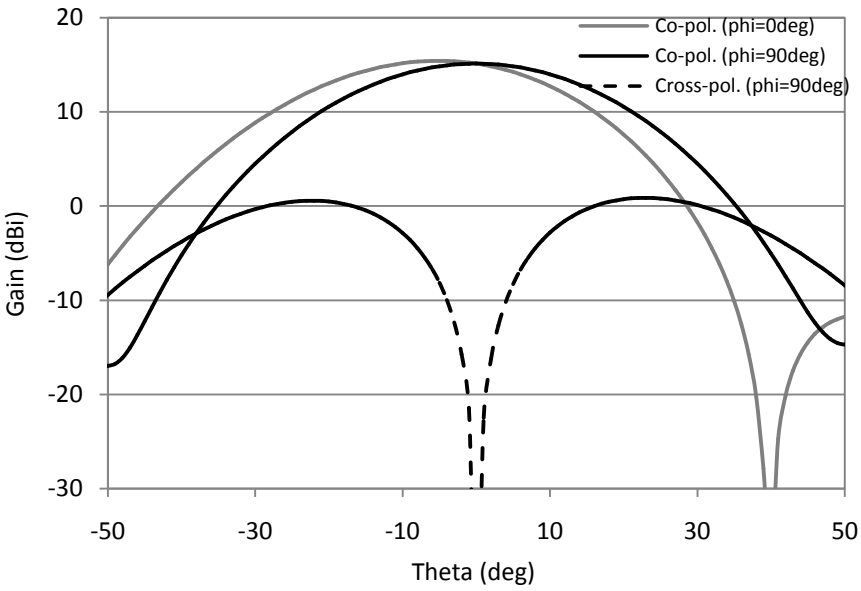

Fig.5.6 Simulated radiation pattern of the broadband corrugated conjugate matched feed horn at 57.5GHz

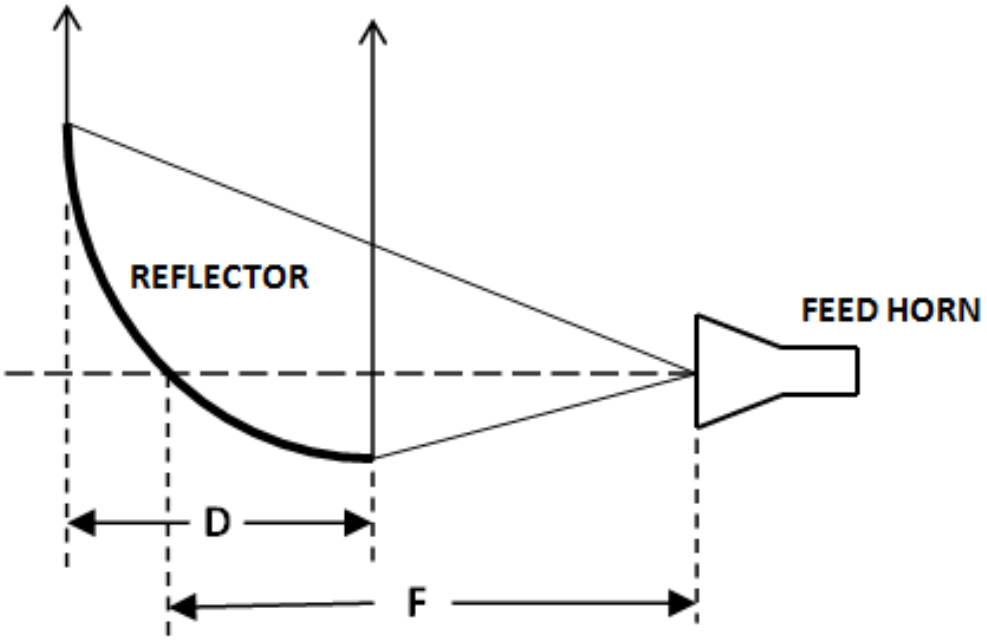

Fig.5.7 Schematic of 90^{O} offset reflector geometry

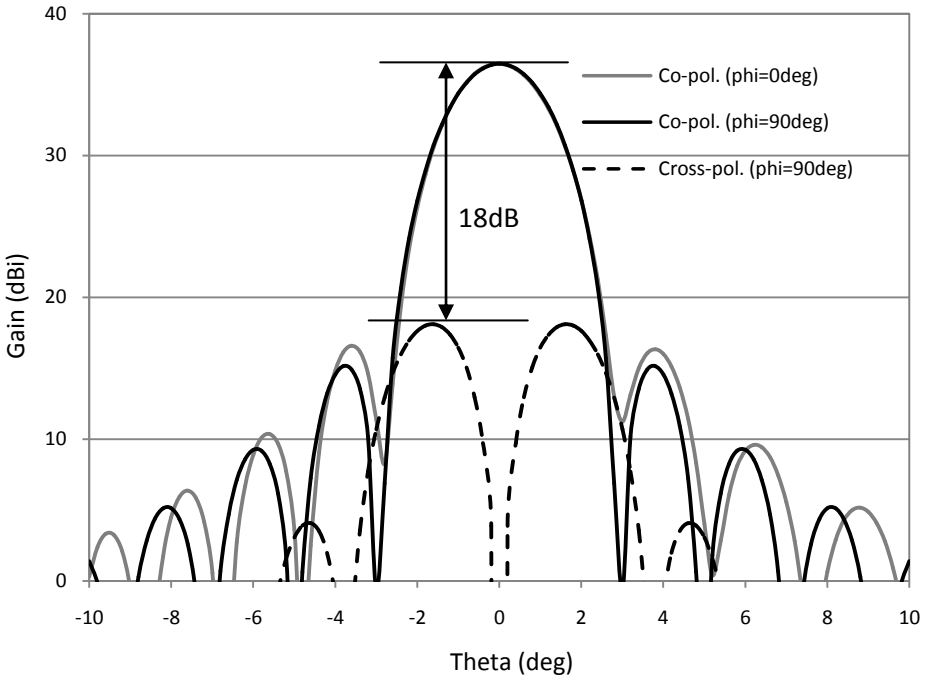

Fig.5.8 Simulated secondary pattern with HE_{11} mode feed horn at 57.5GHz

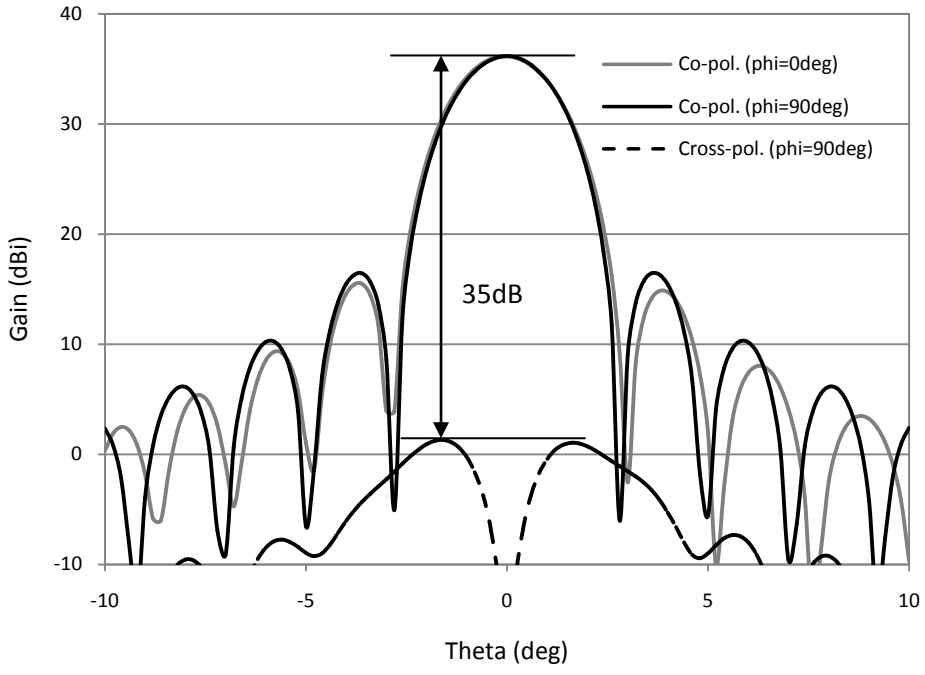

Fig.5.9 Simulated secondary pattern with conjugate matched feed horn at 57.5GHz

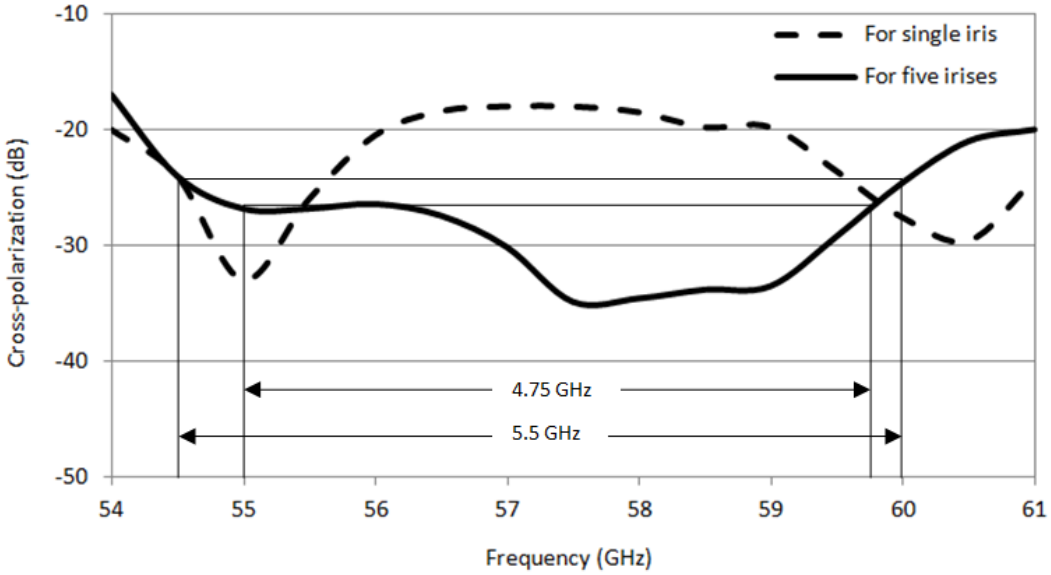

Fig.5.10 Cross-polarization suppression bandwidth (F/D=0.7)

5.3.2 Corrugated Matched Feed For F/D=0.4

The simulated return loss performance of the corrugated conjugate feed horn for reflector having F/D=0.4 and offset angle 90^{o} is shown in Fig.5.11. It is seen from Fig.5.11 that the return loss performance of the horn is better than 22dB over the band. The simulated coupling power in HE_{21} mode relative to HE_{11} mode is presented in Fig.5.12 and the relative phase of HE_{21} w.r.t HE_{11} mode is shown in Fig.5.13. Figure 5.14 shows the simulated radiation pattern of the feed horn at 56.5GHz.

The secondary patterns of the offset reflector having diameter D=138mm, F/D=0.4 and offset angle $\theta_0=90^0$ as shown in Fig.5.7 have been simulated using GRASP/TICRA. The secondary pattern has been simulated using the corrugated feed horn without irises i.e. simple HE_{11} mode horn and the pattern is shown in Fig.5.15. Figure 5.16 shows the secondary simulated pattern with the designed broadband corrugated matched feed horn. The worst secondary cross-polarization using HE_{11} mode feed horn is -14dB over the operating band. The simulated secondary cross-polarization at 56.5GHz is -35dB when the designed broadband

corrugated matched feed is used to illuminate the reflector. Thus there is a maximum improvement in cross-polarization at 56.5GHz and the improvement in cross-polarization is 21dB. Secondary performance of the cross-polarization of the corrugated matched feed as a function of frequency is shown in Fig.5.17. Better than 8dB improvement in cross-polarization is achieved for 8.7% bandwidth.

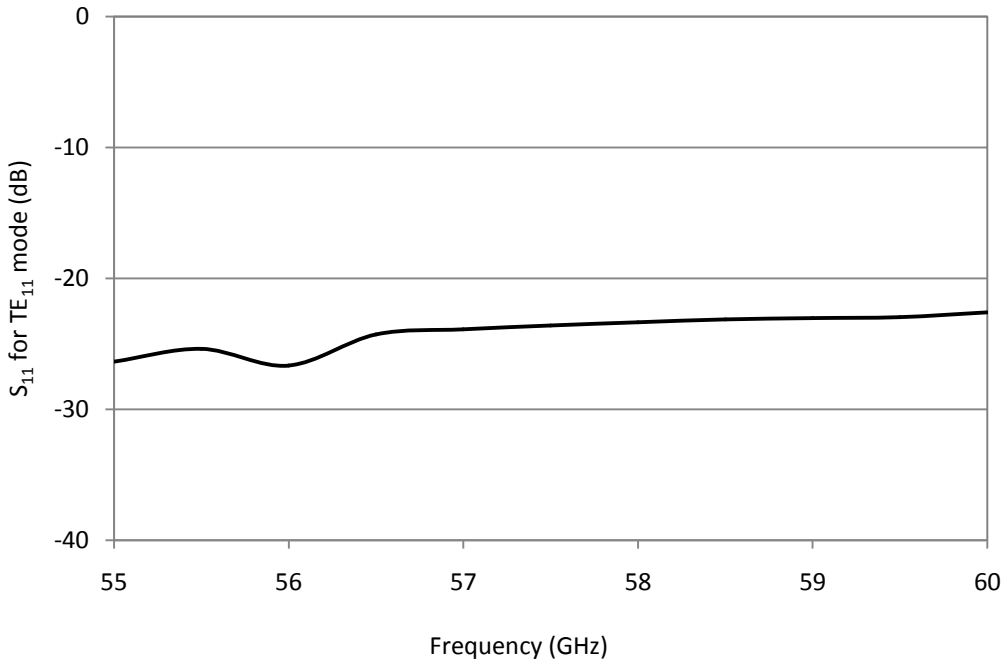

Fig.5.11 Simulated return loss characteristics of the horn

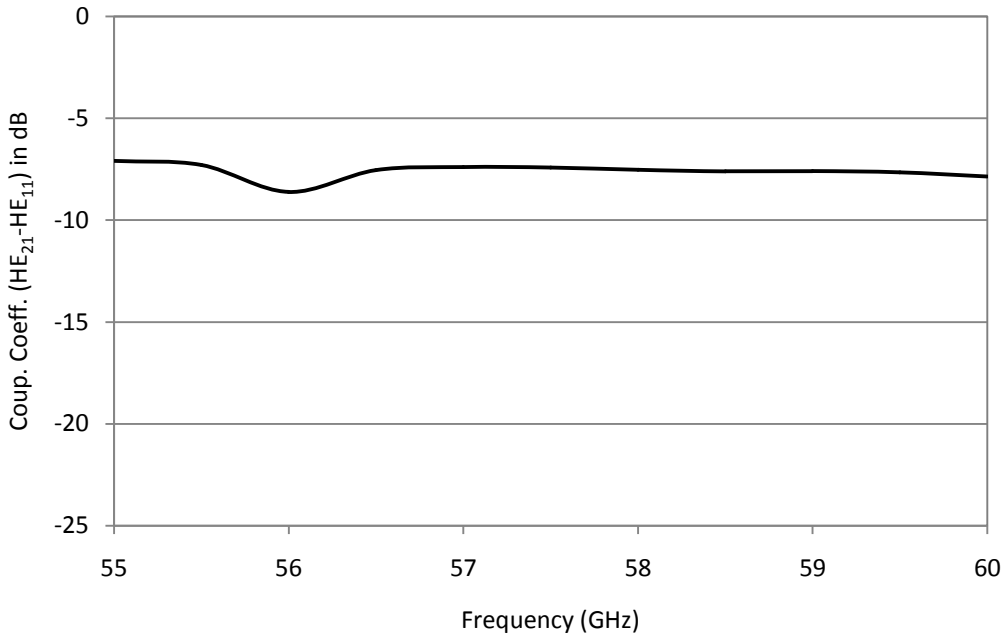

Fig.5.12 Simulated power coupling to HE_{21} mode relative to HE_{11} mode at the aperture of the horn

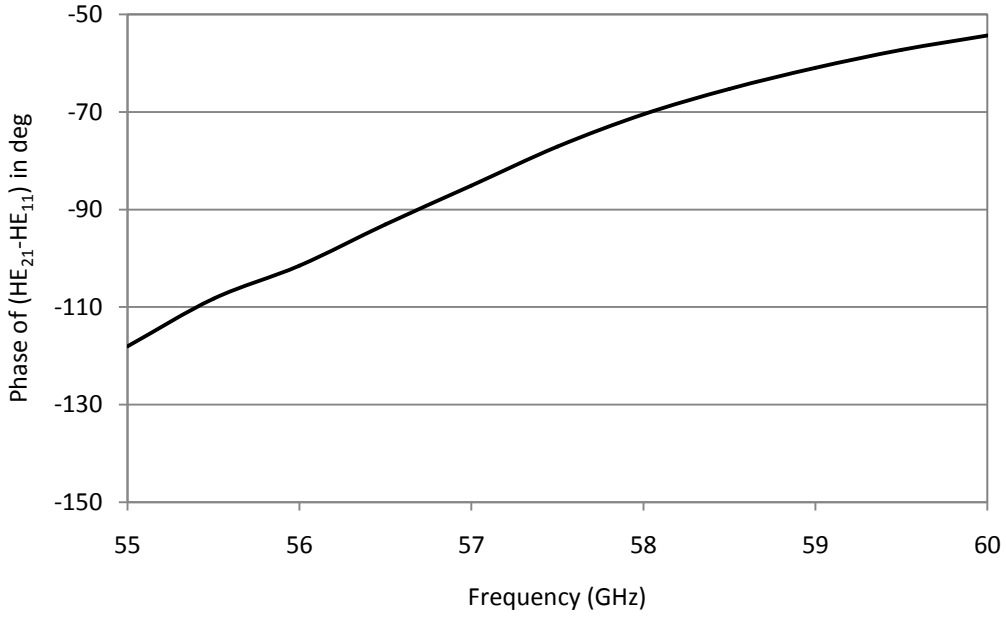

Fig.5.13 Simulated relative phase of HE_{21} mode relative to HE_{11} mode at the aperture of the horn

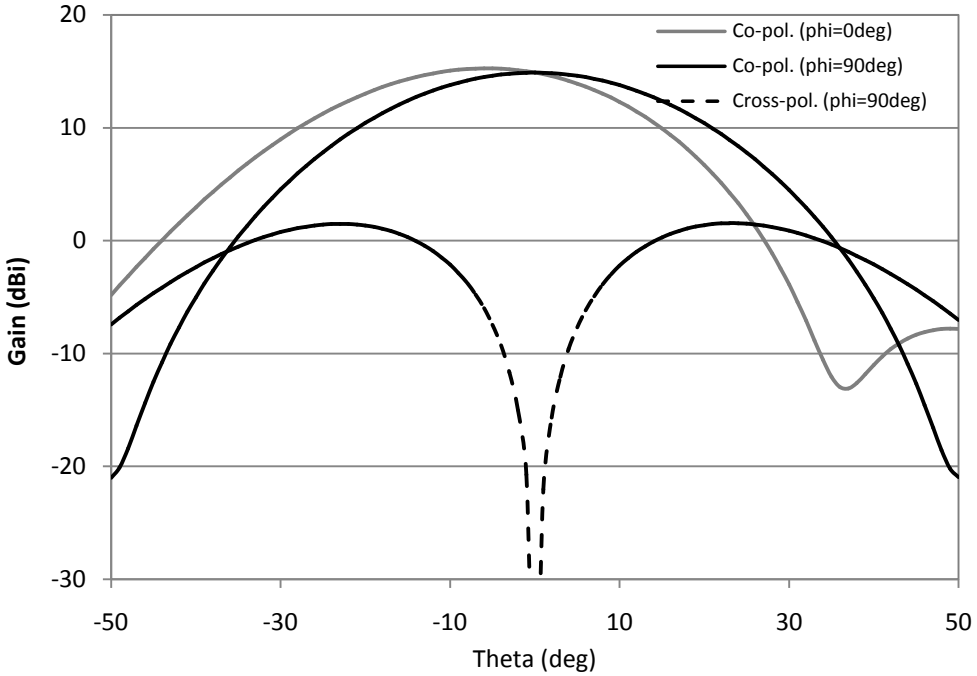

Fig.5.14 Simulated radiation pattern of the broadband corrugated conjugate matched feed horn at 56.5GHz

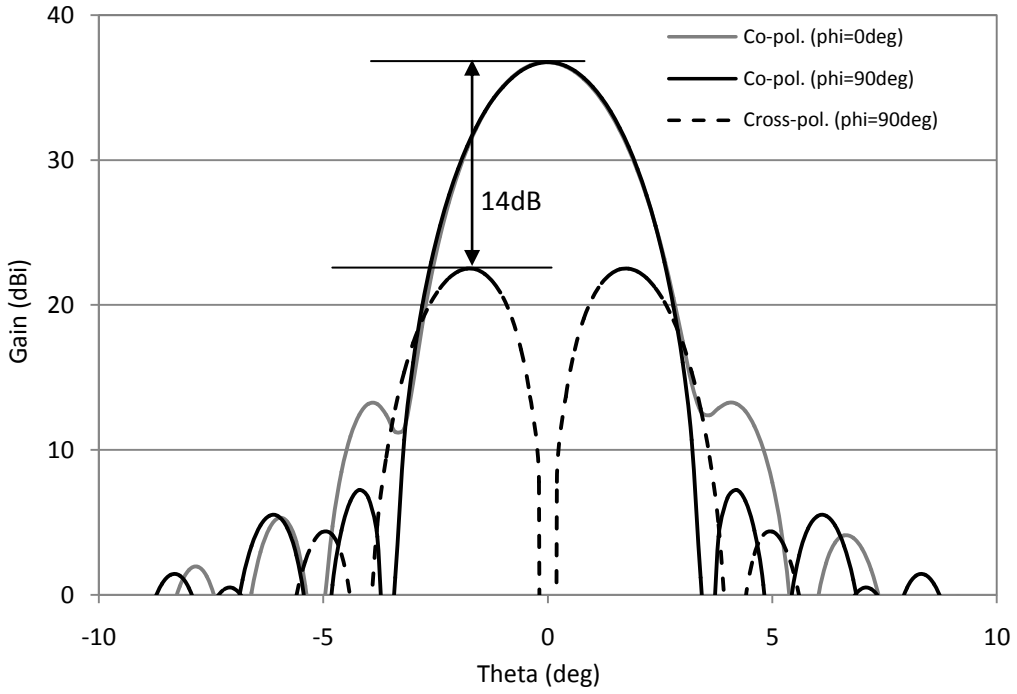

Fig.5.15 Simulated secondary pattern with HE_{11} mode feed horn at 56.5 GHz

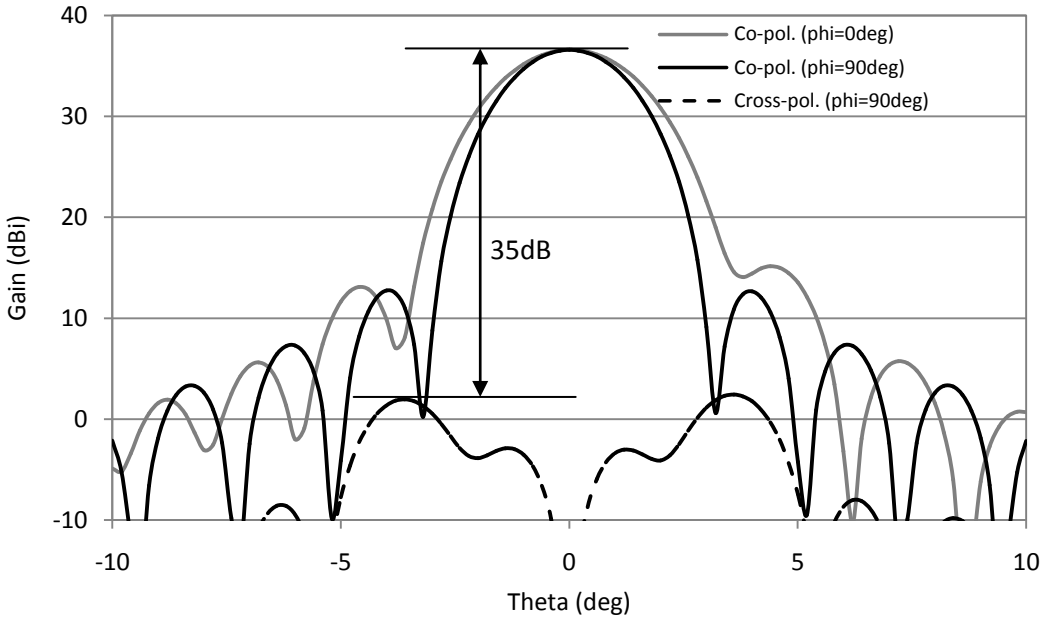

Fig.5.16 Simulated secondary pattern with the conjugate matched feed horn at 56.5GHz

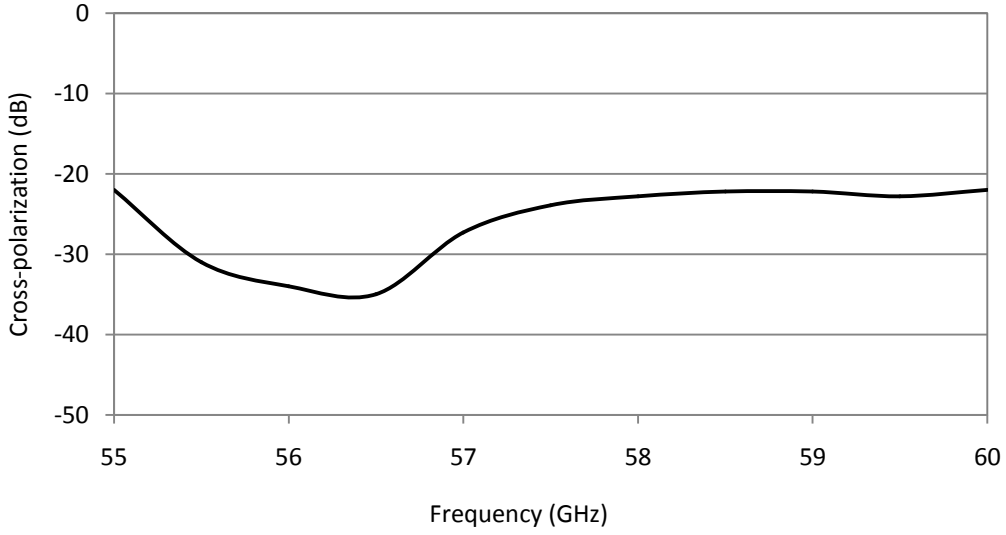

Fig.5.17 Cross-polarization suppression bandwidth (F/D=0.4)

5.4 Conclusion

A novel broadband corrugated conjugate matched feed horn has been designed and simulation results have been presented. The cross-polar performances of 90^0 offset reflector antenna having F/D=0.7 and 0.4 respectively have been simulated using the designed conjugate matched feed horns. It is shown that the proposed matched feed suppresses cross-polarization components significantly over an 8% frequency bandwidth when used as a primary feed with a 90^0 offset parabolic reflector antenna having very low F/D.

CHAPTER 6
CONCLUSION AND FUTURE SCOPE

This chapter presents the conclusions and the summary of the investigations carried out on the broadband conjugate matched feed horn. Section 6.1 describes the conclusions and the important findings of the research. Future scope of work are described in section 6.2.

6.1 Conclusion

In this thesis, a problem of mitigating the undesired high cross-polarization generated in offset parabolic reflector antenna for broad range of frequencies was undertaken. After carrying out detailed literature survey, it was found that no open literature is available dealing with the conjugate matched feed for broadband characteristics. An investigation on cascaded multiple post discontinuity in circular waveguide has been carried out to enhance the bandwidth of the conjugate matched feed horn but it has been found out that only 3% bandwidth is achievable for better than 10dB improvement in cross-polarization. Thus a new discontinuity study has been carried out i.e. off-centered junction in circular waveguide. These discontinuity has been utilized to design and develop a novel configuration of conjugate matched feed horn which can be used for 10% bandwidth for better than 10dB improvement in cross-polarization. The novel concept has been applied to both circular cylindrical structure as well as corrugated structure. Development of such feeds leads to the important technological development in the field of antenna design. The conclusions drawn from the investigations can be briefly summarized as follows:

Matched feed effectively suppresses the unwanted high cross-polarization introduced by the offset geometry in an offset parabolic reflector antenna. In a matched feed, it is necessary that the tangential electric fields at the aperture of the primary feed should be complex conjugate to the focal plane fields of the offset reflector antenna. In order to achieve this matching, the primary feed should support the appropriate higher order mode, in addition to the fundamental mode. Such modes in case of a smooth-walled cylindrical feed are TE_{21} with the fundamental TE_{11} mode, and HE_{21} mode with the fundamental HE_{11} mode in a cylindrical corrugated feed.

For satisfactory operation of the matched feed, it is necessary that the higher order mode should be added in proper amplitude and the phase with respect to the fundamental mode. It has been observed that the amplitudes of the higher order modes strongly depend on the reflector geometry, i.e., F/D ratio and offset angle.

It was observed that, the higher order asymmetric mode in the matched feed generates high cross-polarization in the plane of the primary radiation pattern. However, this high cross-polarization of the feed counter balances the effect of high cross-polarization in the secondary radiation pattern of an offset reflector.

Matched feeds are very suitable for offset reflector configurations having low F/D ratio and high offset angle. Therefore, in practical applications where the low F/D reflector is enforced due to space and weight constraints, the matched feed can be a more suitable option.

In practical applications more wideband performance of the matched feed is required. Thus, in the present thesis, a wideband study of the matched feed has been carried out. Through this study, a novel concept has been realized to design and developed wideband conjugate matched feed horn. With this novel concept, wideband smooth-wall and corrugated conjugate matched feed horn have been

designed. It was found that 10% bandwidth can be achievable for 10dB improvement in the cross-polarization for F/D=0.5 and offset angle=53^{o}.

It is expected that, in near future, for many practical applications, including the beam-scanning, multiple spot beam generation, remote-sensing radiometers, mono-pulse tracking radars, etc. the matched feed will become the most preferred feed option with the offset parabolic reflector antenna.

6.1 Scope for Future Work

In the present thesis, the design of a novel broadband conjugate matched feed horn in cylindrical and corrugated structure have been presented for very low F/D. Presently, 10dB improvement in the cross-polarization has been achieved for 10% bandwidth but as a future work using the same novel concept, further study for improving the bandwidth can be attempted.

Investigations on a multi-mode matched feed using elliptical wave guide structure may be carried out as an advancement of this work. This type of elliptical matched feed will be useful for an application where different beam-widths are required in both E and H planes, while maintaining the low cross-polarization in the secondary radiation pattern. Also wide band design of these feeds can be also studied and carried out. The broadband characteristics of the rectangular matched feed can be studied as a future work.

In the thesis, matched feed designs have been proposed for a single offset parabolic reflector antenna. A new matched feed can also be designed for a shaped offset reflector [19] in which the offset reflector profile is deformed to generate a contoured beam or a shaped beam.

REFERENCES

1. Y. T. Lo, and S. W. Lee, Antenna Handbook, Van Nostrand Reinhold Co., New York, 1988.

2. D. Pujara, S. B. Sharma, and S. B. Chakrabarty, "Historical and Planned Uses of Antenna Technology for the Space-borne Microwave Radiometer," IEEE Antennas and Wave Propagation Magazine, Vol. 53, No. 3, pp. 95-114, June-2011.

3. Samir I. Ghobrial, "Cross-polarization in Satellite and Earth-station Antennas," Proceedings of the IEEE, vol. 65, no. 3, pp. 378-387, March 1977.

4. S. Silver, Microwave Antenna Theory and Design, chapter 12, McGraw-Hill, New York, 1949.

5. Willard V. T. Rusch, "The Current State of the Reflector Antenna Art," IEEE Transactions on Antennas and Propagation, vol. 32, pp. 313-329, April 1984.

6. P. A. Watson, and Samir I. Ghobrial, "Off-axis Polarization Characteristics of Cassegrainian and Front-fed Paraboloidal Antennas," IEEE Transactions on Antennas and Propagation, vol. 20, pp. 691-698, November 1972.

7. Ta-Shing Chu, and R. H. Turrin, "Depolarization Properties of Offset Reflector Antennas," IEEE Transactions on Antennas and Propagation, vol. 21, pp. 339-345, May 1973.

8. M. J. Gans, and R. A. Semplak, "Some Far-field Studies of an Offset Launcher," Bell System Technical Journal, vol. 54, pp. 1319-1340, September 1975.

9. A. W. Rudge, "Multiple-beam Antennas: Offset Reflectors with Offset Feeds," IEEE Transactions on Antennas and Propagation, vol. 23, pp. 317-322, May 1975.

10. Hirokazu Tanaka, and Motoo Mizusawa, "Elimination of Cross Polarization in Offset Dual-Reflector Antennas," Electronics and Communication in Japan, vol. 58-B, pp. 71-78, 1975.

11. B. M. Thomas, "Cross Polarization Characteristics of Axially Symmetric Reflectors," Electronic Letters, vol. 12, pp. 218-219, April 1976.

12. H. C. Minnett, and B. M. Thomas, "Symmetric Reflectors with Zero Depolarization," Electronic Letters, vol. 12, pp. 291-292, May 1976.

13. M. Safak, and P. P. Delogne, “Cross Polarization in Cassegrainian and Front-fed Paraboloidal Antennas,” IEEE Transactions on Antennas and Propagation, vol. 24, pp. 497-501, July 1976.

14. Y. Mizuguch, M. Akagawa, and H. Yokoi, “Offset Dual Reflector Antenna,” IEEE International Symposium on Antennas and Propagation, pp. 2-5, October 1976.

15. A. R. Raab, “Cross-polarization Performance of the RCA SATCOM Frequency Reuse Antenna,” IEEE International Symposium on Antennas and Propagation, pp. 100-104, October 1976.

16. P. J. B. Clarricoats, and G. T. Poulton, “High-efficiency Microwave Reflector Antennas-A Review,” Proceedings of the IEEE, vol. 65, pp.1470-1504, October 1977.

17. Johannes Jacobsen, “On the Cross Polarization of Asymmetric Reflector Antennas for Satellite Applications,” IEEE Transactions on Antennas and Propagation, vol. 25, pp. 276-283, March 1977.

18. A. Kumar, “Reduce Cross-polarization in Reflector-type Antennas,” Microwaves, vol. 17, pp. 48-51, March 1978.

19. A. W. Rudge, and N. A. Adatia, “Offset-parabolic Reflector Antennas: A Review,” Proceedings of the IEEE, vol. 66, pp.1592-1618, December 1978.

20. S. I. Ghobrial, “Off-axis Cross-polarization and Polarization Efficiencies of Reflector Antennas,” IEEE Transactions on Antennas Propagation, vol. 27, pp. 460-466, July 1979.

21. S. I. Ghobrial, “Axial Cross-polarization in Reflector Antennas with Surface Imperfections,” IEEE Transactions on Antennas Propagation, vol. 28, pp. 610-616, September 1980.

22. Per-Simon Kildal, “Losses, Sidelobes, and Cross Polarization Caused by Feed-Support Struts in Reflector Antennas: Design Curves,” IEEE Transactions on Antennas Propagation, vol. 36, pp. 182-190, February 1988.

23. T. S. Chu, “Cancellation of Polarization Rotation in an Offset Paraboloid by a Polarization Grid,” Bell System Technical Journal, vol. 56, pp. 977- 986, July 1977.

24. C. Dragone, “New Grids for Improved Polarization Diplexing of Microwaves in Reflector Antennas,” IEEE Transactions on Antennas Propagation, vol. 26, pp. 459-463, May 1978.

25. W. Strutzman and M. Terada, “Design of offset-parabolic-reflector antennas for low cross-pol. and low sidelobes,” *IEEE Antennas Propag. Mag.*, vol. 35, no. 6, pp. 46–49, Dec. 1993.

26. A. W. Rudge and N. A. Adatia, “New class of primary-feed antennas for use with offset parabolic reflector antennas,” *Electron. Lett.*, vol. 11, pp. 597–599, Nov. 1975.

27. W. Rudge and N. A. Adatia, “Matched-feeds for offset parabolic reflector antennas,” in *Proc. 6th Eur. Microw. Conf.*, Rome, Italy, 1976, pp. 143–147.

28. D. J. Bem, “Electrical-field distribution in the focal region of an offset paraboloid,” in *Proc. IEE*, May 1969, vol. 116, pp. 679–684.

29. K. Bahadori and Y. Rahmat-Samii, “A tri-mode horn feed for gravitationally balanced back-to-back reflector antennas,” in *Proc. IEEE Antennas Propag. Soc. Int. Symp.*, Jul. 2006, pp. 4397–4400.

30. S. B. Sharma, D. Pujara, S. B. Chakrabarty, and V. K. Singh, “Performance comparison of a matched feed horn with a potter feed horn for an offset parabolic reflector,” in *Proc. IEEE Antennas Propag. Soc. Int.Symp.*, Jul. 2008, pp. 1–4.

31. S. B. Sharma, D. Pujara, S. B. Chakrabarty, and V. K. Singh, “Improving the cross-polar performance of an offset parabolic reflector antenna using a rectangular matched feed,” *IEEE Antennas Wireless Propag. Lett.*, vol. 8, pp. 513–516, 2009.

32. S. B. Sharma, Dhaval Pujara, S. B. Chakrabarty, **Ranajit Dey**, and V. K. Singh, “Design and Development of a Conjugate Matched Feed for an Offset Parabolic Reflector Antenna,” IET Microwaves, Antennas & Propagation, Vol. 4, Iss. 11, pp. 1782–1788, Nov.2010.

33. S. B. Sharma, Dhaval Pujara, S. B. Chakrabarty, and **Ranajit Dey**, "Cross-Polarization Cancellation in an Offset Parabolic Reflector Antenna Using a Corrugated Matched Feed" *IEEE Antennas Wireless Propag. Lett.*, vol. 8, pp. 861–864, 2009.

34. S.B. Sharma, V.K. Singh, **Ranajit Dey** and S.B. Chakrabarty, "Analysis of a Post Discontinuity in Oversized Circular Waveguide", IEEE Trans. Microw. Theory Tech., vol. 57, no. 8, pp. 1989-1995, Aug. 2009.

35. **Ranajit Dey**, S. B. Chakrabarty, Rajeev Jyoti and Thomas Kurian, "Higher Order Mode Analysis of Dual Post Discontinuity in a Circular Waveguide", IETE Journal of Research, Vol. 62, Issue-1, PP. 55-62, 2016.

36. **Ranajit Dey**, S. B. Chakrabarty, Rajeev Jyoti, "Analysis and Application of Triple Post Discontinuity in Circular Waveguide", Electromagnetics, Vol. 36, No. 2, 67–77, 2016.

37. **Ranajit Dey**, S. B. Chakrabarty, Rajeev Jyoti, "Scattering Analysis of Cascaded Off-centered Circular Waveguides", Under review in Electromagnetics Journal (Taylor and Francis)

38. K. M. Prasad and Lotfollah Shafai, "Improving the symmetry of radiation patterns for offset reflectors illuminated by matched feeds," IEEE, Transactions on Antenna and Propagation , vol. 36, no. 1, pp. 141-144, Jan. 1988.

39. S. B. Sharma, V. K. Singh, and S B Chakrabarty, "Multi-frequency waveguide orthomode transducer," IEEE Trans. Microw. Theory Tech., vol. 53, no. 8, pp. 2604-2609, Aug. 2005.

40. Zhongxiang Shen and Robert H. MacPhie, "Scattering by a Thick Off-Centered Circular Iris in Circular Waveguide", IEEE Trans. on Microwave Theory and Techniques, Vol.43, No. 11, November 1995.

41. R. W. Scharstein and A. T. Adams, 'Galerkin solution for the thin circular iris in a TE11 mode circular waveguide', IEEE Trans. Microwave Theory Tech., vol. 36, pp. 106-113, Jan. 1988.

42. R. R. Mansour and R. H. MacPhie, 'Scattering at an N-furcated parallel plate waveguide junction', IEEE Trans. Microwave Theory Tech., vol. MTT-33, pp. 830~835, Sept. 1985.

43. N. Marcuivitz, 'Waveguide Handbook', R.L Series, Vol. 10, McGraw Hill Book Co., New York, 1951

44. M. Abramowitz and I. A. Stegun, 'Handbook of Mathematical Functions', New York: Dover, 1965.

45. J. D. Wade and R. H. MacPhie, 'Scattering at circular-to-rectangular waveguide junctions', IEEE Trans. Microwave Theory Tech., vol.MTT34, pp. 1085-1091, Nov. 1986.

46. W. J. English, 'The circular waveguide step-discontinuity transducer', IEEE Trans. Microwave Theory Tech., vol. MIT-21, pp. 633-636, Oct. 1973.

47. L. Carin, K. J. Webb and S. Weinreb, 'Matched windows in circular waveguide', IEEE Trans. Microwave Theory Tech., vol. 36, pp.1359-1362, Sept. 1988.

48. K.Watson, A. W. Rudge, and N. A. Adatia, “Dual-polarized mode generator for cross-polar compensation in parabolic reflector antennas,” in Proc. 8th Eur. Microw. Conf., Paris, France, 1978, pp. 183–187.

49. P. J. B. Clarricoats, and A. D. Olver, Corrugated Horns for Microwave Antennas, IEEE Press, 1984.

50. H. C. Minnett, and MacA. B. Thomas, “A Method of Synthesizing Radiation Patterns with Axial Symmetry,” IEEE Transactions on Antennas Propagation, vol. 14, pp. 654-656, September 1966.

51. P. J. B. Clarricoats, and P. K. Saha, “Propagation and Radiation Behavior of Corrugated Feeds, Part 1,” Proceedings of the IEE, (118), pp. 1167-1176, September 1971.

52. R.W. Gruner and W.J. English, "Antenna design studies for a U.S. domestic satellite", Comsat Tech. Rev., vol.4, 2, pp.413-447, Fall 1974

53. K.C. Lang, M.K. Eick and D.T. Nakatani, "A 6/4 and 30/20 dual foci offset parabolic reflector antennas", IEEE Trans. Antennas and Propagation, vol. AP-24, pp. 859-865, Nov. 1976.

LIST OF PUBLICATIONS BASED ON THE THESIS

Papers Published:

1. **Ranajit Dey**, S. B. Chakrabarty, Rajeev Jyoti, "Broadband Conjugate Matched Feed Horn- A Novel Concept", IEEE Antennas and Wireless Propagation Letters, Vol. 15, PP. 496-499, 02,March-2016.

2. **Ranajit Dey**, S. B. Chakrabarty, Rajeev Jyoti and Thomas Kurian, "Higher Order Mode Analysis of Dual Post Discontinuity in a Circular Waveguide", IETE Journal of Research, Vol. 62, Issue 1, PP. 55-62, 2016.

3. **Ranajit Dey**, S. B. Chakrabarty, Rajeev Jyoti, "Analysis and Application of Triple Post Discontinuity in Circular Waveguide", Electromagnetics, Vol. 36, No. 2, 67–77, 2016.

4. **Ranajit Dey**, S. B. Chakrabarty, Rajeev Jyoti and Thomas Kurian, "Synthesis and Analysis of Multimode Profile Horn using Mode Matching and Evolutionary Algorithm", IET Microwave Antennas and Propagation, Vol. 10, No. 3, PP. 276-282, 2016.

5. **Ranajit Dey**, S. B. Chakrabarty and Rajeev Jyoti, "Analysis of a Coaxial Probe-fed Circular waveguide", Microwave and Optical Technology Letters, Vol.55, No.11, November 2013.

Paper Communicated:

6. **Ranajit Dey**, "Broadband Corrugated Conjugate Matched Feed Horn", Communicated to Microwave and Optical Technology Letters.